Anticancer efficacy of selected South African phytomedicines in a three-dimensional colorectal cancer model

[Antikanker-doeltreffendheid van geselekteerde Suid-Afrikaanse fitomedisyne in 'n drie-dimensionele kolorektale kankermodel]

T Smit

orcid.org/ 0000-0002-2934-8639

Dissertation submitted in fulfilment of the requirements for the degree *Master of Science in Pharmaceutics* at the North West University

Supervisor: Prof C Gouws

Co-supervisor: Dr C Calitz

Co-Supervisor: Prof K Wrzesinski

Examination: November 2019

Student number: 24970247

The more that you read,

the more things you will know.

The more that you learn,

the more place you'll go.

- Dr.-Seuss

ACKNOWLEDGEMENTS

First and foremost, to my **Heavenly Father** who gave me this wonderful opportunity, thank you for the emotional strength and determination in completing this dissertation.

To my amazing parents, **Alfred and Karin Smit**, thank you for believing in me and giving me encouragement, love and support during these rough two years. To my brothers, **Alfred and Stefan Smit**, thank you for always being interested and giving praise and support.

To my homeslices (**Monique, Mardi, Sharissa**) and my flatmate (**Miki**) words cannot describe how much you mean to me. Thank you for being family.

To all the new friends I have made, thank you all for keeping me sane, giving support and distractions when needed. I would not have been able to this without you.

Prof C Gouws, thank you for all that you have taught me. Thank you for giving a helping hand and a shoulder to cry on. It was a privilege to have had a mentor as excellent as you.

Prof K Wrzesinski, thank you for always giving comments and advice even when I did everything wrong. Thank you for sharing your knowledge and passion.

To **Roan Swanepoel** and **Jacques Rossouw**, thank you for helping me when I knew nothing! To **Liezaan van der Merw**e, thank you for all your help and support.

To **Dr H Svitina**, **Dr C Willers**, **Dr L Twete, Dr C Calitz,** thank you for all that you have done for me, without you it would not have been possible.

Prof Josias H Hamman, thank you for always being willing to explain something or to give a new perspective.

To the "**Afrikaanse Akademie vir Wetenskap en Kuns**", thank you for giving me the opportunity to develop the language I love and providing me with funding.

To the **North-West University** for also providing financial support.

ABSTRACT

Millions of patients die from cancer each year, with colorectal cancer being one of the leading causes. Chemotherapeutic drugs are routinely used in cancer treatment, but unfortunately these treatments have severe side effects. This contributes to the increasing popularity of phytomedicine use during cancer therapy. The use of phytomedicines is popular because they are seen as “safe and natural”, even though there is little concrete proof of their efficacy. *Sutherlandia frutescens* and *Xysmalobium undulatum* are South African medicinal plants that are widely used for a variety of diseases, and they have also been proposed to have anticancer potential.

Both plants contain various bioactive compounds with potential activity in the treatment of cancer and other diseases. These compounds, however, could potentially interact with co-administered conventional drugs which can result in serious side effects or decreased pharmacological efficacy of the co-administered drug. The cytochrome P450 (CYP450) enzyme family is responsible for the metabolism of most commercially available drugs. Phytomedicines may change the expression or activity of these CYP450 enzymes, which may lead to phytomedicine-drug interactions.

Three-dimensional (3D) cell culture models have been proposed to bridge the gap between *in vitro* anticancer and drug biotransformation studies, and the human *in vivo* system. The current gap is a result of the lack of physiological relevance of the highly used two-dimensional (2D) models. In this study, LS180 colorectal cancer cells were cultured as 3D sodium alginate encapsulated spheroids in clinostat based bioreactors. Their growth and viability were subsequently characterised for 20 days, and the ideal window in which to perform experiments was determined.

The 3- (4,5- dimethylthiazol- 2- yl)- 2,5- diphenyltetrazolium bromide (MTT) assay was then used to establish half maximal inhibitory concentrations for *S. frutescens* and *X. undulatum* crude aqueous extracts, as wells as for the standard chemotherapeutic drug, paclitaxel. The determined MTT values were then used to validate and implement the established 3D model. During model characterization, validation and implementation, the following parameters were measured:

soluble protein content, intracellular adenosine triphosphate levels (ATP), extracellular adenylate kinase (AK), glucose consumption and *CYP3A4* and *CYP2D6* gene expression.

Use of the model for anticancer treatment screening was validated using two concentrations of paclitaxel, and treatment continued for 96 h. It was established that the LS180 3D cell model could be used for future anticancer activity screening, as paclitaxel caused a decrease in cell growth, viability and glucose consumption in the model. Furthermore, relative expression of the *CYP3A4*, *CYP2D6* and P-glycoprotein genes all increased relative to the untreated control group. These are typical resistance-producing changes known to be a result of paclitaxel treatment.

The model was then used to evaluate the anticancer potential of the two selected South African phytomedicines. The LS180 cell spheroids were treated with two concentrations of each of the phytomedicines for 96 h. Crude aqueous *S. frutescens* extract caused a marked decrease in the soluble protein content, and caused the ATP per protein content and AK per protein content to decrease below detectable limits after only 4 h exposure. *S. frutescens* also resulted in a decrease in glucose consumption. Treatment with the *X. undulatum* aqueous extract also resulted in decreased soluble protein content, as well as decreased cell viability and glucose consumption. The results suggested that *S. frutescens* and *X. undulatum* could have treatment potential against colorectal cancer.

It was concluded that the LS180 sodium alginate encapsulated spheroid model could be used for future anticancer treatment and drug biotransformation screening. Furthermore, the two phytomedicines have colorectal anticancer potential as determined by in vitro tests, and this needs to be studied further to determine the clinical significance of their activities.

Keywords: *anticancer; cell viability; colorectal cancer; drug biotransformation; phytomedicine; three-dimensional cell culture.*

UITTREKSEL

Miljoene pasiënte sterf jaarliks as gevolg van kanker, met kolorektale kanker wat een van die hoof oorsake is. Chemoterapeutiese middels word gereeld tydens kankerbehandeling gebruik, maar ongelukkig het hierdie behandelings ernstige newe-effekte. Dit dra by tot die toenemende gewildheid van fitomedisyne-gebruik tydens kankerterapie. Die gebruik van fitomedisyne is gewild omdat dit gesien word as 'veilig en natuurlik', al is daar min konkrete bewyse van hul effektiwiteit. *Sutherlandia frutescens* en *Xysmalobium undulatum* is Suid-Afrikaanse medisinale plante wat wyd gebruik word vir 'n verskeidenheid siektes, en daar word ook voorgestel dat hulle antikanker potensiaal het.

Albei plante bevat verskillende bioaktiewe verbindings met potensiële aktiwiteit in die behandeling van kanker en ander siektes. Hierdie verbindings kan egter moontlike interaksie hê wanneer dit tesame met ander middels gebruik word, wat kan lei tot ernstige newe-effekte of 'n verminderde farmakologiese effektiwiteit van die toegediende medisyne. Die sitochroom P450 (CYP450) ensiemfamilie is verantwoordelik vir die metabolisme van die meeste kommersieel beskikbare medisyne. Fitomedisyne kan die uitdrukking of aktiwiteit van hierdie CYP450-ensieme verander, wat kan lei tot fitomedisyne-geneesmiddels interaksies.

Drie-dimensionele (3D) selkultuurmodelle is voorgestel om die gaping tussen *in vitro*-antikanker- en geneesmiddelbiotransformasiestudies en die menslike *in vivo*-stelsel te oorbrug. Die huidige gaping is die gevolg van die gebrek aan fisiologiese relevansie van die hoogs gebruikte twee-dimensionele (2D) modelle. In hierdie studie is LS180 kolorektale kankerselle gekweek as 3D natriumalginaat geënkapsuleerde sferoïede in klinostaat-gebaseerde bioreaktors. Hulle groei en lewensvatbaarheid is daarna vir 20 dae gekarakteriseer, en die ideale tydperk om toekomstige eksperimente uit te voer, is bepaal.

Die 3- (4,5-dimetieltiasol- 2- iel)- 2,5-difenieltetrasolium bromied (MTT) toets is gebruik om die half maksimale inhiberingskonsentrasies vir *S. frutescens* en *X. undulatum* ru

water ekstrakte te bepaal, asook vir die standaard chemoterapeutiese geneesmiddel, paklitaksel. Die vasgestelde MTT-waardes is daarna gebruik om die gevestigde 3D-model te valideer en te implementeer. Tydens modelkarakterisering, validering en implementering is die volgende parameters gemeet: oplosbare proteïeninhoud, intrasellulêre adenosientrifosfaatvlakke (ATP), ekstrasellulêre adenilaatkinase (AK), glukoseverbruik en *CYP3A4* en *CYP2D6* geenuitdrukking.

Die gebruik van die model vir antikankerbehandeling sifting is gevalideer met behulp van twee konsentrasies van paklitaksel, en die behandeling is vir 96 uur voortgesit. Daar is vasgestel dat die model gebruik kan word vir toekomstige siftingstoetse om antikanker aktiwiteit te bepaal, aangesien paklitaksel 'n afname in selgroei, sellewensvatbaarheid en glukoseverbruik in die model veroorsaak het. Verder het die relatiewe geenuitdrukking van *CYP3A4*, *CYP2D6* en P-glikoproteïen toegeneem relatief tot die onbehandelde kontrolegroep. Hierdie is tipiese weerstandigheidsmeganismes wat voorkom na paklitaksel behandeling.

Die model is gevolglik gebruik om die antikanker potensiaal van die twee Suid-Afrikaanse fitomedisynes te evalueer. Die sferoïede is vir 96 uur met twee afsonderlike konsentrasies van elk van die fitomedisyne behandel. Ru water ekstrakte van *S. frutescens* het 'n merkbare afname in die oplosbare proteïeninhoud veroorsaak en die ATP per proteïeninhoud en AK per proteïeninhoud het na slegs 4 ure van blootstelling onder waarneembare grense gedaal. *S. frutescens* blootstelling het ook gelei tot 'n afname in glukoseverbruik. Behandeling met *X. undulatum* ru water ekstrakte het ook gelei tot 'n verlaagde oplosbare proteïeninhoud, sellewensvatbaarheid asook glukoseverbruik. Die resultate het voorgestel dat *S. frutescens* en *X. undulatum* behandelingspotensiaal teen kolorektale kanker kan hê.

Daar is tot die gevolgtrekking gekom dat die LS180 natriumalginaat geënkapsuleerde sferoïed model gebruik kan word vir toekomstige antikankerbehandeling- en biotransformasiesifting. Verder het die twee fitomedisynes antikanker potensiaal, wat verdere ondersoek vereis.

Sleutelwoorde: *antikanker; sellewensvatbaarheid; kolorektale kanker; geneesmiddelbiotransformasie; fitomedisyne; drie-dimensionele sel kulture.*

TABLE OF CONTENTS

LIST OF FIGURES

Chapter 1

Chapter 2

Chapter 3

Chapter 4

Appendices

LIST OF TABLES

Chapter 2

Chapter 3

Chapter 4

LIST OF ABBREVIATIONS

2D	Two-dimensional
3D	Three-dimensional
µg	Microgram
A	
AIDS	Acquired immunodeficiency syndrome
AK	Adenylate kinase
ANOVA	Analysis of variance
ATCC	American Tissue Culture Collection
ATP	Adenosine triphosphate
ATPase	Adenosine triphosphatase
B	
BAM	Bioarray matrix
BSA	Bovine serum albumin
C	
$CaCl_2$	Calcium chloride
$CaCl_2.2H_2O$	Calcium chloride dihydrate
cDNA	Complementary deoxyribonucleic acid
CO_2	Carbon dioxide
Ct	Threshold cycle

CYP450	Cytochrome P450
D	
DIY	Do it yourself
DMEM	Dulbecco's Modified Eagle's medium
DMSO	Dimethyl sulfoxide
DNA	Deoxyribonucleic acid
E	
EDTA	Ethylenediaminetetraacetic acid
Eme1	Essential meiotic structure-specific endonuclease 1
F	
FBS	Foetal bovine serum
G	
GAPDH	Glyceraldehyde 3-phosphate dehydrogenase
H	
HIV	Human immunodeficiency virus HIV
I	
IC	Inhibition concentration
IC_{50}	50% inhibitory concentration
L	
LC-MS	Liquid chromatography-mass spectrometry
LD_{50}	50% lethal dose concentration

M

MDR1	Multidrug resistant gene
mRNA	Messenger ribonucleic acid
MTHFR	Methylenetetrahydrofolate reductase
MTT	3- (4,5- dimethylthiazol- 2- yl)- 2,5- diphenyltetrazolium bromide

N

NaCl	Sodium chloride
NADP	Nicotinamide adenine dinucleotide phosphate
NEAA	Non-essential amino acids
NWU	North-West University

P

PBS	Phosphate buffered saline
PDA	Photodiode array
P-gp	P-glycoprotein
PXR	Pregnane X receptor

Q

qPCR	Real-time polymerase chain reaction-based
qRT-PCR	Quantitative reverse transcription polymerase chain reaction

R

RNA	Ribonucleic acid
rpm	Rotations per minute

S

S. frutescens	*Sutherlandia frutescens*
SFFW	*Sutherlandia frutescens*
SU1	Cycloartane-like triterpene glycoside

T

TBP	TATA-box binding protein

U

UPLC	Ultra-performance liquid chromatography

W

WHO	World Health Organisation

X

X. undulatum	*Xysmalobium undulatum*
XU174	*Xysmalobium undulatum*

CHAPTER 1

This chapter presents the background, justification, problem statement, general aim, specific objectives and chapter layout for this study. An experimental approach is illustrated and finally the publication status of the research, with the specific contributions of the authors are given.

1.1. Introduction

Cancer remains a global burden despite the medical advances made every day. Patients suffering from this disease are usually desperate for a cure, or to simply reduce the severe side effects of conventional treatment. To this end, they frequently turn to alternative treatments which usually include plant-based medicines or phytomedicines. Although these treatments may be curative or beneficial, they may also have adverse effects. When used simultaneously with the prescribed chemotherapeutic drugs, they may also interact with the treatment.

When studying these phytomedicines as potential treatment sources, the standard drug development pipeline must still be followed. However, the current models used in this pipeline lacks physiological relevance, to such an extent that only an estimated 3.4% of new drug candidates are successful in clinical trials (Wong *et al*., 2019). New models with better correlation to human physiology are therefore urgently needed to increase the successful screening of potential treatments.

1.2. Background and justification

Approximately 80% of the world's population living in third world countries rely on phytomedicines for their primary health care needs (Aziz *et al*., 2017). Phytomedicines are commonly used by traditional healers to treat a variety of symptoms and ailments, including fever, headache, colds, diabetes and cancer (Baskar *et al*., 2012). In 2018, cancer was responsible for an estimated 9.6 million deaths worldwide, with colorectal cancer accounting for 1.8 million cases annually. Of these deaths, approximately 70% occurred in low- and middle-income countries (WHO, 2018). Although some types of cancers are preventable, colon cancer is often detected only in its advanced stages when symptoms become apparent (Mishra *et al*., 2013).

According to Brenner *et al*. (2007), advanced adenoma transition rates are strongly age-dependent, meaning that older patients are more likely to develop colorectal cancer. Patients aged 50 years and older account for more than 90% of colorectal cancer cases (Haggar & Boushey, 2009). Several options are available for the treatment of colorectal cancer, including surgery, chemotherapy, radiation therapy, immunotherapy and nutritional support therapy (Mishra *et al*., 2013). Surgical resection remains the primary treatment option for patients with colorectal cancer, however, more than half of the patients eventually die of metastatic related diseases. Chemotherapy as a treatment option for patients with advanced colorectal cancer aims to prolong patient survival rates, maintain the quality of life, as well as provide symptomatic treatment

(Simmonds, 2000). Older patients, however, are less likely to tolerate the treatment well as age is a risk factor for chemotherapeutic toxicity, and these treatments are known for side effects of varying severity (Carr *et al*., 2008; Hurria *et al*., 2011). The latter is one of the reasons that there is often an increase in the use of phytomedicines by cancer patients. The general public belief is that these phytomedicines can improve cancer related symptoms and kill tumour cells with fewer adverse effects when compared to standard chemotherapeutic treatment options (Oga *et al.,* 2016).

According to Baskar *et al*. (2012), plants have been a useful source in identifying new, clinically significant anticancer compounds. As a result, an astonishing 60% of currently used anticancer agents are derived from natural sources (Fouché *et al*., 2006). Neuwinger (2000) compiled a list of African medicinal plants which includes more than 5 400 medicinal plant taxa with more than 16 300 medicinal uses (Van Wyk, 2011). *Sutherlandia frutescens*, commonly known as cancer bush, is a South African medicinal plant found along the west coast of the Western Cape (Van Wyk, 1997; Chinkwo, 2005). Traditional healers have claimed that *S. frutescens* has anticancer properties and this has been partially validated (Chinkwo, 2005). The indigenous plant *Xysmalobium undulatum,* also known as Uzara, is one of the most widely used phytomedicines in South Africa (Vermaak *et al*., 2014). Phytomedicines known to contain plant cardenolides, such as *X. undulatum*, have recently emerged as promising new agents in treating diseases such as cancer (Krishna *et al*., 2015). Exploring the possibility of new chemotherapeutic agents is still an important field in drug discovery and development. However, establishing the efficacy as well as the pharmacological and toxicological effects of these new chemotherapeutic agents are essential (Saeidnia *et al*., 2015).

Most commercially available drugs are metabolised by the cytochrome P450 (CYP450) family, particularly CYP3A4 and 2D6 (Amacher, 2010). The metabolic processing pathway of commercial drugs is usually well known, including their influence on CYP450 enzymes. This, however, does not hold true for phytomedicines. There is a general lack of *in vivo* data regarding the safety, efficacy and metabolism-associated interactions of plants indigenous to Africa, particularly medicinal plants, and this requires extensive study (Gouws & Hamman, 2018). It is also of utmost importance to identify the possible effects of phytomedicines on CYP450 expression and activity, as this will enable prediction of possible pharmacokinetic interactions due to concomitant use of prescribed medicines and phytomedicines (Bo *et al*., 2016).

In vitro systems, specifically the use of immortalised cell lines, have long served as the gold standard to establish pharmacokinetic and pharmacodynamic drug interactions during preclinical

drug discovery and development (Zhang *et al*., 2012, Saeidnia *et al*., 2015; Jaroch *et al*., 2018). According to Wrzesinski *et al.* (2014) there are two extreme conditions for cell growth, namely classical two-dimensional (2D) cell cultures and three-dimensional (3D) cell cultures. The second is characterised by cells which have reached dynamic equilibrium, resulting in mimetic tissue-like conglomerates. Literature has indicated that there are differences between cellular morphology when comparing 3D and 2D models (Bonnier *et al.,* 2015). This may be because 2D-cultured cells are inherently unable to simulate the microenvironment of cells and organs *in vivo,* which grow three dimensionally (Imamura *et al.,* 2015). Furthermore, using animals in research is now also ethically challenging (Festing & Wilkinson, 2007), requiring new and better high throughput *in vitro* models and assays for research such as drug biotransformation and cancer treatment screening (Gouws & Hamman, 2018). Recent studies have indicated that 3D cell culture models can bridge the resultant gap between *in vitro* and *in vivo* studies (Hoarau-Véchot *et al.,* 2018), and is therefore an ideal model for preclinical studies.

1.3. Problem statement

Patients from low-income communities are particularly at risk for the development of colorectal cancer. Colorectal cancer treatment usually involves both tumour ablation and treatment with well-established chemotherapeutic drugs. The latter is known to result in severe side effects, especially in the elderly, resulting in a loss of patient compliance. It is for this reason that the worldwide use of phytomedicines for the treatment of cancer is increasing. The cost of chemotherapeutic treatment in low-income communities also attributes to the higher level of alternative medicine use in these communities. These phytomedicines are also seen as “safe and natural”, although data concerning their pharmacokinetic profiles, safety and pharmacological activity in terms of cancer treatment are scarce. This is particularly true for plants indigenous to Africa.

Furthermore, these phytomedicines are frequently used concomitantly with prescribed medicines, often without the knowledge of the primary caregiver. This increases the likelihood of herb-drug interactions, which may have detrimental effects on treatment efficacy or toxicity. For this reason, the study of the potential effect of these phytomedicines on the CYP450 enzyme family is of utmost importance. Identifying any effects of these phytomedicines on the expression or activity of CYP450 will allow the prediction of potential pharmacokinetic interactions.

Although *in vitro* models such as 2D cell culture models and *in vivo* animal models have long served as the gold standard in preclinical drug discovery, these models are afflicted by various shortcomings and restrictions. Conventional cell culture models only provide limited information due to a lack of physiological relevance in terms of tumour complexity and architecture, while the use of animal models in research causes an ethical dilemma and still has interspecies differences. Therefore, it is clear that a need exists for new 3D screening models to study pharmacological activity and CYP450 expression and activity in the preclinical screening of African phytomedicines used to treat cancer.

1.4. General aim

The aim of this project is to validate a sodium alginate encapsulated 3D spheroid model of the LS180 colorectal cancer cell line as a potential model for drug biotransformation and anticancer activity screening of new compounds and phytomedicines.

1.5. Specific objectives

The specific objectives for the study are:

1. To optimise a 3D sodium alginate encapsulated, clinostat-based spheroid model of the LS180 cell line, and to characterise it in terms of cell viability (intracellular adenosine triphosphate (ATP), extracellular adenylate kinase (AK) and glucose consumption), growth (soluble protein content) and CYP3A4 and CYP2D6 expression (real-time polymerase chain reaction-based (qPCR) gene expression assay).
2. To determine the 50% inhibitory concentration (IC_{50}) of the selected African phytomedicines, *S. frutescens* and *X. undulatum* crude aqueous extracts, as well as a standard chemotherapeutic drug, paclitaxel, in the 2D LS180 cell model using the 3- (4,5- dimethylthiazol- 2- yl)- 2,5- diphenyltetrazolium bromide (MTT) assay.
3. To validate the use of the established 3D spheroid LS180 model for the *in vitro* screening of chemotherapeutic treatments for colorectal cancer, using the standard chemotherapeutic drug, paclitaxel, at concentrations based on the 2D IC_{50} concentrations.
4. To evaluate the anticancer treatment potential of crude aqueous extracts of *S. frutescens* and *X. undulatum* in the established *in vitro* 3D LS180 model in terms of viability and growth, at concentrations based on the 2D IC_{50} concentrations.

5. To evaluate the effects of crude extracts of *S. frutescens* and *X. undulatum* on CYP3A4 and CYP2D6 gene expression in the 3D LS180 model.

A flow diagram depicting the experimental approach of the study to address these objectives is presented in **Figure 1.1**.

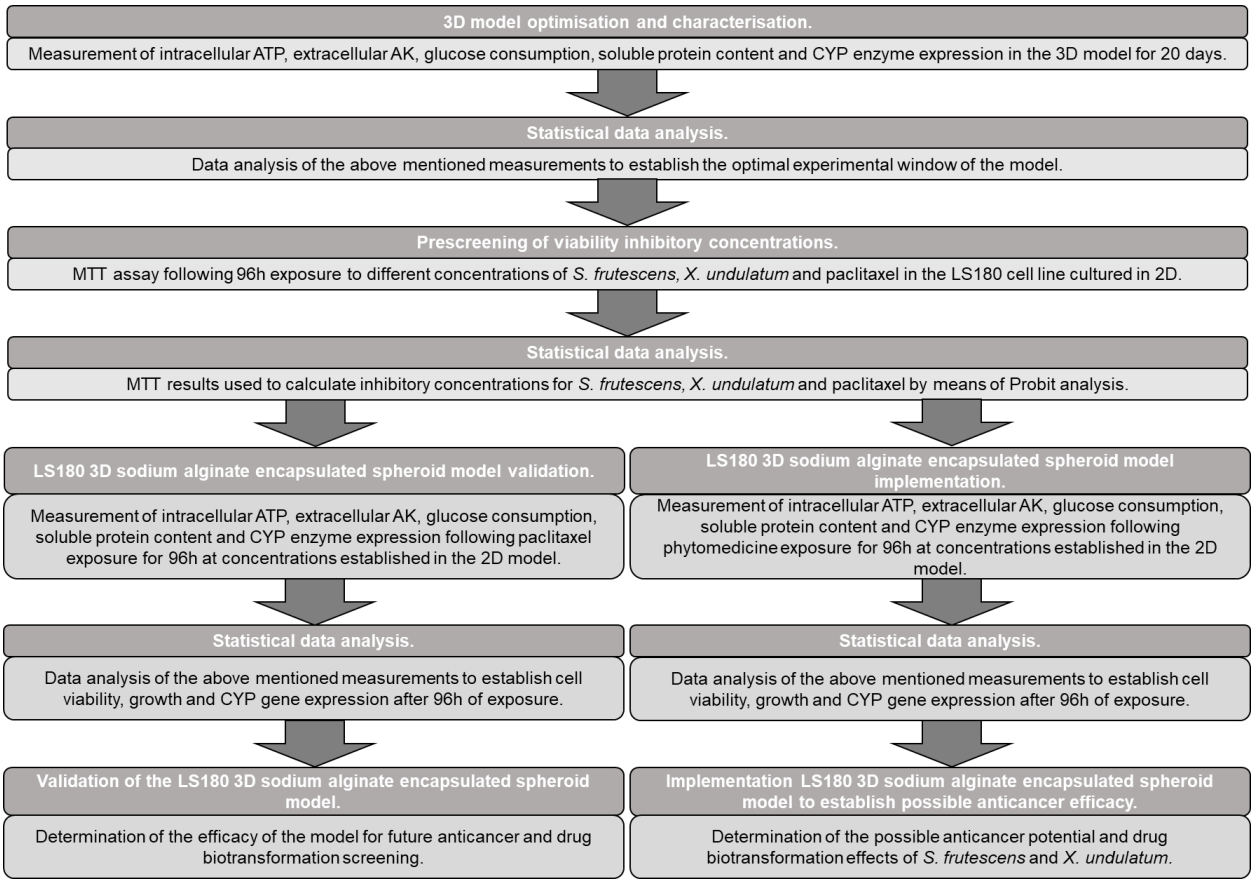

Figure 1.1: A flow diagram depicting the experimental aspects of the study.

1.6. Chapter layout of dissertation

This dissertation is a compilation of chapters consisting of the following:

Chapter 1 presents the background, justification, problem statement, general aim, specific objectives and chapter layout for this study. An experimental approach is illustrated and finally the publication status of the research, with the specific contributions of the authors are given.

Chapter 2 consists of a literature review, providing an overview of cancer, specifically colorectal carcinoma, and the traditional use of African phytomedicine in the treatment thereof. Furthermore, this literature review will also consider drug biotransformation in the context of African phytomedicine use. To this extent, the importance of *in vitro* cell culture models in studying cancer treatment and drug biotransformation will be discussed, with the specific focus on current 2D and novel 3D cell culture models for these applications.

Chapter 3 describes all materials and methods used during this study. This includes: basic cell culturing and cell seeding, the MTT assay, optimisation and characterisation of the 3D sodium alginate encapsulated spheroid model, as well as validation and implementation of the model.

Chapter 4 presents the results and discussion following the preliminary anticancer activity screening with the MTT assay, as well as the optimisation and characterisation of the LS180 3D sodium alginate encapsulated spheroid model, validation of this model for anticancer treatment screening, induction of the CYP450 enzyme family and, finally, implementation of the model to evaluate the potential use of *S. frutescens* and *X. undulatum* in the treatment of colorectal cancer.

Chapter 5 presents concluding remarks on the LS180 3D sodium alginate encapsulated spheroid model, its characterization and its validation for use in anticancer treatment screening and drug biotransformation evaluations. Furthermore, the potential use of *S. frutescence* and *X. undulatum* in the treatment of colorectal cancer is reflected on, and future recommendations are also presented.

References are included at the end of each individual chapter.

Appendix A includes the certificate of analysis of all plant material used during the study.

Appendix B includes the results of the liquid chromatography-mass spectrometry analysis done to characterise the *S. frutescens* extract.

Appendix C includes the results of the ultra-high pressure liquid chromatography (UPLC) analysis done to characterise the *X. undulatum* extract.

Appendix D includes the cell viability inhibition data following 96 h of exposure to different concentrations of paclitaxel on the LS180 cell line.

Appendix E includes the cell viability inhibition data following 96 h of exposure to different concentrations of *S. frutescens* extracts on the LS180 cell line.

Appendix F includes the cell viability inhibition data following 96 h of exposure to different concentrations of *X. undulatum* extracts on the LS180 cell line.

Appendix G includes the amplification data following real-time polymerase chain reaction-based gene expression assay (qRT-PCR) of the untreated control group, *S. frutescens* groups and *X. undulatum* groups.

1.7. Publication status of research

A manuscript emanating from the research has been accepted for publication in the journal *ACS Medical Chemistry Letters*.

The characterisation and validation of the LS180 sodium alginate encapsulated spheroid model was an extension of work by Calitz (2017).

- Smit, T., Calitz, C., Willers, C., Svitina, H., Hamman, J.H., Gouws, C. & Wrzesinksi, K. 2019. Characterisation of an alginate encapsulated LS180 spheroid model for anti-colorectal cancer compound screening. *ACS Medical Chemistry Letters*. Status: manuscript accepted.

Abstract:

Colorectal cancer is one of the leading causes of cancer-related deaths. A main problem for its treatment is resistance to chemotherapy, requiring the development of new drugs. The success rate of new candidate cancer drugs in clinical trials remains dismal. Three-dimensional (3D) cell culture models have been proposed to bridge the current gap between in vitro chemotherapeutic studies and the human in vivo, due to shortcomings in the physiological relevance of the commonly used two-dimensional cell culture models. In this study, LS180 colorectal cancer cells were cultured as 3D sodium alginate encapsulated spheroids in clinostat bioreactors. Growth and viability were evaluated for 20 days to determine the ideal experimental window. The 3- (4,5-dimethylthiazol- 2- yl)- 2,5- diphenyltetrazolium bromide assay was then used to establish half maximal inhibitory concentrations for the standard chemotherapeutic drug, paclitaxel. This concentration was used to further evaluate the established 3D model. During model characterization and evaluation soluble protein content, intracellular adenosine triphosphate levels, extracellular adenylate kinase, glucose consumption and P-glycoprotein (P-gp) gene expression were measured. Use of the model for chemotherapeutic treatment screening was evaluated using two concentrations of paclitaxel, and treatment continued for 96 h. Paclitaxel

caused a decrease in cell growth, viability and glucose consumption in the model. Furthermore, relative expression of P-gp increased compared to the untreated control group. This is a typical resistance-producing change, seen in vivo and known to be a result of paclitaxel treatment. It was concluded that the LS180 sodium alginate encapsulated spheroid model could be used for testing new chemotherapeutic compounds for colorectal cancer.

Author Contributions: conceptualization, Prof C Gouws and Prof K Wrzesinski; methodology, Prof K Wrzesinski, Dr C Calitz, Miss T Smit and Dr H Svitina; validation, Miss T Smit, Dr C Willers and Dr H Svitina; formal analysis, Miss T Smit and Dr H Svitina; investigation, Miss T Smit, Dr C Calitz, Dr C Willers and Dr H Svitina; resources, Prof JH Hamman, Prof C Gouws and Prof K Wrzesinski; data curation, Miss T Smit, Dr H Svitina, Prof C Gouws and Prof K Wrzesinski; writing—original draft preparation, Miss T Smit and Dr C Calitz; writing—review and editing, Dr C Willers, Prof JH Hamman, Prof C Gouws and Prof K Wrzesinski; visualization, Miss T Smit, Dr C Calitz and Dr H Svitina; supervision, Prof JH Hamman, Prof C Gouws and Prof K Wrzesinski; project administration, Prof C Gouws ; funding acquisition, Prof C Gouws and Prof K Wrzesinski.

The method development and the validation results were also presented at the 3rd CellFit Annual Meeting, 10-12 October 2019, in Athens, Greece by Prof C Gouws. CellFit is a European network of excellence (COST Action CA16119), with competence on all levels within fundamental biology, bio-engineering as well as clinical research. CellFit aims to translate the present basic knowledge in cell control, cell repair and regeneration from the laboratory bench to the clinical application.

- Smit, T., Calitz, C., Willers, C., Thete, L., Hamman, J.H., Gouws, C. & Wrzesinski, K. 2019. *Developing a sodium alginate encapsulated three-dimensional colorectal cell spheroid model for biotransformation and anticancer activity evaluation*. The extracellular vesicles paradigm of intracellular communication, 10 – 12 October 2019, Athens, Greece.

Abstract:

The use of phytomedicines is popular worldwide for a wide variety of ailments because they are seen as "safe and natural", even though there is little concrete proof of their efficacy. The use of phytomedicines by cancer patients is common and increasing due to the belief that it has less

adverse effects in comparison to other treatments. The anticancer potential of these African phytomedicines have not been extensively studied, and there have been many discrepancies between their findings and clinical reports. Bioactive compounds could be medically efficacious, but in many instances these compounds are yet to be fully characterised, identified and validated. These bioactive compounds can potentially also interact with coadministered conventional drugs, which can cause serious side effects or decreased pharmacological efficacy of the coadministered drug. Phytomedicines may change the expression or activity of the human cytochrome P450 enzymes which may lead to phytomedicine-drug interactions.

To bridge the gap between in vitro studies and the human in vivo system, we developed a novel three-dimensional spheroid model to study colorectal cancer treatment and biotransformation. The LS180 cells were encapsulated in Sodium Alginate, and the subsequent spheroids maintained in bioreactors on a clinostat-based rotating drive unit for 42 days. Viability and growth of the spheroids were continually assessed through parameters such as intracellular adenosine triphosphate, extracellular adenylate kinase, glucose consumption and protein content. Metabolic equilibrium of the spheroid model was observed from 10 days, and the potential use of the model to evaluate anticancer activity was assessed through treatment with a standard chemotherapeutic drug and aqueous extracts of Sutherlandia frutescens and Xysmalobium undulatum for 4 days. The effect of these treatments on the gene expression of the CYP3A4 enzyme was determined and to confirm biotransformation activity in the model, metabolism of indinavir (known CYP3A4 substrate) was measured through LC-MS/MS.

References:

Amacher, D.E. 2010. The effects of cytochrome P450 induction by xenobiotics on endobiotic metabolism in pre-clinical safety studies. *Toxicology mechanisms and methods*, 20:159-166.

Aziz, M.A., Khan, A.H., Adnan, M. & Izatullah, I. 2017. Traditional uses of medicinal plants reported by the indigenous communities and local herbal practitioners of Bajaur Agency, federally administrated tribal areas, Pakistan. *Journal of ethnopharmacology*, 198:268-281.

Baskar, A.A., Al. Numair, K.S., Alsaif, M.A. & Ignacimuthu, S. 2012. *In vitro* antioxidant and antiproliferative potential of medicinal plants used in traditional Indian medicine to treat cancer. *Redox report*, 17:145-156.

Bo, L., Baosheng, Z., Yang, L., Mingmin, T., Beiran, L., Zhiqiang, L. & Huaqiang, Z. 2016. Herb-drug enzyme-mediated interactions and the associated experimental methods: a review. *Journal of traditional Chinese medicine*, 36:392-408.

Bonnier, F., Keating, M.E., Wrobel, T.P., Majzner, K., Baranska, M., Garcia-Munoz, A., Blanco, A. & Byrne, H.J. 2015. Cell viability assessment using the Alamar blue assay: a comparison of 2D and 3D cell culture models. *Toxicology in vitro*, 29:124-131.

Brenner, H., Hoffmeister, M., Stegmaier, C., Brenner, G., Altenhofen, L. & Haug, U. 2007. Risk of progression of advanced adenomas to colorectal cancer by age and sex: estimates based on 840 149 screening colonoscopies. *Gut*, 56:1585-1589.

Calitz, C. 2017. Establishing three-dimensional cell culture models to measure biotransformation and toxicity. Potchefstroom:NWU. (Thesis- PhD).

Carr, C., Ng, J. & Wigmore, T. 2008. The side effects of chemotherapeutic agents. *Current anaesthesia & critical care*, 19:70-79.

Chinkwo, K.A. 2005. *Sutherlandia frutescens* extracts can induce apoptosis in cultured carcinoma cells. *Journal of ethnopharmacology*, 98:163-170.

Festing, S. & Wilkinson, R. 2007. The ethics of animal research. *European molecular biology organization (EMBO) reports*, 8:526-530.

Fouché, G., Khorombi, T.E., Kolesnikova, N.I., Maharaj, V.J., Nthambeleni, R. & Van der Merwe, M.R. 2006. Investigation of South African plants for anticancer properties. *Pharmacology online*, 3:494-500.

Gouws, C. & Hamman, J.H. 2018. Recent developments in our understanding of the implications of traditional African medicine on drug metabolism. *Expert opinion on drug metabolism & toxicology*, 14:161-168.

Haggar, F.A. & Boushey, R.P. 2009. Colorectal cancer epidemiology: incidence, mortality, survival, and risk factors. *Clinics in colon and rectal surgery*, 22:191-197.

Hoarau-Véchot, J., Rafii, A., Touboul, C. & Pasquier, J. 2018. Halfway between 2D and animal models: are 3D cultures the ideal tool to study cancer-microenvironment interactions? *International journal of molecular sciences*, 19:181-205.

Hurria, A., Togawa, K., Mohile, S.G., Owusu, C., Klepin, H.D., Gross, C.P., Lichtman, S.M., Gajra, A., Bhatia, S., Katheria, V. & Klapper, S. 2011. Predicting chemotherapy toxicity in older adults with cancer: a prospective multicenter study. *Journal of clinical oncology*, 29:3457-3465.

Imamura, Y., Mukohara, T., Shimono, Y., Funakoshi, Y., Chayahara, N., Toyoda, M., Kiyota, N., Takao, S., Kono, S., Nakatsura, T. & Minami, H. 2015. Comparison of 2D-and 3D- culture models as drug-testing platforms in breast cancer. *Oncology reports*, 33:1837- 1843.

Jaroch, K., Jaroch, A. & Bojkoa, B. 2018. Cell cultures in drug discovery and development: The need of reliable *in vitro* - *in vivo* extrapolation for pharmacodynamics and pharmacokinetics assessment. *Journal of pharmaceutical and biomedical analysis*, 147:297-312.

Krishna, A.B., Manikyam, H.K., Sharma, V.K. & Sharma, N. 2015. Plant cardenolides in therapeutics. *International journal of indigenous medicinal plants*, 48:1871-1896.

Mishra, J., Drummond, J., Quazi, S.H., Karanki, S.S., Shaw, J.J., Chen, B. & Kumar, N. 2013. Prospective of colon cancer treatments and scope for combinatorial approach to enhanced cancer cell apoptosis. *Critical reviews in oncology/hematology*, 86:232-250.

Neuwinger, H.D. 2000. African traditional medicine: A dictionary of plant use and applications. Stuttgart: Medpharm Scientific Publishers.

Oga, E.F., Sekine, S., Shitara, Y. & Horie, T. 2016. Pharmacokinetic herb-drug interactions: insight into mechanisms and consequences. *European journal of drug metabolism and pharmacokinetics*, 41:93-108.

Saeidnia, S., Manayi, A. & Abdollahi, M. 2015. From *in vitro* experiments to *in vivo* and clinical studies; pros and cons. *Current drug discovery technologies*, 12:218-224.

Simmonds, P.C. 2000. Palliative chemotherapy for advanced colorectal cancer: systematic review and meta-analysis. *Colorectal cancer collaborative group*, 321: 531-535.

Vermaak, I., Enslin, G.M., Idowu, T.O. & Viljoen, A.M. 2014. *Xysmalobium undulatum* (uzara) – review of an antidiarrhoeal traditional medicine. *Journal of ethnopharmacology*, 156:135-146.

Van Wyk, B.E. 1997. Medicinal Plants of South Africa. Pretoria: Briza Publishers.

Van Wyk, B.E. 2011. The potential of South African plants in the development of new medicinal products. *South African journal of botany*, 77:812-829.

Wong, C.H., Siah, K.W. & Lo, A.W. 2019. Estimation of clinical trial success rates and related parameters. *Biostatistics*, 20:273-286.

World Health Organization (WHO). 12 Sep. 2018. Cancer fact sheet. http://www.who.int/en/news-room/fact-sheets/detail/cancer Date of access: 6 February 2019.

Wrzesinski, K., Rogowska-Wrzesinska, A., Kanlaya, R., Borkowski, K., Schwämmle, V., Dai, J., Joensen, K.E., Wojdyla, K., Carvalho, V.B. & Fey, S.J. 2014. The cultural divide: exponential growth in classical 2D and metabolic equilibrium in 3D environments. *PloS one*, 9:e106973.

Zhang, D., Luo, G., Ding, X. & Lu, C. 2012. Preclinical experimental models of drug metabolism and disposition in drug discovery and development. *Acta pharmaceutica sinica B*., 2:549-561.

CHAPTER 2

This chapter consists of a literature review, providing an overview of cancer, specifically colorectal carcinoma, and the traditional use of African phytomedicine in the treatment thereof. Furthermore, this literature review will also consider drug biotransformation in the context of African phytomedicine use. To this extent, the importance of *in vitro* cell culture models in studying cancer treatment and drug biotransformation will be discussed, with the specific focus on current two-dimensional and novel three-dimensional cell culture models for these applications.

2.1. Introduction

The use of animals in research has become frowned upon, with institutions such as the United States Environmental Protection Agency going as far as to announce a deadline of 2035 for the elimination of animal research (Grimm, 2019). The implementation of the 3 “R’s” (Reduction, Replacement and Refinement) through development of *in silico* or *in vitro* assays has therefore become an essential element of risk assessment (Jaroch *et al*., 2018). During drug biotransformation studies primary cultured hepatocytes, liver slices and microsomes are valuable *in vitro* models. Their use, however, is hindered by the scarcity of suitable human liver samples. Different cell line models have therefore been proposed for drug metabolism screening to overcome some screening limitations in recent years (Donato *et al*., 2008). The use of *in vitro* systems such as cell lines makes it possible to estimate the *in vivo* pharmacokinetic response with relatively good correlation (Jaroch *et al*., 2018).

Tumour-derived cell lines are also often used as models in cancer research. Nonetheless, these cell-lines carry millions of deviations from the tumours from which they originated (Goodspeed *et al*., 2016). Since the burden of cancer remains substantial, especially in Africa, finding new anticancer drugs is still crucial in drug discovery and development. Investigating the potential activity, pharmacological and toxicological effects of these new drugs are some of the useful applications of *in vitro* models (Saeidnia *et al*., 2015).

2.2. Cancer

Cancers are diseases in which continuously dividing somatic cells kill by invading, subverting and eroding the normal surrounding tissues (Evan & Vousden, 2001). Mitosis is a process through which most of the normal cells in our bodies replicate. When there are enough cells, they stop growing through various processes, such as contact inhibition (Kalyanaraman, 2017). When a normal cell proliferates uncontrollably, it can cause genetic instabilities and alterations can accumulate within the cell which transforms a normal cell into a malignant cell (Iqbal *et al.,* 2017). When cells become malignant they divide continuously without any signalling response for apoptosis.

Cancer has various aetiologies and multiple stages induced by the deregulation of genetic and epigenetic programming. This can happen due to factors such as infections, chemical carcinogenesis and hormonal perturbation, to name a few (Schuster-Bockler & Lehner, 2012; Supek & Lehner, 2015; Wynendaele *et al*., 2015; Bouyahya *et al*., 2018). The incidence and

behaviour of specific types of cancers are also related to numerous factors, including sex, age, race, genetic disposition, as well as exposure to environmental carcinogens. Of all the factors mentioned environmental exposure is probably the most important, with constant human exposure to deoxyribonucleic acid (DNA)-damaging agents (Kastan & Bartek, 2004; Katzung *et al*., 2012). Although various types of cancer forms exist in humans, lung, breast and colorectal cancers are most common (Ferlay *et al*., 2010).

2.2.1. Colorectal cancer

In 2018, cancer was responsible for an estimated 9.6 million deaths worldwide. Of these deaths, approximately 70% occurred in low- and middle-income countries (WHO, 2018). Colorectal cancer is the most common type of gastrointestinal malignancy and nearly 145 000 new cases are reported annually in the United States of America (Katzung *et al*., 2012). Colorectal cancer begins as a benign adenomatous polyp, which then develops into an advanced adenoma with high-grade dysplasia and lastly progresses to an invasive cancer (Markowitz & Bertagnolli, 2009). Although some types of cancers are preventable, colon cancer is often detected only in its advanced stages when symptoms become apparent (Mishra *et al*., 2013). Some of these symptoms include rectal bleeding, diarrhoea or constipation (changes in bowel habit), loss of weight, abdominal pain and anaemia (Hamilton & Sharp, 2004). These symptoms are, however, also common with some benign conditions and the clinician must decide which patients are at higher risk and warrant further investigation (Astin *et al*., 2011). One of the main problems for the treatment of colorectal cancer is the development of resistance to chemotherapy and the disease progression to metastatic cancer (Naghibalhossaini *et al*., 2017).

Various risk factors for colorectal cancer exist. Some of these risk factors are non-modifiable, such as age, and the likelihood of colorectal cancer increases after the age of 40. A personal history with inflammatory bowel disease (Crohn's disease and/or ulcerative colitis) is also a risk factor as these inflammatory conditions increase the individual's overall risk of developing cancer. Furthermore, family history is a risk factor as up to 20% of patients with colorectal cancer has a family history of the disease with approximately 5-10% being a consequence of recognized hereditary conditions (Haggar & Boushey, 2009).

2.2.2. Current treatment options for colorectal cancer

Several options are available for treating cancer through surgery, chemotherapy, radiation

therapy, immunotherapy and nutritional support therapy (Mishra *et al*., 2013). The treatment method, however, is dependent on the location and the stage of the tumour (Singh *et al*., 2016). Chemotherapy is often used in combination with other treatments, and it is also common for different classes of chemotherapeutic drugs to be combined. Some of these classes include: alkylating agents, antimetabolites, plant alkaloids, cytotoxic antibodies and platinum compounds (Katzung *et al.* 2012). Chemotherapy is currently used in three main clinical settings, the first being primary induction chemotherapy where chemotherapy is the primary treatment. Secondly, as neoadjuvant chemotherapy for patients with localized cancer and for which local therapies exist, but they are not completely effective. Lastly, as adjuvant chemotherapy to local treatment modalities, such as surgery or radiation therapy (Katzung *et al.* 2012).

Over the past few decades, literature has emphasised the relevance of cell cycle deregulation in cancer (Malumbres & Barbacid, 2009). The cell cycle is a sequential routine in which cells reproduce by replication of DNA, followed by division of the nucleus and separation of the cytoplasm to yield two daughter cells (Massagué, 2004). The cell cycle is controlled by numerous mechanisms ensuring that correct cell division takes place (Vermeulen *et al*., 2003). Various chemotherapeutic agents target specific phases in the cell cycle and are known as cell cycle-specific agents, but cell cycle-nonspecific agents are also used clinically as shown in **Table 2.1** (Katzung *et al*., 2012).

Table 2.1. Two major classes of anticancer agents and their cell cycle effects (Katzung *et al*., 2012)

Cell Cycle-Specific Agents	**Cell Cycle-Nonspecific Agents**
Antimetabolites targeting the S-Phase	**Alkylating agents**
Capecitabine	Altretamine
Cladribine	Bendamustine
Clofarabine	Busulfan
Cytarabine (ara-C)	Carmustine
Fludarabine	Chlorambucil
5-Fluorouracil (5-FU)	Cyclophosphamine

Cell Cycle-Specific Agents	Cell Cycle-Nonspecific Agents
Gemcitabine	Dacarbazine
6-Mercaptopurine (6-MP)	Lomustine
Methotrexate (MTX)	Mechlorethamine
Nelarabine	Melphalan
Pralatrexate	Temozolomide
6-Thioguanine (6-TG)	Thiotepa
Epipodophyllotoxin (topoisomerase II inhibitor) targeting the G_1 and S-Phase	**Antitumor antibiotics**
Etoposide	Dactinomycin
Taxanes targeting the M-Phase	Mitomycin
Albumin-bound paclitaxel	**Camptothecins (Topoisomerase I inhibitors)**
Cabazitaxel	Irinotecan
Paclitaxel	Topotecan
Vinca alkaloids targeting the M-Phase	**Platinum analogues**
Vinblastine	Carboplatin
Vincristine	Cisplatin
Vinorelbine	Oxaplatin
Antimicrotubule inhibitor targeting the M-Phase	**Anthracyclines**
Ixabepilone	Daunorubicin
Antitumor antibiotics targeting G_2 and M-Phase	Doxorubicin
Bleomycin	Epirubicin
	Idarubicin
	Mitoxantrone

According to Simmonds (2000) there is no universally accepted standard therapy for colorectal cancer, and the route of administration and the duration of the treatment varies extensively. To identify the best treatment strategy for a patient with metastatic colorectal cancer, the staging should include at least clinical examination, blood counts, liver adrenal testing and a computerized tomography scan of the abdomen and chest (Van Cutsem *et al*., 2014). But, according to the same source, the backbone of first-line treatment chemotherapy, alone or in combination, consists of a fluoropyrimidine (like fluorouracil) in various combinations and schedules. Other first-line treatments can include fluorouracil with leucovorin and irinotecan, or oxaliplatin alone or in combination with bevacizumab (Van Cutsem *et al*., 2009).

Paclitaxel is an anticancer agent that acts by disrupting cell functions by stabilization of microtubules, which consequently leads to apoptosis (Koziara *et al*., 2006). Combination of 5-fluorouracil together with paclitaxel is an attractive approach as this ads cell-killing by means of apoptosis to the radio-sensitization action of 5-fluorouracil. Paclitaxel thus exerts its cytotoxic effects through different mechanisms as 5-fluorouracil, and has no cross-resistance with it (Kennedy *et al*., 2000).

2.3. Traditional use of phytomedicines

For many centuries, medicines derived from plants have been the principal agents used in primary health care (Sheeja *et al*., 2006; Fasinu *et al.,* 2012). Although it is difficult to get exact estimates, it has been proposed that 60 to 85% of native Africans use herbal medicines, many of these in combination with other prescribed drugs (Van Wyk *et al.,* 2009). This may be because of the common misconception that herbal remedies are safe and harmless because of their “natural” origin (Cohen & Ernst, 2010). Traditional African medicines are also believed to be useful in a wide variety of ailments and disorders, including cancer, human immunodeficiency virus/acquired immunodeficiency syndrome (HIV/AIDS), diabetes, depression, deep vein thrombosis, headaches and many more. Phytomedicines contain bioactive compounds which are believed to be medically efficacious, but in many instances these bioactive compounds are yet to be fully characterised, identified and validated (Sasidharan *et al*., 2011). South Africa, like many developing countries, has no official herbal pharmacopoeia providing monographs of indigenous medicinal plants, and this industry is also very poorly regulated (Patel *et al.,* 2010). There are approximately 3 000 plants used in traditional healing practices in South Africa (Van Wyk *et al*., 2009). This enormous diversity represents a very valuable resource for not only commercial development, but also for basic scientific study (Van Wyk, 2008). According to the World Health

Organisation (WHO) (2013) there is a great and urgent need for further research into African phytomedicines, as they are continuously consumed without concrete proof of their safety and efficacy. The WHO also indicated in their Regional Strategy for Traditional Medicine in the Western Pacific (2011–2020), that one of the key strategic objectives for 2011-2020 is to include traditional medicine in the national healthcare system (WHO, 2012).

South Africa has made significant progress to integrate traditional and complementary medicine into the legislative framework for healthcare practitioners. It is estimated that approximately 25 000 traditional and complementary medicines have been submitted to the Medicines Control Council to facilitate the implementation of the Accelerated Registration Programme (Gqaleni *et al*., 2007).

2.3.1. Phytomedicine use in cancer therapy

Complementary and alternative medicine is used by one third to half of cancer patients throughout the world (Jermini *et al*., 2019). It is also interesting to know that when oncologists discuss treatment options for patients, an interest in the use of complementary and alternative medicine has grown together with questions about its use in cancer treatment (Lee *et al*., 2014). Phytomedicine use is common and increasing; this is due to the belief that it can improve cancer related symptoms, kill the tumour cells and have less adverse effects in comparison to other treatments (Oga *et al.,* 2016). Due to the high morbidity and mortality rate of cancer, there has been an increased scientific interest in the discovery of anticancer agents from natural sources (Kaur *et al.,* 2018). Numerous plants and their phytochemicals have been shown to have the potential to inhibit development and progression of cancer (Aung *et al.*, 2017; Iqbal *et al*., 2017). Colchicine, podophyllotoxin, taxol, vinblastine and vincristine are anticancer drugs derived from plants (Singh *et al.*, 2016). According to Wang *et al*. (2007), three saponins isolated from *P. ginseng* were found to effectively inhibit cell proliferation of glioma, pancreatic, breast, prostate and lung cancer cells. *Allium sativum*, more commonly known as garlic, contains a manganese superoxide dismutase that has inhibitory effects on the growth of porcine endothelial cells, as well as B16 mouse melanoma cells *in vitro* (Sfaxi *et al*., 2009). The twigs and leaves of *Larrea tridentana*, otherwise known as chaparral, can be used as an anticancer agent but must rather be avoided due to its severe hepatotoxicity (Katzung *et al.*, 2012). Various South African medicinal plants are used by traditional healers to treat cancer and its symptoms including *Bidens pilosa*, *Centella asiatica*, *Cnicus benedictus*, *Sutherlandia frutescens*, *Hypoxis hemerocallidea* and *Solanum aculeastrum* (Maness *et al*., 2012).

2.3.2. Phytomedicine-drug interactions

Phytomedicines contain many bioactive compounds that can potentially interact with co-administered conventional drugs, and this can cause serious side effects or affect pharmacological efficacy of the co-administered drug (Negi *et al*., 2008). In phytomedicine-drug pharmacokinetic interactions the cytochrome P450 (CYP450) enzymes and the efflux transporter, P-glycoprotein (P-gp), have been shown to play a central role. More than half of ingested phytomedicines are likely to interact with the CYP450 enzyme family, responsible for metabolising many medications (Bo *et al*., 2016). The most recognised phytomedicine-drug interaction associated with CYP450 enzymes are that of St. John's wort. When co-administered with conventional drugs, St. John's wort may render many medications less effective, and the consequences may be severe (Gurley *et al*., 2008).

The risk of phytomedicine-drug interactions is increasing and this public health problem can be accompanied by life-threatening adverse drug events, prolonged hospitalization and even death (Ekor, 2014; Awortwe *et al*., 2018). Some of the most frequent reactions include allergic reactions, gastrointestinal problems and in severe cases hepatotoxicity, neurotoxicity and nephrotoxicity (Jermini *et al*., 2019). An accurate estimate of the prevalence of herbal products used concomitantly with conventional drugs are difficult, as consumers of herbal products seldom inform their healthcare practitioners (Gardiner *et al*., 2006; Brantley *et al*., 2014).

In a study by Yates *et al*. (2005) it was indicated that 90% of the cancer patients surveyed used at least one form of complementary and alternative medicine and 80% were using between one and four during their cancer treatment. In a study conducted by Ramos-Esquivel *et al*. (2017) they indicated that a possible 122 phytomedicine-drug interactions were detected among 75 patients accounting for 50.3% of the entire sample population. For the purpose of this study, only the potential effects of interactions on drug metabolism will be discussed in depth.

2.4. Drug biotransformation

Drug metabolism or drug biotransformation is defined as the process by which a drug is chemically converted in the body to metabolites, and this is usually through an enzymatic process (Shargel *et al*., 2012). Various routes of administration are used in clinical medicine. The use of each route is effected by convenience (e.g. oral), to maximize the concentration at the site of action and minimize it elsewhere (e.g. topical), to prolong the duration of drug absorption (e.g. transdermal) or to avoid the first-pass metabolism effect (Katzung *et al*., 2012). The rapid

metabolism of orally administered drugs before reaching the systemic circulation is termed the first-pass effect or pre-systemic elimination. Some routes of administration, such as intravenous and transdermal may, however, cause drug distribution within the body prior to first-pass metabolism by the liver (Shargel *et al*., 2012). After an oral drug is absorbed in the intestines it is transported via the portal circulation to the liver, where it will be subject to hepatic first-pass metabolism. This biotransformation of the drug is one of the most important factors that can influence the overall therapeutic and toxicity profile of a drug, as it can directly affect bioavailability (Brandon *et al.,* 2003). During drug metabolism the parent drug will undergo phase I oxidation, followed by phase II conjugation (Yan & Cardwell, 2001).

A key step in the metabolism process is catalysed by the CYP450 enzyme family (Coon *et al.*, 1992; Brandon *et al.*, 2003; Lübberstedt *et al*., 2011). Phytomedicines have multiple components and modes of action, which may change the expression or activity of the human CYP450 enzymes and may potentially lead to herb-drug interactions (Zadoyan & Fuhr, 2012).

2.4.1. Cytochrome P450 enzyme family

The CYP450 family are key enzymes in phase I oxidation, and can be divided into families and sub-families based on their nucleotide sequence homology, with each family having a high degree of substrate specificity (Li, 2001; Fasinu *et al*., 2012). The CYP1, 2 and 3 families are responsible for the metabolism of most foreign substances (xenobiotics), including 70 - 80% of drugs in clinical use (Zanger & Schwab, 2013). CYP3A4 is the most abundant of these enzymes, and metabolises more than 60% of prescribed drugs in the human body. The CYP2D6 enzyme is also of great importance in drug metabolism, since 20 - 25% of commercially used drugs are metabolised by this enzyme (Ingelman-Sundberg, 2005).

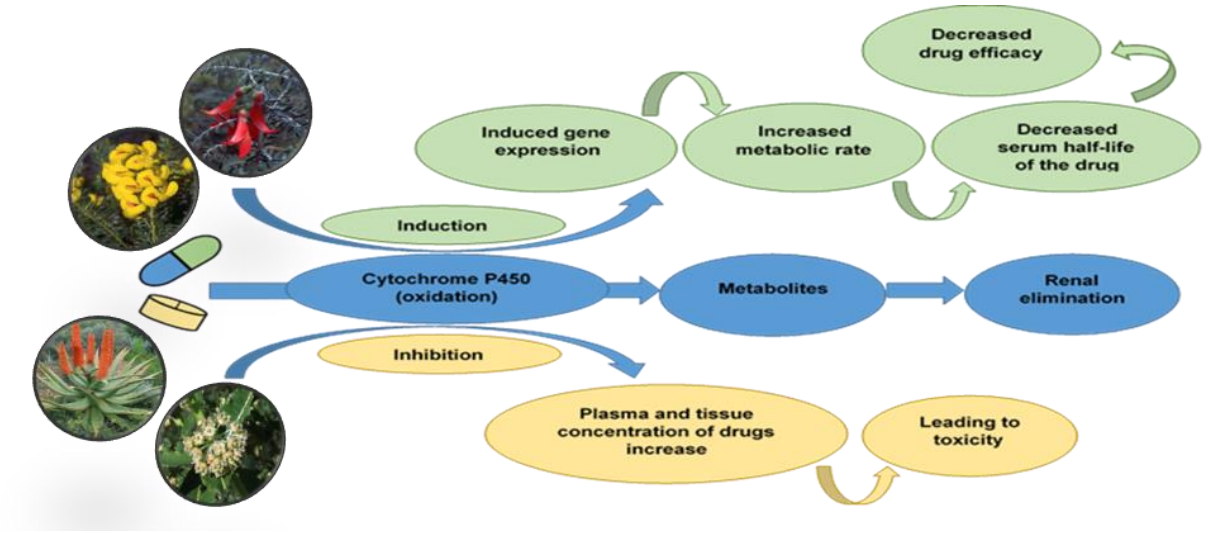

Figure 2.1. Cytochrome P450 interactions and their potential effects on dug bioavailability and toxicity (Van Wyk, 2008; Mukherjee *et al.,* 2011)

Induction or inhibition of CYP450 expression or activity by phytoconstituents can subsequently increase or decrease the bioavailability or efficacy of co-administered substrates, as can be seen in **Figure 2.1** (Minocha *et al*., 2011). After repeated administration of a xenobiotic, CYP induction can occur by increasing the rate of enzyme synthesis. CYP enzyme inhibition can occur by physical blocking of the CYP enzyme activity (Mukherjee *et al.,* 2011).

2.4.2. Cytochrome P450 gene expression

CYP450 enzymes are found in almost all human tissues, as illustrated in **Figure 2.2**. The highest abundance and largest number of individual CYP isoforms are found in the liver, the main site of detoxification in the body (Pelkonen *et al.,* 2008). The CYP isoforms most expressed in the liver are CYP3A4, 2C9, 2C8, 2E1 and 1A2, followed by CYP2A6, 2D6, 2B6, 2C19 and 3A5 which are less ample, but still of importance. Some CYPs are expressed only extrahepatically (CYP2J2, 1A1 and 1B1) (Zanger & Schwab, 2013). The pregnane X receptor (PXR) is part of the nuclear receptor superfamily of ligand-activated transcription factors. PXR is one of the receptors that regulate the expression of phase I and phase II xenobiotic metabolising enzymes and transporters (Moon & Gwak, 2015), and this is also one of the sites of action where substances such as phytochemicals may influence CYP450 levels through induction or attenuation.

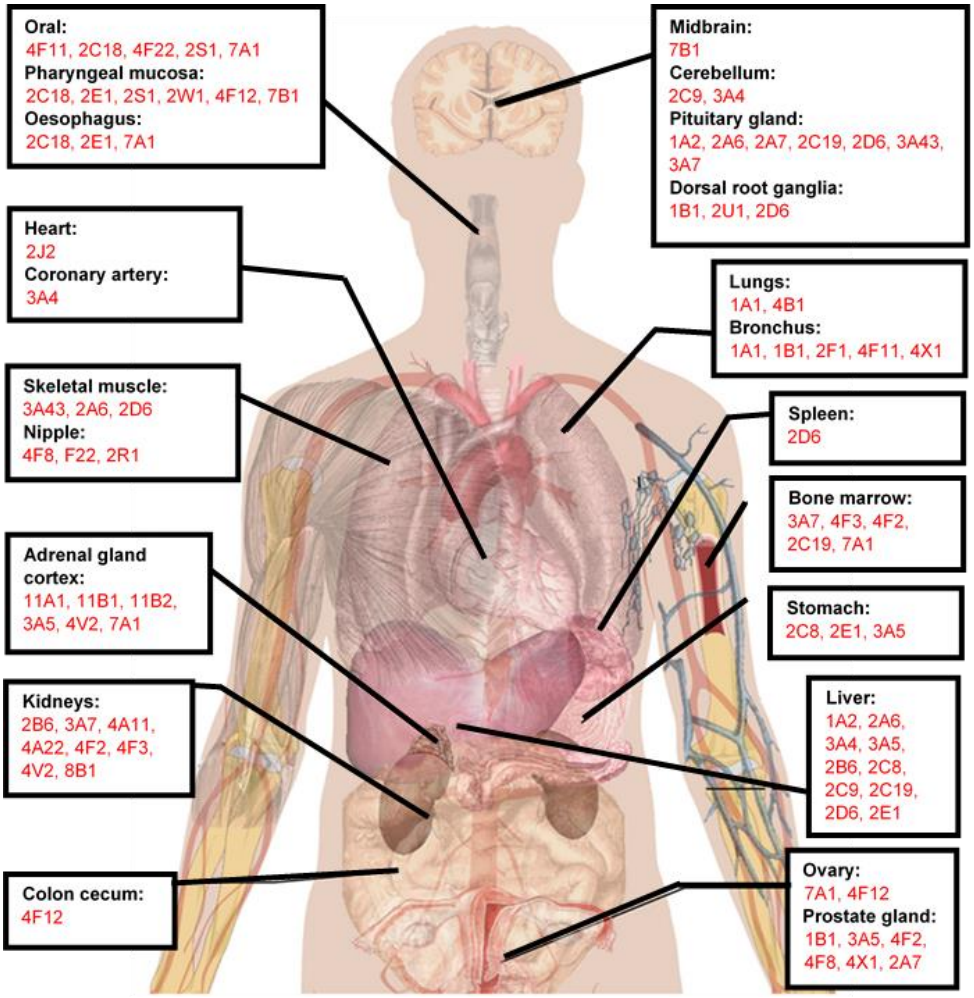

Figure 2.2. A body map of cytochrome P450 enzyme expression (image adapted from Preissner *et al.,* 2013).

Levels of CYP450 expression may differ from person to person, influenced mainly by the following factors (Zanger & Schwab, 2013):

- **Genetic polymorphisms**

  A genetic polymorphism is a discontinuous genetic variation, resulting in the occurrence of several different types of individuals amongst members of a single species (Encyclopaedia Britannica, 1998). The metabolic enzyme capacity of CYPs are not equal in all members of a population, thus the metabolic conversion and excretion rates of drugs can vary between individuals (Van der Weide & Steijns, 1999). This inter-individual variability can be translated into four major phenotypes: extensive metabolisers having high activity, poor metabolisers

lacking enzyme activity, intermediate metabolisers having normal activity and ultra-rapid metabolisers having more than two genes encoding active enzymes (Ingelman-Sundberg, 2004).

- **Epigenetic alterations**

Epigenetics is the study of the chemical modification of specific genes or gene-associated proteins of an organism (Encyclopaedia Britannica, 2017). The term epigenetics were invented to describe the occurrence of heritable changes in gene function that are not based on DNA sequence variations (Zanger & Schwab, 2013). These alterations include DNA methylation and post-transcriptional alterations of the histones involved in the packaging of the DNA strand (Rodriguez-Antona *et al.,* 2010). These alterations can result in changes in expression and translation of the CYP enzymes.

- **Non-genetic host factors**

According to Zanger & Schwab (2013), sex, age and disease state are three key, non-genetic host factors that play a vital role in CYP expression and function in individuals. If we take age for example; CYP1A2, CYP2B6, CYP2C19, CYP2D6 and CYP2E1 activity appears to decrease with age, whereas CYP2A6 and CYP4A11 activity appears to increase with age (Parkinson *et al.,* 2004).

2.4.2.1. Induction and attenuation of cytochrome P450 gene expression

Gene expression of CYP450 can be induced via activation of members of the nuclear receptor super-family, which includes PXR (Amacher, 2010). CYP enzyme induction is usually the result of an increase in gene transcription, but some nontranscriptional mechanisms are also known to be involved (Lin & Lu, 1998). Nuclear receptor activation will then result in an increased amount of CYP450 messenger ribonucleic acid (mRNA) which, after translation, will result in increased enzyme levels. More enzyme will, in turn, lead to faster oxidation and clearance of the substrate drugs (Bibi, 2008).

In drug therapy there are two possible consequences following CYP450 induction. The first being a reduction in the pharmacological effect of the drug, caused by an increase in drug metabolism which effectively removes the drug from circulation. Secondly, the induction process may create an undesirable imbalance between “toxification” and “detoxification” (Lin & Lu, 1998). A wide variety of CYP3A4 inducers are known, including carbamazepine, phenobarbital, phenytoin,

rifampicin, ritonavir, St. John's wort, etc. (Pelkonen *et al.,* 2008). According to the Flockhart Table™, rifampicin and dexamethasone are clinically important inducers of the CYP2D6 enzyme (Flockhart, 2007).

Attenuation or downregulation of gene expression will work exactly opposite to induction, primarily resulting in decreased levels of the associated enzymes and therefore reduced removal of substrate drugs from the circulation. Attenuation is, however, not a frequent result of exposure to phytomedicines.

Induction and downregulation of gene expression is not an instant process, and can take anything from 48 hours, to two weeks.

2.4.3. Cytochrome P450 enzyme activity

Following oral administration, the concentration of the drug in circulation will decrease due to intestinal and hepatic metabolism by the CYP450 enzyme family (Pond & Tozer, 1984; Coon *et al.*, 1992; Brandon *et al.*, 2003; Lübberstedt *et al.,* 2011). The measure of activity of the relevant CYP enzymes present can greatly influence this rate of drug removal from the circulation, and lower activity will result in lower levels of metabolism.

2.4.3.1. Inhibition of cytochrome P450 activity

CYP450 inhibitors can block the metabolic activity of one or more CYP450 enzymes to various degrees, and some phytochemicals can also act as inhibitors of these enzymes (Lynch & Price, 2007). There are three mechanisms of CYP450 inhibition, namely competitive, non-competitive and mechanism-based inhibition (Bibi, 2008). These mechanisms can emerge as reversible or irreversible loss of activity (Yan & Caldwell, 2001).

- **Competitive inhibition**

  Competitive inhibition takes place when the "perpetrator" xenobiotic, including phytochemicals, binds to the active site of an enzyme and thereby prevents the "victim" drug from binding. For example, when two substrates of the same enzyme isoform are administered concomitantly, they may demonstrate competitive inhibition. The consequence is that a much higher dose of the "victim" drug is needed to compete for the binding sites available (Brantley *et al.,* 2014). In a recent study by Tsujimoto *et al.* (2017), the results suggested that cabbage, onion and green pepper juices may competitively inhibit CYP3A4

activity. Ciprofloxacin is also an example of a drug that causes competitive inhibition when given in combination with other xenobiotics (Pelkonen *et al.*, 2008).

- **Non-competitive inhibition**

When there is an enzyme interaction of a ligand at a site other than the substrate-binding site, the result will be non-competitive inhibition (De Montellano, 2015). This binding affects the structure of the enzyme, and therefore alters the ability of the substrate to bind to the active site. Thus, increasing the concentration will not affect the degree of inhibition (White, 2016). Curcumin is an example of a phytomedicine which can cause non-competitive inhibition with respect to CYP2D6 and CYP2C9 (Appiah-Opong *et al.*, 2007).

- **Mechanism-based inhibition**

During mechanism-based inhibition the reactive intermediates are able to inactivate the CYP450 enzyme in three different ways. Firstly, through covalent adduction to an amino acid residue within the enzyme active site. Secondly, by arylation or alkylation of the prosthetic heme moiety. And lastly, via the destruction of the heme group, which leads to heme-derived products which forms cross-links with the CYP450 apoprotein (Zhou, 2008). There is a long list of known mechanism-based CYP3A4 inhibitors, including macrolide antibiotics, anti-HIV agents, antidepressants, calcium channel blockers, steroids and several herbal and dietary components (Zhou, 2008).

2.5. *Sutherlandia frutescens*

S. frutescens (also known as cancer bush) is a member of the pea family, indigenous to South Africa, Lesotho, South-Eastern Botswana and southern Namibia (Aboyade *et al.*, 2014). As shown in **Figure 2.3.**, it is a shrub with fine greyish green leaves and red, butterfly shaped flowers that is traditionally used by many South Africans to treat a variety of conditions (Tai *et al.*, 2004; Aboyade *et al.*, 2014). *S. frutescens* is one of the most reputable remedies consumed amongst patients living with HIV/AIDS in South Africa (Gericke, 2001), although it is traditionally claimed that *S. frutescens* can be used for almost any disease (Van Wyk, 2008). Some of these conditions include diabetes, internal cancers, stress, fever, wounds, appetite stimulant, HIV/AIDS, muscle wasting and countless more (Van Wyk & Albrecht, 2008). *S. frutescens* capsules commercially available contain 300 mg dried, powdered leaves and are recommended to be taken twice daily (Van Wyk & Albrecht, 2008). In an extensive toxicological screening study in a primate model using doses 9 times higher than the recommended dose of 9 mg/kg/day, no haematological,

clinical of physiological toxicity was indicated (Mills *et al*., 2005). According to Seier *et al*. (2002), the Medical Research Council of South Africa conducted a detailed safety study of *S. frutescens* showing no signs of toxicity in more than 50 parameters tested (Van Wyk, 2008). A clinical phase I study conducted by Johnson *et al*. (2007), found that 800 mg/day was well tolerated with no indication of toxicity.

Figure 2.3. Images of *Sutherlandia frutescens*. 1- Image of the entire plant; 2- Image of the flowers; 3- Image of the pods.

2.5.1. Traditional preparations and uses of *Sutherlandia frutescens*

The first records of its use came from Dutch colonist in the Cape, who most likely came to know of it through the local San and Khoi (Pappe, 1847). *S. frutescens* decoctions prepared by traditional healers can consist of various parts of the plant, including the flowers, stem, leaves and even the roots, depending on the medical need of the patient (Aboyade *et al*., 2014). Traditional healers will collect fresh plant material, dry them and then grind them into a powder using two stones. This preparation is usually infused in hot or boiling water, left to cool and then given to the patient (Aboyade *et al*., 2014). It is traditionally used as a tea or an aqueous extract (Vorster *et al*., 2012). Decoctions of the plant is used to wash wounds and eyes and to reduce fevers (Van Wyk & Van Staden, 2002). Infusions of the leaves and stems can be used to treat cancers, fever, diabetes, rheumatism, stomach ailments and kidney and liver problems (Thring & Weitz, 2006). *S. frutescens* is currently available in various dosage forms such as capsules,

tablets, gels, ointments and creams for topical application, as well as liquid extracts (Van Wyk & Albrecht, 2008).

2.5.2. Biologically active constituents of *Sutherlandia frutescens*

The pharmacological activity of *S. frutescens* may be due to the chemical composition of its leaves, containing the following active constituents: L-canavanine, L-arginine, hexadecenoic acid, pinitol, triterpenoid, saponins and γ-sitosterol (Leisching *et al.,* 2015). But it has been noted that the chemical and genetic makeup of *S. frutescens* vary across geographical areas (Van Wyk & Albrecht, 2008). Canavanine is a potent L-arganine antagonist and has documented anticancer activity (Crooks & Rosenthal, 1994; Swaffar *et al*., 1995). L-canavanine is a structural analogue of L-arganine and a natural insecticide. Because of its close similarity to arginine it can interfere with arginine metabolism, which leads to the formation of dysfunctional proteins (Mitri *et al*., 2009). L-canavanine has also been reported to have antiviral activity against influenza and retroviruses, thus its use in the treatment of HIV (Mills *et al*., 2005). Another constituent, D-pinitol has also been suggested for the treatment of wasting in cancer and AIDS patients, although the evidence thereof is scant (Mills *et al*., 2005). Pinitol has been claimed to have an insulin-like action by improving glycaemic control and stimulation of glucose uptake, and is therefore used in the treatment of diabetes (Aboyade *et al*., 2014). The triterpenoids identified in *S. frutescens* are SU1 and SU2. These compounds are known to have biological activity and are used against bacteria, fungi and viruses. The mode of actions of these compounds are, however, still unknown (Ifeanyi, 2009).

2.5.3. *Sutherlandia frutescens* in the treatment of cancer

The long-standing traditional claims that *S. frutescens* possesses anticancer properties have been partially validated (Stander *et al*., 2009). According to Stander *et al*. (2009) a *S. frutescens* aqueous extract of 10 mg/ml demonstrated a reduction in cell viability in a human breast adenocarcinoma cell line (MCF-7) and in a human non-tumorigenic epithelial mammary gland cell line (MCF-12A) following 72 hours of exposure. It was also reported that *S. frutescens* can be beneficial in cancer treatment as it can induce cytotoxicity (Chinkwo, 2005). Tai *et al*. (2004) and Reid *et al*. (2006) also reported that *S. frutescens* has anticancer and anti-mutagenic effects (Van Wyk, 2008). Swanepoel (2018) reported possible anticancer and cytotoxic effects for *S. frutescens* in various small-cell lung cancer cell lines. Vorster *et al*. (2012) revealed that

S. frutescens aqueous extracts affect proliferation, morphology and cell cycle dynamics of MCF-7 and MCF-12A cells to varying degrees, and in a time and dose dependant manner. Phulukdaree *et al*. (2010) revealed that at concentrations higher than 6 mg/ml the *S. frutescens* extract was not cytotoxic in the tested kidney cell lines (LLC-PK1 and MDBK cell lines), but it did possess the potential to increase oxidative stress, promote apoptosis and alter the integrity of mitochondrial membranes.

2.5.4. The influence of *Sutherlandia frutescens* on drug biotransformation

S. frutescens has been shown to cause a concentration-dependant inhibition of CYP1A2, CYP2A6, CYP2C8, CYP2C9, CYP2C12 and CYP3A4/5 in a study conducted by Fasinu *et al*. (2013). Minocha *et al*. (2011) concluded that the concomitant use of *S. frutescens* with low-therapeutic prescription drugs could lead to herb-drug interactions, as well as only partial efficacy of such drugs. Ifeanyi (2009) also confirmed that *S. frutescens* extracts could directly interact with CYP450 enzymes. Mills *et al*. (2005) demonstrated the effects of *S. frutescens* on CYP3A4, P-gp and PXR *in vitro* and found that it produced near complete inhibition of CYP3A4 (96%). Relatively high concentrations of extract were used in the study, but they tentatively suggest that ingestion of *S. frutescens* could lead to bi-directional drug interactions and loss of therapeutic effects (Mills *et al*. 2005).

2.6. *Xysmalobium undulatum*

X. undulatum (Uzara) is a traditional herbal medicine indigenous to sub-Saharan Africa (Bester, 2009). It belongs to the family *Apocynaceae* (Krishna *et al*., 2015) and has a long history of use not only in South Africa, but also in Germany where it was introduced into the pharmaceutical markets as early as 1911 (Van Wyk, 2008). The plant grows to a height of 0.5 - 2.0 m, and it has large hairy and heart shaped leaves (**Figure 2.4**). Uzara also has prominent yellowish flowers growing in clusters around the stem (Bester, 2009; Vermaak *et al*., 2014). It is, however, the roots of the plant that are of medicinal importance and these bitter, fleshy roots are extensively used in South African traditional medicine (Van Wyk & Gericke, 2000; Vermaak *et al.,* 2014). These roots are pale brown outside and white inside with a peculiar sweet, somewhat nauseating smell (Van Wyk *et al*., 2009). Its uses include the treatment of abscesses, afterbirth cramps, diarrhoea, headaches, stomach cramps and wounds (Van Wyk, 2008). Uzara is a widely used herbal remedy in South Africa (Schmelzer & Gurib-Fakim, 2011; Vermaak *et al.,* 2014), and although the

plant has been marketed since early in the last century, there is no data on quality control protocols for Uzara (Kanama *et al.,* 2016).

Figure 2.4. Images of *Xysmalobium undulatum*. 1- Image of the whole plant; 2- Image showing the hairy fruit.

2.6.1. Traditional preparations and uses of *Xysmalobium undulatum*

The roots and the leaves of the plant are used in traditional remedies, but it is noteworthy that the stems were found to be poisonous (Reid *et al*., 2006). According to Van Wyk *et al*. (2009), half a cup of powdered root is boiled in one litre of water, and half a cup of this intensively bitter infusion is then taken twice daily. The powdered root can also be snuffed for the treatment of headaches and hysteria or applied directly to wounds and abscesses (Van Wyk, 2008). The Zulu people grind the stem and use it as an emetic in poisoning, while the Tswana people chew a piece of the root as an antidote for food poisoning. Uzara is not only used as medicine, but the powdered root is mixed into porridge by Zimbabweans and used as an aphrodisiac (Vermaak *et al*., 2014).

2.6.2. Biologically active constituents of *Xysmalobium undulatum*

The roots of the plant are harvested and contain cardiac glycosides, of which uzarin is the best known compound. The major compounds of the roots are uzarin and xysmalorin, but it also contains small amounts of allouzarin and alloxysmalorin (Van Wyk *et al*., 2009). Other active

constituents include ascleposide, pachygenol, uzaroside, pregnenolone and β-sitosterol (Vermaak *et al*., 2014). Glycosides are known for their inhibitory effect on intestinal motility, as well as their digitalis-like effect on the heart at high doses (Van Wyk, 2008). Uzara contains the following plant cardenolides: xysmalobin, uzarin, xysmalorin, uzaroside, ascleposide and glucoascleposide (Singh, 2011).

2.6.3. *Xysmalobium undulatum* in the treatment of cancer

Calitz *et al*. (2018) observed anti-proliferating effects of crude water extracts of *X. undulatum* in both two-dimensional (2D) and three-dimensional (3D) HepG2/C3A hepatocarcinoma cell line models at concentrations of 350 - 750 mg/kg. It is also noteworthy that this growth inhibition was more extensive in the 3D cell culture model compared to the 2D cell culture model. Swanepoel (2018) also indicated that uzara could possibly have anticancer effects, regardless of the risk of cytotoxicity for normal tissues when used at high concentrations. Wong and colleagues (2011) assesed the antiproliferative activities of five selected *Apocynaceae* species, and they found that the extracts of *C. gigantea* and *V. glabra* inhibited the growth of six different human cancer cell lines. One hundred and nine cardenolides have been isolated thus far from the *Apocynaceae* family, and interestingly a quarter of them are reported to have anticancer activity (Wen *et al*., 2016). According to Krishna *et al*. (2015), cardenolides have emerged as promising agents to treat cancer because their P-gp inhibitory properties make them excellent targets. They can also inhibit cell death and enhance proliferation in normal cells. These cardenolides are also natural Na^+/K^+-adenosine trifosfatase (ATPase) ligands that can affect numerous signalling cascades and suppress tumour growth (Krishna *et al*., 2015). In a study conducted by Delebinski (2015) they evaluated the effects of 20 steroid glycosides, including uzarin, on the proliferation and apoptotic induction in 143B osteosarcoma cells. They found that uzarin had no effect on apoptotic induction in mitochondrial potential nor inhibition of proliferation.

2.6.4. The influence of *Xysmalobium undulatum* on drug biotransformation

Because of the digitalis-like effect of the glycosides, it should not be used concomitantly with other cardiac glycosides as cross-reaction has been reported (Thürmann *et al*., 2004; Abd-El-Maeboud *et al*., 2014). Data regarding the biotransformation pathway of *X. undulatum*, including the effects thereof on the CYP450 enzyme family, is extremely scarce. Further research into this topic is needed.

2.7. *In vitro* models for colorectal cancer and drug biotransformation screening

During the pre-clinical drug development phase, as well as in non-clinical studies conducted to launch a drug, *in vitro* methods play a vital role (Hariparsad *et al*., 2006). *In vitro* studies aimed at understanding the molecular progression of cancer or identifying new and effective anticancer agents, rely on the availability of a versatile platform that closely resembles the pathophysiological features of the tumour and microenvironment *in vivo* (Xu *et al*., 2014). During *in vitro* toxicological studies, a platform that mimics the reproduction of normal tissues and portions of functional organs, as well as mimicry of tumour formation is required (Lelièvre *et al*., 2017). One such platform is the use of cell lines, which are vastly used in research today because they are easy to maintain, represent important features of certain cancers and are extremely useful to unravel biochemical pathways (Kimlin *et al*., 2013). Tumour cells are also routinely used to assess the mechanisms of toxicity that could help improve anticancer treatments (Katt *et al*., 2016;).

Many Bioresource centres offer characterised models of various types of cancer cell lines that are routinely used (Kapałczyńska *et al*., 2018). Numerous colon cancer cell lines are currently employed in research for example: CT-116, HCT-15, LoVo, RKO, SW1116, SW48, SW620, SW948, NCI-H508, ALA, CaCo-2, COLO 320 etc. Although there are numerous cell lines one could use, one cell line that has potential for both colorectal cancer treatment research, as well as drug biotransformation research, is the LS180 cell line. This colorectal cancer cell line has also been characterised and used for various *in vitro* studies (Tsujimoto *et al*., 2017).

2.7.1. The LS180 colorectal cancer cell line

The LS180 cell line is a microvillus expressing human colon carcinoma cell line. It is mainly used to study CYP450 enzyme inhibition, induction and transport of drugs *in vitro* (Li *et al.,* 2003; Collet *et al.,* 2004; Brandon *et al.,* 2006). According to Engman *et al.* (2001) and Brandon *et al.* (2006), the LS180 cells express many of the CYP450 isoforms, including CYP1A2 and CYP3A4 (Brandin *et al.,* 2007). The LS180 cell line could be an excellent cell line to study CYP450 induction, as they express PXR (Gupta *et al.,* 2008). Brandin *et al.* (2007) used the LS180 cell line to study the effects of certain herbal medicines on CYP1A2 and CYP3A4 enzyme induction, and the cell line was also used by Tsujimoto *et al.* (2017) to demonstrate that cabbage and onion juice significantly inhibit CYP3A4 enzyme activity. Aiba and colleagues investigated the suitability of the LS180 cell line to study intestinal first pass metabolism, CYP3A4 and multidrug resistant gene (MDR1) mRNA induction, and found that the LS180 cell line may be used

to examine regulation mechanisms responsible for intestinal CYP3A4 expression (Aiba *et al*., 2005).

Human colorectal cancer cell lines are commonly used in preclinical systems to study cancer. These cells are important and have provided many insights into tumour and cell biology (Mouradov *et al*., 2014). The LS180 cell was used in a study to determine the impact of thymidylate synthase and methylenetetrahydrofolate reductase genotypes on the sensitivity to 5-fluorouracil treatment in colorectal cancer. It was revealed that the LS180 cell line showed higher resistance to 5-fluorouracil treatment than the other cell lines (HT29/219 and SW1116) used during the study, because of the difference in 6-bp ins variant of the methylenetetrahydrofolate reductase (MTHFR) genotypes (Naghibalhossaini *et al*., 2017). In a study conducted by Tomoda *et al*. (2009) they used various cell lines, including the LS180 cell line, to provide functional evidence for essential meiotic structure-specific endonuclease 1 (Eme1) as a marker of cisplatin resistance. In this study it was established that cisplatin sensitivity correlated well with Eme1 levels.

2.7.2. Two-dimensional versus three-dimensional cell culturing

According to Wrzesinski *et al.* (2014), there are two extreme conditions for cell growth, namely the classical 2D culturing techniques and the second being characterised by cells which have reached dynamic equilibrium growing in 3D tissues or tissue-like conglomerates. 3D cell cultures can be defined as cells arranged into structures that resemble their organization *in vivo* (Lelièvre *et al*., 2017). Literature has indicated that there are differences between cellular morphology when comparing 3D and 2D models (Bonnier *et al.,* 2015). This may be because 2D-cultured cells are unable to simulate the microenvironment of cells and organs *in vivo,* which grow three dimensionally (Imamura *et al.,* 2015). These conventional cell monolayers are grown under simplified and unrealistic conditions and do not fully reflect the essential physiology of real tissue (Hoarau-Véchot *et al.,* 2018). When comparing 2D and 3D cultured cells, there are changes throughout the entire cell as the cells adapt from exponential growth to a dynamic equilibrium (Wrzesinki *et al,* 2014). A few of these changes include: increased protein to DNA ratio, reduced protein oxidation, increased adenosine triphosphate (ATP) levels, nuclear arrangement, cytoskeleton rearrangement and more (Wrzesinki *et al,* 2014).

It has recently been claimed that 3D cell culture models can bridge the gap between *in vitro* and *in vivo* studies (Hoarau-Véchot *et al.,* 2018). Kapałczyńska *et al*. (2018) and Hoarau-

Véchot *et al*. (2018) compiled a tables comparing 2D and 3D culture methods. In **Table 2.2**. it is evident that there are substantial differences between the two. Choosing the type of culture to be used will be dependent on the type of experiments to be performed.

Table 2.2. A comparison between two-dimensional and three-dimensional cell culture models (Adapted from Hoarau-Véchot *et al*., 2018; Kapałczyńska *et al*., 2018).

Type of culture	2D	3D
Time of culture formation	Minutes to hours	Hours to days
***In vivo* correlation limitations**	Do not mimic the *in vivo* structures of the tissues or tumour mass	*In vivo* tissues and organs are in 3D form and thus this technique mimics the *in vivo* environment
Cell differentiation	Non spontaneous	Could be spontaneous via cellular contact or soluble factors
Cell interactions	Deprived cell-cell and cell-extracellular environment interactions, not *in vivo*-like microenvironments	Proper interactions of cell-cell and cell-extracellular environment similar to the *in vivo* microenvironment
Characteristics of cells	Changes in morphology and cell divisions there is also a loss of diverse phenotype and polarity	Preserved cell morphology and cell divisions, diverse phenotype and polarity
Access to essential compounds	In contrast to the *in vivo* environment, this technique offers unlimited access to oxygen, nutrients, metabolites and signalling molecules	Variable access to oxygen, nutrients, metabolites and signalling molecules which is the same as *in vivo*
Molecular mechanisms	Changes in gene expression, mRNA splicing, topology and biochemistry of cells	Expression of genes, splicing, topology and biochemistry of cells as *in vivo*
Multicellular study	Better when studying immune responses	Good in co-culture, but complicated with more than two cell types
Cost of maintaining a culture	Cheaper with more commercially available tests and media	More expensive, more time-consuming, with fewer commercially available tests

2.7.3. Three-dimensional cell culturing techniques

3D culturing has been around for decades and one of the first 3D cultures were carried out by Hamburg and Solomon in soft agar solution in the 1970's (Kapałczyńska *et al*., 2018). Since then, various 3D culturing methods have been developed in an effort to provide models that produce structures that are *in vivo*-like (Breslin & O'Driscoll, 2013). Some of the most commonly used 3D cell culturing techniques are described below.

- Forced floating technique

  This relatively simple method (depicted in **Figure 2.5.**) prevents cell attachment to the vessel surface by modifying the surface, resulting in forced floating of cells. This promotes cell-cell contact which finally results in the formation of spheroids after centrifugation (Breslin & O'Driscoll, 2013).

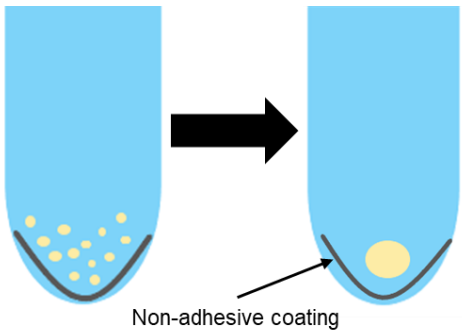

Figure 2.5. Image indicating the forced floating technique were cells are in suspension and centrifuged to form a spheroid.

- Hanging drop spheroid cultures

  During this method illustrated in **Figure 2.6.**, a small aliquot of about 20 µl of a single cell suspension is pipetted into the wells of a 60-well MicroWell MiniTray. The cell density can also be adapted depending on the size of the desired spheroid. Following seeding, the tray is inverted and the cell suspension aliquots turn into hanging drops. Cells accumulate at the tip and are allowed to form spheroids (Breslin & O'Driscoll, 2013).

- Agitation-based approaches

  During this approach, a cell suspension is placed into a container and the suspension is kept in motion by stirring or rotating (**Figure 2.7.**). The continuous motion of the cell suspension inhibits cells to attach to the container wall, but instead form cell-cell interactions and finally form spheroids (Breslin & O'Driscoll, 2013).

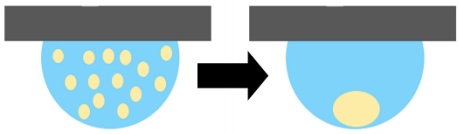

Figure 2.6. Image indicating the hanging drop technique where cells are in suspension and then form a spheroid.

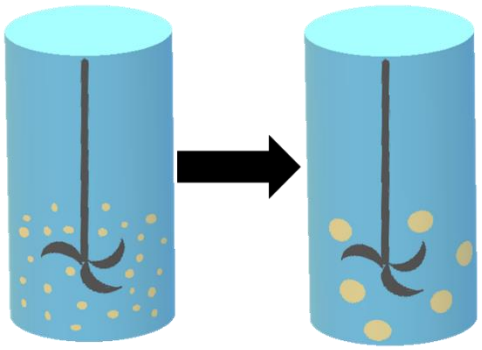

Figure 2.7. Image of illustrating one of the agitation based approaches where the continuous motion of cells causes cell-cell interactions and spheroids form.

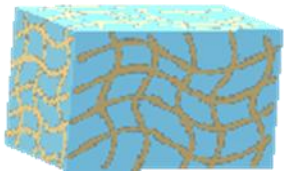

Figure 2.8. Image of a scaffold that can be employed during 3D cell culturing.

- Matrices and scaffolds

  Matrices and scaffolds are employed in 3D cell culturing to serve as an extra cellular matrix to support the growth of cell in 3D, as shown in **Figure 2.8**. Cells can either be imbedded in the matrix or grown on top of it. Pre-fabricated scaffolds can also be used. Cells are seeded in the scaffolds and can then migrate between fibres of the scaffold and attach to them (Breslin & O'Driscoll, 2013).

- Microfluidic cell culture platforms

  Microfluidic systems comprise of a main microfluidic channel which is an array of micropillars through which a cell suspension is passed (**Figure 2.9.**). The micropillar array immobilises cells within the pillars and supports cell-cell interactions. A collagen matrix is then passed through the system and forms a thin layer over the cells (Breslin & O'Driscoll, 2013).

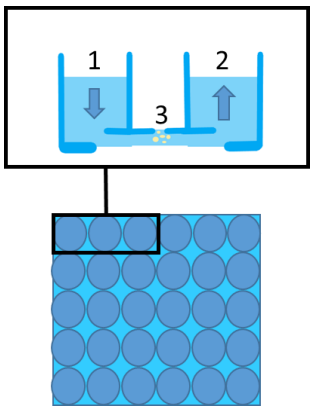

Figure 2.9. Image indicating a microfluidic system. Three connected wells make up one microfluidic unit. Number 1 indicates the inlet reservoir, 2 indicated the outlet reservoir and 3 indicates the cell chamber.

Each of these 3D culturing techniques have different advantages and disadvantages aiding in the choice of technique for a specific purpose as seen in **Table 2.3.**

Cell spheroid cultures are simple 3D models that can be created from a wide variety of cell types and form due to the tendency of adherent cells to aggregate (Haycock, 2011). Various methods can also be employed to achieve a 3D spheroid culture. Some of these methods include:

- <u>Pellet cultures</u>

  The pellet culture technique uses centrifugal force to concentrate cells on the bottom of a conical tube to maximize the opportunity for cell-cell interactions and spheroid formation (Achilli *et al*., 2012).

- <u>Spinner cultures</u>

  This culturing technique is one of the agitation based approaches described above (Achilli *et al*., 2012).

Table 2.3. Advantages and disadvantages of a few three-dimensional cell culturing techniques (adapted from Breslin & O'Driscoll, 2013).

Culturing technique	Advantages	Disadvantages
Forced-floating	• Relatively simple and inexpensive • Suitable for high-throughput testing • Easy access to produced spheroids	• Variable cell size and shape • Do it yourself (DIY) plate-coating is relatively labour intensive
Hanging drop	• Inexpensive when using 96-well plates • Suitable for high-throughput testing • Easy access to produced spheroids	• More expensive if using specialised plates • Labour intensive if preparing plates in-house • Small culture volume makes medium exchange, without disturbing cells, difficult
Agitation-based approaches	• Simple to culture cells • Large-scale production achievable • Motion of culture assists in nutrient transport • Easy access to produced spheroids	• Specialized equipment needed • No control over number of cells and spheroid size • Time consuming if used for high-throughput screening • Cells possibly exposed to shear forces in spinner flasks
Matrices and scaffolds	• Provide 3D support that mimics *in vivo* • Some incorporate growth factors	• Can be expensive for large-scale production • Can have difficulty in retrieving cells following 3D culture formation
Microfluidic cell platforms	• Described as suitable for high-throughput testing	• Specialized equipment needed, making it expensive • Further analysis of 3D cultures produced may be difficult

- Hanging drop

As described above, this method can also be used to form co-cultured heterotypic spheroids (Achilli *et al*., 2012).

- Liquid overlay

Cells are seeded on low-attachment plates as this promotes cell-cell aggregation. The plate is then rocked, and with a small amount of shaking, the cells aggregate into spheroids (Achilli *et al*., 2012).

- Rotating wall vessels

This creates a microgravity environment that maintains cells in suspension and allows cells to aggregate into spheroids (Achilli *et al*., 2012).

- External force

This method uses external forces like electric fields, magnetic forces and ultrasound to concentrate mono-dispersed cells into high density that facilitates cell aggregation (Achilli *et al*., 2012).

- Microfluidics

As described above, this technique can be used to create size-controlled spheroids for high-throughput screening (Achilli *et al*., 2012).

- Microfabricated microstructures

Single suspensions are seeded into microwells following distribution by gravity and hydrodynamic forces. This eventually leads to the assembly into aggregates according to microwell geometry (Lin & Chang, 2008).

- Cultures grown in concentrated medium or in gel-like substances

In this technique, a single cell suspension is encapsulated by substances with gelling properties and grown inside it (Kapałczyńska *et al*. 2018).

2.7.4. Static and dynamic 3D cell culturing systems

Concentration gradients exist in all tissues for oxygen, pH, soluble components such as nutrients as well as cellular metabolites. These concentration gradients affect various cell behaviours including cell motility, cell migration and cell signalling which can have an impact on chemotaxis and morphogenesis in normal tissue development (Langhans, 2018). According to Wrzesinski & Fey (2018), one of the main differences in cells cultured 2D and 3D is concentration gradients.

There is also a difference in concentration gradient when comparing static systems and dynamic systems. For static systems, where there is no flow of nutrients, the concentration gradients fall rapidly towards the centre of the spheroid and there is a very big diffusion depletion zone around each spheroid. When looking at dynamic or irrigated systems, where media flows past the spheroids, the diffusion depletion zone around the spheroid is much smaller (Wrzesinski & Fey, 2018). In **Figure 2.10.** a few examples are given for different static or dynamic culturing systems.

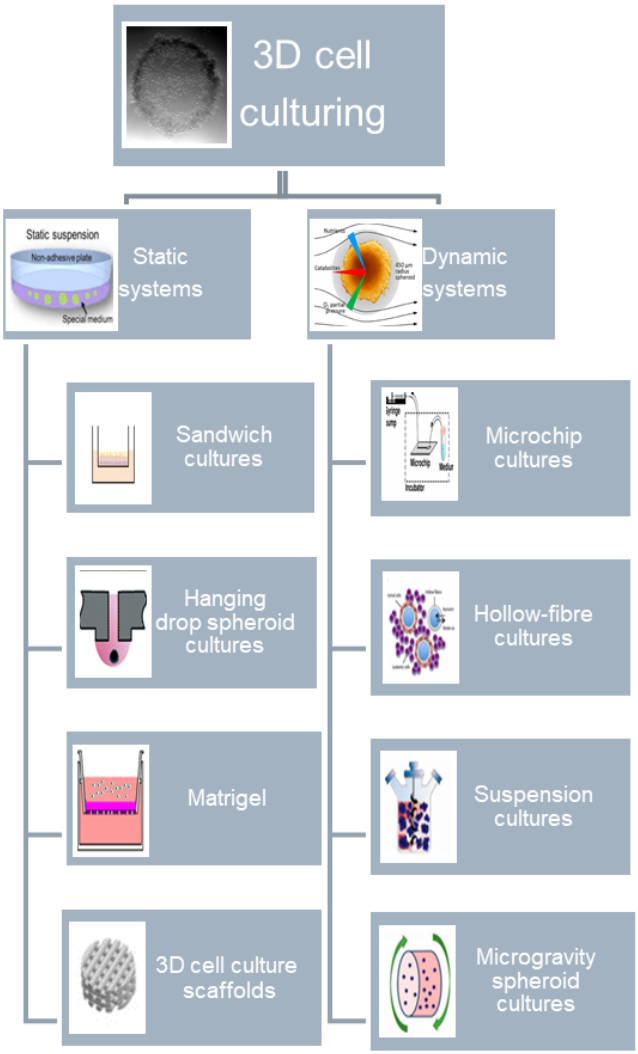

Figure 2.10. Diagram showing a few different static and dynamic cell culturing systems (Image adapted from Tanaka *et al*., 2006; Partridge & Flaherty, 2009; Tung *et al*., 2011; Usuludin *et al*., 2012; Pereira & Bártolo, 2015; McKee & Chaudhry, 2017; Wrzesinki & Fey, 2018).

According to McKee & Chaudhry (2017), there are several approaches to maintain, expand and differentiate spheroid cultures using different 3D culture systems. One such a system is the dynamic clinostat-based rotating bioreactor and Bioarray matrix drive (BAM) system developed by Fey & Wrzesinski (2012) (indicated in **Figure 2.11.**). Bioreactors are devices in which spheroids develop under closely monitored and tightly controlled environmental operating conditions (i.e. pH, temperature, shear stress, pressure, nutrient supply and waste removal) (Khetani & Bhatia, 2006). Bioreactors induce the mixing of oxygen and nutrients throughout the medium and reduce the concentration boundary layer at the construct surface, as commonly found in static cultures (Martin *et al*., 2004).

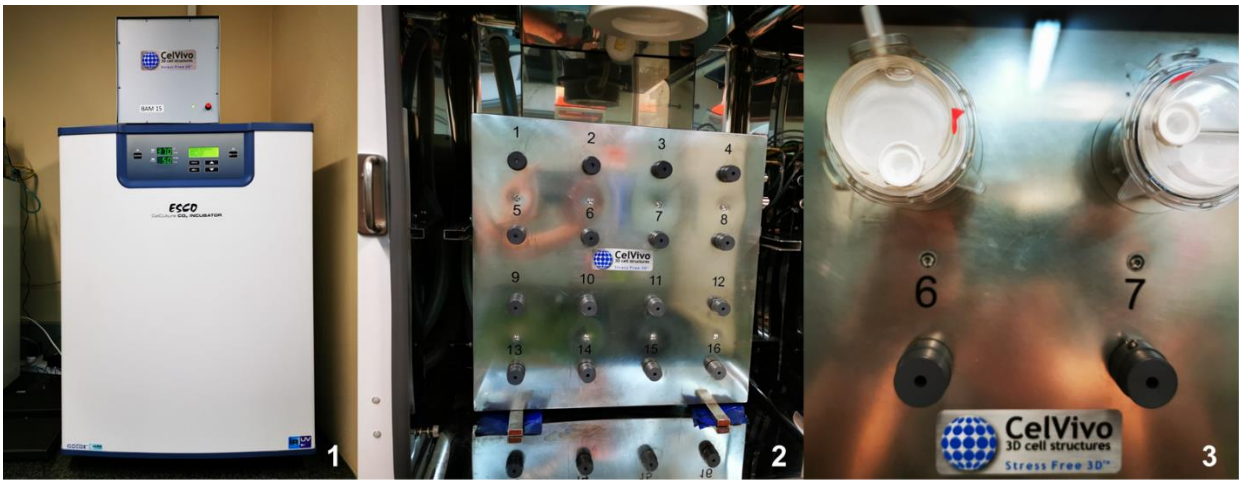

Figure 2.11. Image indicating the clinostat-based rotating bioreactor and Bioarray matrix (BAM) drive system. 1- Image of the incubator and BAM system used. 2- Image of the drive unit of the BAM system with 16 rotors. 3- Image of two clinostat based bioreactors on their individual rotors.

Fey & Wrzesinski (2012) used the clinostat-based bioreactor and BAM system to construct 3D spheroids from an immortal human hepatocyte cell line (HepG2/C3A). During this study they determined the 50% lethal dose (LD_{50}) value of six compounds on cells cultured 2D and 3D. The results of the 3D spheroid model were superior to the results obtained from the 2D model and this data also more closely correlates with *in vivo* lethal blood plasma levels. In another study by Wrzesinski *et al*. (2014) they cultured the HepG2/C3A immortal human hepatocytes as spheroids for 21 days in the clinostat-based bioreactors. They analysed the proteome and cellular architecture of these spheroids in comparison with their 2D cultured counterpart. They found that

these two extremes differ dramatically in terms of a multitude of protein changes.

2.7.5. Sodium alginate cell encapsulation

Alginates are anionic polysaccharides extracted from brown seaweed, composed of β-D-mannuronic acid and α-L-guluronic acid. These alginates form hydrogels when cross-linked with multivalent cations, such as Ca^{2+}, Ba^{2+} or Fe^{2+} (Tan & Takeuchi, 2007). Alginates have numerous biomedical applications including pharmaceutical applications like delivery of small chemical drugs and protein delivery, wound dressings for acute and chronic wounds, various applications in the field of cell culture and lastly, in tissue regeneration with protein delivery (Lee & Mooney, 2012).

According to Le Roux *et al*. (1999), alginate cross-linked with Ca^{2+} has been popularized for *in vitro* cell culture and tissue engineering applications. This is due to its biocompatibility, low toxicity, relatively low cost, as well as mild gelation by addition of bivalent cations (Lee & Mooney, 2012). Furthermore, alginates have a relatively inert aqueous environment, they have high gel porosity which allows for high diffusion rates and they are biodegradable under normal physiological conditions (Gombotz & Wee, 1998; Chung *et al*., 2002). Cell encapsulation technologies are based on the immobilization of cells within a semipermeable membrane. This membrane will protect the encapsulated cells from mechanical stress, while allowing bidirectional diffusion of oxygen, nutrients and waste (Murua *et al*., 2008).

Ashton and colleagues (2007) used sodium alginate for creating alginate hydrogels with adjustable degradation rates that can be used as scaffolds for stem cells. It has also been indicated that purified alginate gels were able to support proliferation of rat marrow cells and their differentiation along the osteoblastic lineage after encapsulation. This indicates that sodium alginate has potential to act as a tissue-engineering scaffold on which tissues may be formed (Wang *et al*., 2003). Alessandri *et al*. (2013) designed cell-encapsulating hollow, permeable and elastic alginate shells. This method allows efficient preparation and long-term culture of multicellular spheroids. This technique also overcomes the disadvantages of low production rate and size variability. Mhanna *et al*. (2014) used alginate sulphate as a hydrogel for autologous chondrocyte implantation that allows cells to synthesize their own matrix, maintain their cartilage phenotype and proliferate. 3D alginate scaffolds were also used by Godugu *et al*. (2013) to successfully develop a 3D-lung tumour model that can be used in the future to predict the anticancer effects of various drugs.

2.7.6. Two-dimensional versus three-dimensional models for anticancer and biotransformation studies

Cell-based assays are widely used during the anticancer drug screening process (Lama *et al*., 2013). Lama *et al*. (2013) conducted a study to compare the 50% inhibitory concentration (IC_{50}) values of 41 known anticancer drugs used to treat H292 non-small lung cancer, in both a 2D culture as well as in a 3D spheroid culture. It was found that there was a very low correlation ($R^2 = 0.35$) between the two models, which emphasizes the importance of 3D cultures. Furthermore, a previous study by Smitskamp-Wilms *et al*. (1998) also showed that colon cancer cells were 1 000 times more resistant to gemcitabine in 3D cultures than in 2D cultures.

In a study conducted by Lu *et al*. (2012) they constructed a hollow fiber based organoid culture of hepatocytes and evaluated glucose metabolism in comparison to 2D and sandwich cultures. They concluded that this system is an improved *in vitro* platform for physiological/pathological glucose metabolism studies and pharmacological investigations on anti-diabetes drugs.

A novel HepaRG spheroid model that represents a simple approach for obtaining physiological relevant levels of xenobiotic metabolism and hepatocellular functionality was established by Ramaiahgari *et al*. (2017). This model is stable for at least 28 days and exhibits hallmarks of hepatocyte functionality including physiologically relevant drug metabolizing activities, liver enzyme inducibility, and evidence of biliary excretion functionality. This consequently indicates that the 3D model is superior to the 2D cultured HepaRG cells.

2.8. Summary

Establishing new 3D cell culturing systems to evaluate anticancer potential and biotransformation pathways of drugs will be a valuable asset for future research. These 3D cell culture models have the potential to bridge the gap between *in vitro* research and the *in vivo* situation, without using animal models. Furthermore, plants are important sources for new anticancer drugs and their potential use in this field is worthy of exploring.

It is, however, also of utmost importance to establish the biotransformation pathways of these phytomedicines, especially their effect on the CYP450 enzyme family. These effects may lead to pharmacokinetic interactions during concomitant use with prescribed medicines, potentially resulting in toxic levels of a drug or treatment failure.

References:

Abd-El-Maeboud, K.H., Kortam, M.A., Ali, M.S., Ibrahim, M.I. & Mohamed, R.M. 2014. A preliminary pilot randomized crossover study of uzara (*Xysmalobium undulatum*) versus ibuprofen in the treatment of primary dysmenorrhea. *PloS one*, 9:e104473.

Aboyade, O.M., Styger, G., Gibson, D. & Hughes, G. 2014. *Sutherlandia frutescens*: the meeting of science and traditional knowledge. *The journal of alternative and complementary medicine*, 20:71-76.

Achilli, T.M., Meyer, J. & Morgan, J.R. 2012. Advances in the formation, use and understanding of multi-cellular spheroids. *Expert opinion on biological therapy*, 12:1347-1360.

Aiba, T., Susa, M., Fukumori, S. & Hashimoto, Y. 2005. The effects of culture conditions on CYP3A4 and MDR1 mRNA induction by 1α, 25-dihydroxyvitamin D3 in human intestinal cell lines, Caco-2 and LS180. *Drug metabolism and pharmacokinetics*, 20:268-274.

Alessandri, K., Sarangi, B.R., Gurchenkov, V.V., Sinha, B., Kießling, T.R., Fetler, L., Rico, F., Scheuring, S., Lamaze, C., Simon, A. & Geraldo, S. 2013. Cellular capsules as a tool for multicellular spheroid production and for investigating the mechanics of tumor progression *in vitro*. *Proceedings of the National academy of sciences*, 110:14843-14848.

Amacher, D.E. 2010. The effects of cytochrome P450 induction by xenobiotics on endobiotic metabolism in pre-clinical safety studies. *Toxicology mechanisms and methods*, 20:159-166.

Appiah-Opong, R., Commandeur, J.N., Van Vugt-Lussenburg, B. & Vermeulen, N.P. 2007. Inhibition of human recombinant cytochrome P450s by curcumin and curcumin decomposition products. *Toxicology*, 235:83-91.

Ashton, R.S., Banerjee, A., Punyani, S., Schaffer, D.V. & Kane, R.S. 2007. Scaffolds based on degradable alginate hydrogels and poly (lactide-co-glycolide) microspheres for stem cell culture. *Biomaterials*, 28:5518-5525.

Astin, M., Griffin, T., Neal, R.D., Rose, P. & Hamilton, W. 2011. The diagnostic value of symptoms for colorectal cancer in primary care: a systematic review. *British journal of general practice*, 61:e231-e243.

Aung, T.N., Qu, Z., Kortschak, R.D. & Adelson, D.L. 2017. Understanding the effectiveness of natural compound mixtures in cancer through their molecular mode of action. *International journal of molecular sciences,* 18: 656-276.

Awortwe, C., Makiwane, M., Reuter, H., Muller, C., Louw, J. & Rosenkranz, B. 2018. Critical evaluation of causality assessment of herb–drug interactions in patients. *British journal of clinical pharmacology*, 84:679-693.

Bester, S.P. 2009. *Xysmalobium undulatum* (L,) Aitonf. var undulatum. Plantzafrica, official website of the South African National Biodiversity Institute (SANBI), Pretoria. Available at: http://pza.sanbi.org/xysmalobium-undulatum, [Date of access: 28 Feb. 2018].

Bibi, Z. 2008. Role of cytochrome P450 in drug interactions. *Nutrition and metabolism*, 5:1-10.

Bo, L., Baosheng, Z., Yang, L., Mingmin, T., Beiran, L., Zhiqiang, L. & Huaqiang, Z. 2016. Herb-drug enzyme-mediated interactions and the associated experimental methods: a review. *Journal of traditional Chinese medicine*, 36:392-408.

Bonnier, F., Keating, M.E., Wrobel, T.P., Majzner, K., Baranska, M., Garcia-Munoz, A., Blanco, A. & Byrne, H.J. 2015. Cell viability assessment using the Alamar blue assay: a comparison of 2D and 3D cell culture models. *Toxicology in vitro*, 29:124-131.

Bouyahya, A., Bakri, Y., Et-Touys, A., Assemian, I.C.C., Abrini, J., & Dakka, N. 2018. *In vitro* antiproliferative activity of selected medicinal plants from the North-West of Morocco on several cancer cell lines. *European journal of integrative medicine,* 18:23-29.

Brandin, H., Viitanen, E., Myrberg, O. & Arvidsson, A.K. 2007. Effects of herbal medicinal products and food supplements on induction of CYP1A2, CYP3A4 and MDR1 in the human colon carcinoma cell line LS180. *Phytotherapy research*, 21:239-244.

Brandon, E.F.A., Raap, C. D., Meijerman, I., Beijnen, J. H. & Schellens, J. H. 2003. An update on *in vitro* test methods in human hepatic drug biotransformation research: Pros and cons. *Toxicology and applied pharmacology*, 189:233-246.

Brandon, E.F.A., Bosch, T.M., Deenena, M.J., Levinka, R., Van der Wal, E., Van Meerveld, J.B.M., Bijl, M., Beijnen, J.H., Schellens, J.H.M. & Meijerman, I. 2006. Validation of *in vitro* cell models used in drug metabolism and transport studies; genotyping of cytochrome P450, phase II enzymes and drug transporter polymorphisms in the human hepatoma (HepG2), ovarian carcinoma (IGROV-1) and colon carcinoma (CaCo-2, LS180) cell lines. *Toxicology and applied pharmacology*, 211:1-10.

Brantley, S., Argikar, A., Lin, Y.S., Nagar, S. & Paine, M.F. 2014. Herb-drug interactions: challenges and opportunities for improved predictions. *Drug metabolism and disposition*, 42:301-317.

Breslin, S. & O'Driscoll, L. 2013. Three-dimensional cell culture: the missing link in drug discovery. *Drug discovery today*, 18:240-249.

Calitz, C., Hamman, J.H., Viljoen, A.M., Fey, S.J., Wrzesinski, K. & Gouws, C. 2018. Toxicity and anti-prolific properties of *Xysmalobium undulatum* water extract during short-term exposure to two-dimensional and three-dimensional spheroid cell cultures. *Toxicology mechanisms and methods*, 28:641-652.

Chinkwo, K.A. 2005. *Sutherlandia frutescens* extracts can induce apoptosis in cultured carcinoma cells. *Journal of ethnopharmacology*, 98:163-170.

Chung, T.W., Yang, J., Akaike, T., Cho, K.Y., Nah, J.W., Kim, S.I. & Cho, C.S. 2002. Preparation of alginate/galactosylated chitosan scaffold for hepatocyte attachment. *Biomaterials*, 23:2827-2834.

Cohen, P.A. & Ernst, E. 2010. Safety of herbal supplements: a guide for cardiologists. *Cardiovascular therapeutics*, 28:246-253.

Collet, A., Tanianis-Hughes, J. & Warhurst, G. 2004. Rapid induction of P-glycoprotein expression by high permeability compounds in colonic cells *in vitro*: a possible source of transporter mediated drug interactions. *Biochemistry and pharmacology*, 68:783-790.

Coon, M. J., Ding, X. X., Pernecky, S. J. & Vaz, A. D. 1992. Cytochrome P450: Progress and predictions. *Federation of American societies for experimental biology journal*, 6:669-673.

Crooks, P.A. & Rosenthal, G.A. 1996. University of Kentucky Research Foundation. Use of L-canavanine as a chemotherapeutic agent for the treatment of pancreatic cancer. U.S. Patent 5,552,440.

Delebinski, C.I., Georgi, S., Kleinsimon, S., Twardziok, M., Kopp, B., Melzig, M.F. & Seifert, G. 2015. Analysis of proliferation and apoptotic induction by 20 steroid glycosides in 143B osteosarcoma cells *in vitro*. *Cell proliferation*, 48:600-610.

De Montellano, P.R.O. 2015. Cytochrome P450: structure, mechanism, and biochemistry. 4th ed. Cham: Springer Science and Business Media.

Donato, M.T., Lahoz, A., Castell, J.V. & Gómez-Lechón, M.J. 2008. Cell lines: a tool for *in vitro* drug metabolism studies. *Current drug metabolism*, 9:1-11.

Ekor, M. 2014. The growing use of herbal medicines: issues relating to adverse reactions and challenges in monitoring safety. *Frontiers in pharmacology*, 4:1-10.

Encyclopaedia Britannica. 1998. Polymorphism. https://www.britannica.com/science/polymorphism-biology, [Date of access: 26 Feb. 2018].

Encyclopaedia Britannica. 2017. Epigenetics. https://www.britannica.com/science/epigenetics, [Date of access: 26 Feb. 2018].

Engman, H.A., Lennernäs, H., Taipalensuu, J., Otter, C., Leidvik, B. & Artursson, P. 2001. CYP3A4, CYP3A5, and MDR1 in human small and large intestinal cell lines suitable for drug transport studies. *Journal of pharmaceutical sciences*, 90:1736-1751.

Evan, G.I. & Vousden, K.H. 2001. Proliferation, cell cycle and apoptosis in cancer. *Nature*, 411:342-348.

Fasinu, P.S., Bouic, P.J. & Rosenkranz, B. 2012. An overview of the evidence and mechanisms of herb-drug interactions. *Frontiers in pharmacology*, 3:1-19.

Ferlay, J., Shin, H.R., Bray, F., Forman, D., Mathers, C. & Parkin, D.M. 2010. Estimates of worldwide burden of cancer in 2008: GLOBOCAN 2008. *International journal of cancer*, 12:2893-2917.

Fey, S.J. & Wrzesinski, K. 2012. Bioreactor with lid for easy access to incubation cavity. USA PA 61/423, 145, 2010; DK PCT/DK2011/050466.

Flockhart, D.A. 2007. Drug interactions: cytochrome P450 drug interaction table. https://medicine.iupui.edu/clinpharm/ddis/main-table/, [Date of access: 15 March 2018].

Gardiner, P., Graham, R.E., Legedza, A.T., Eisenberg, D.M. & Phillips, R.S. 2006. Factors associated with dietary supplement use among prescription medication users. *Archives of internal medicine*, 166:1968-1974.

Gericke, N. 2001. Sutherlandia and AIDS patients: update 13 March 2001. *Australian journal of medical herbalism*, 13:17-18.

Godugu, C., Patel, A.R., Desai, U., Andey, T., Sams, A. & Singh, M. 2013. AlgiMatrix™ based 3D cell culture system as an *in-vitro* tumor model for anticancer studies. *PloS one*, 8:e53708.

Gombotz, W.R. & Wee, S. 1998. Protein release from alginate matrices. *Advanced drug delivery reviews*, 31:67-285.

Goodspeed, A., Heiser, L.M., Gray, J.W. & Costello, J.C. 2016. Tumor-derived cell lines as molecular models of cancer pharmacogenomics. *Molecular cancer research*, 14:3-13.

Gqaleni, N., Moodley, I., Kruger, H., Ntuli, A. & McLeod, H. 2007. Traditional and complementary medicine: health care delivery. *South African health review*, 2007:175-188.

Grimm, D. 2019. U.S. EPA to eliminate all mammal testing by 2035. https://sci-hub.tw/https://www.sciencemag.org/news/2019/09/us-epa-eliminate-all-mammal-testing-2035 Date of access: 3 Oct. 2019.

Gupta, A., Mugundu, G.M., Desai, P.B., Thummel, K.E. & Unadkat, J.D. 2008. Intestinal human colon adenocarcinoma cell line LS180 is an excellent model to study pregnane X receptor, but not constitutive androstane receptor, mediated CYP3A4 and multidrug resistance transporter 1 induction: Studies with anti-human immunodeficiency virus protease inhibitors. *Drug metabolism and disposition*, 36:1172-1180.

Gurley, B.J., Swain, A., Hubbard, M.A., Williams, D.K., Barone, G., Hartsfield, F., Tong, Y., Carrier, D.J., Cheboyina, S. & Battu, S.K. 2008. Clinical assessment of CYP2D6-mediated herb–drug interactions in humans: Effects of milk thistle, black cohosh, goldenseal, kava kava, St. John's wort, and Echinacea. *Molecular nutrition and food research*, 52:755-763.

Haggar, F.A. & Boushey, R.P. 2009. Colorectal cancer epidemiology: incidence, mortality, survival, and risk factors. *Clinics in colon and rectal surgery*, 22:191-197.

Hamilton, W. & Sharp, D. 2004. Diagnosis of colorectal cancer in primary care: the evidence base for guidelines. *Family practice*, 21:99-106.

Hariparsad, N., Sane, R.S., Strom, S.C. & Desai, P.B. 2006. *In vitro* methods in human drug biotransformation research: implications for cancer chemotherapy. *Toxicology in vitro*, 20:135-153.

Haycock, J.W. 2011. 3D cell culture: a review of current approaches and techniques. (In 3D cell culture: methods and protocols. Switzerland: Springer Science+Business Media. p. 1-15).

Hoarau-Véchot, J., Rafii, A., Touboul, C. & Pasquier, J. 2018. Halfway between 2D and animal models: are 3D cultures the ideal tool to study cancer-microenvironment interactions? *International journal of molecular sciences*, 19:181.

Ifeanyi, E. 2009. An investigation into the bioactivity of *Sutherlandia frutescens* (Cancer bush). Stellenbosch: University of Stellenbosch. (Dissertation-MSc).

Imamura, Y., Mukohara, T., Shimono, Y., Funakoshi, Y., Chayahara, N., Toyoda, M., Kiyota, N., Takao, S., Kono, S., Nakatsura, T. & Minami, H. 2015. Comparison of 2D-and 3D-culture models as drug-testing platforms in breast cancer. *Oncology reports*, 33:1837-1843.

Ingelman-Sundberg, M. 2004. Pharmacogenetics of cytochrome P450 and its applications in drug therapy: the past, present and future. *Trends in pharmacological sciences*, 25:193-200.

Ingelman-Sundberg, M. 2005. Genetic polymorphisms of cytochrome P450 2D6 (CYP2D6): clinical consequences, evolutionary aspects and functional diversity. *The pharmacogenomics journal*, 5:6.

Iqbal, J., Abbasi, B.A., Mahmood, T., Kanwal, S., Ali, B., Shah, S.A. & Khalil, A.T. 2017. Plant-derived anticancer agents: A green anticancer approach. *Asian pacific journal of tropical biomedicine*, 7:1129-1150.

Jaroch, K., Jaroch, A. & Bojkoa, B. 2018. Cell cultures in drug discovery and development: The need of reliable *in vitro-in vivo* extrapolation for pharmacodynamics and pharmacokinetics assessment. *Journal of pharmaceutical and biomedical analysis*, 147:297-312.

Jermini, M., Dubois, J., Rodondi, P.Y., Zaman, K., Buclin, T., Csajka, C., Orcurto, A. & Rothuizen, L.E. 2019. Complementary medicine use during cancer treatment and potential herb-drug interactions from a cross-sectional study in an academic centre. *Scientific reports*, 9:5078-5089.

Johnson, Q., Syce, J., Nell, H., Rudeen, K. & Folk, W.R. 2007. A randomized, double-blind, placebo-controlled trial of *Lessertia frutescens* in healthy adults. *PloS clinical trials*, 2:e16.

Kalyanaraman, B. 2017. Teaching the basics of cancer metabolism: Developing antitumor strategies by exploiting the differences between normal and cancer cell metabolism. *Redox biology*, 12:833-842.

Kanama, S., Viljoen, A., Enslin, G., Kamatou, G., Chen, W., Sandasi, M. & Idowu, T. 2016. Uzara–A quality control perspective of *Xysmalobium undulatum*. *Pharmaceutical biology*, 54:1272-1279.

Kapałczyńska, M., Kolenda, T., Przybyła, W., Zajączkowska, M., Teresiak, A., Filas, V., Ibbs, M., Bliźniak, R., Łuczewski, Ł. & Lamperska, K. 2018. 2D and 3D cell cultures–a comparison of different types of cancer cell cultures. *Archives of medical science*, 14:910.

Kastan, M.B. & Bartek, J. 2004. Cell-cycle checkpoints and cancer. *Nature*, 432:316.

Katt, M.E., Placone, A.L., Wong, A.D., Xu, Z.S. & Searson, P.C. 2016. *In vitro* tumor models: advantages, disadvantages, variables, and selecting the right platform. *Frontiers in bioengineering and biotechnology*, 4:1-14.

Katzung, B.G., Masters, S.B. & Trevor, A.J. 2012. Basic and Clinical Pharmacology. 12th ed. New York: McGraw-Hill. 949-965.

Kaur, V., Kumar, M., Kumar, A., Kaur, K., Dhillon, V.S. & Kaur, S. 2018. Pharmacotherapeutic potential of phytochemicals: Implications in cancer chemoprevention and future perspectives. *Biomedicine & pharmacotherapy*, 97: 564-586.

Kennedy, A.S., Harrison, G.H., Mansfield, C.M., Zhou, X.J., Xu, J.F. & Balcer-Kubiczek, E.K. 2000. Survival of colorectal cancer cell lines treated with paclitaxel, radiation, and 5-FU: Effect of TP53 or hMLH1 deficiency. *International journal of cancer*, 90:175-185.

Khetani, S.R. & Bhatia, S.N. 2006. Engineering tissues for *in vitro* applications. *Current opinion in biotechnology*, 17:524-531.

Kimlin, L.C., Casagrande, G. & Virador, V.M. 2013. *In vitro* three-dimensional (3D) models in cancer research: an update. *Molecular carcinogenesis*, 52:167-182.

Koziara, J.M., Whisman, T.R., Tseng, M.T. & Mumper, R.J. 2006. In-vivo efficacy of novel paclitaxel nanoparticles in paclitaxel-resistant human colorectal tumors. *Journal of controlled release*, 112:312-319.

Krishna, A.B., Manikyam, H.K., Sharma, V.K. & Sharma, N. 2015. Plant cardenolides in therapeutics. *International journal of indigenous medicinal plants*, 48:1871-1896.

Lama, R., Zhang, L., Naim, J.M., Williams, J., Zhou, A. & Su, B. 2013. Development, validation and pilot screening of an *in vitro* multi-cellular three-dimensional cancer spheroid assay for anti-cancer drug testing. *Bioorganic & medicinal chemistry*, 21:922-931.

Langhans, S.A. 2018. Three-dimensional *in vitro* cell culture models in drug discovery and drug repositioning. *Frontiers in pharmacology*, 9:1-14.

Lee, K.Y. & Mooney, D.J. 2012. Alginate: properties and biomedical applications. *Progress in polymer science*, 37:106-126.

Lee, R.T., Barbo, A., Lopez, G., Melhem-Bertrandt, A., Lin, H., Olopade, O.I. & Curlin, F.A. 2014. National survey of US oncologists' knowledge, attitudes, and practice patterns regarding herb and supplement use by patients with cancer. *Journal of clinical oncology*, 32:4095-4101.

Leisching, G., Loos, B., Nell, T. & Engelbrecht, A.M. 2015. *Sutherlandia frutescens* treatment induces apoptosis and modulates the PI3-kinase pathway in colon cancer cells. *South African journal of botany*, 100:20-26.

Lelièvre, S.A., Kwok, T. & Chittiboyina, S. 2017. Architecture in 3D cell culture: an essential feature for *in vitro* toxicology. *Toxicology in vitro*, 45:287-295.

Le Roux, M.A., Guilak, F. & Setton, L.A. 1999. Compressive and shear properties of alginate gel: effects of sodium ions and alginate concentration. *Journal of biomedical materials research: an official journal of the society for biomaterials, the Japanese society for biomaterials, and the Australian society for biomaterials and the Korean society for biomaterials*, 47:46-53.

Li, A.P. 2001. Screening for human ADME/Tox drug properties in drug discovery. *Drug discovery today*, 6:356-366.

Li, Q., Sai, Y., Kato, Y., Tamai, I. & Tsuji, A. 2003. Influence of drugs and nutrients on transporter gene expression levels in CaCo-2 and LS180 intestinal epithelial cell lines. *Pharmaceutical research*, 20:1119-1124.

Lin, J.H. & Lu, A.Y. 1998. Inhibition and induction of cytochrome P450 and the clinical implications. *Clinical pharmacokinetics*, 35:361-390.

Lin, R.Z. & Chang, H.Y. 2008. Recent advances in three-dimensional multicellular spheroid culture for biomedical research. *Biotechnology journal: healthcare nutrition technology*, 3:1172-1184.

Lu, Y., Zhang, G., Shen, C., Uygun, K., Yarmush, M.L. & Meng, Q. 2012. A novel 3D liver organoid system for elucidation of hepatic glucose metabolism. *Biotechnology and bioengineering*, 109:595-604.

Lübberstedt, M., Müller-Vieira, U., Mayer, M., Biemel, K.M., Knöspel, F., Knobeloch, D., Nüssler, A.K., Gerlach, J.C. & Zeilinger, K. 2011. HepaRG human hepatic cell line utility as a surrogate for primary human hepatocytes in drug metabolism assessment *in vitro*. *Journal of pharmacological and toxicological methods*, 63:159-68.

Lynch, T. & Price, A. 2007. The effect of cytochrome P450 metabolism on drug response. *American family physician*, 76:391-396.

Malumbres, M. & Barbacid, M. 2009. Cell cycle, CDKs and cancer: a changing paradigm. *Nature reviews cancer*, 9:153-166.

Maness, L., Goktepe, I. & Ahmedna, M. 2012. *In vitro* cancer research on ancient herbal remedies: a changing trend. *Journal of applied pharmaceutical science*, 2:13-20.

Markowitz, S.D. & Bertagnolli, M.M. 2009. Molecular basis of colorectal cancer. *New England journal of medicine*, 361:2449-2460.

Martin, I., Wendt, D. & Heberer, M. 2004. The role of bioreactors in tissue engineering. *Trends in biotechnology*, 22:80-86.

Massagué, J. 2004. G1 cell-cycle control and cancer. *Nature*, 432:298-306.

McKee, C. & Chaudhry, G.R. 2017. Advances and challenges in stem cell culture. *Colloids and surfaces B: biointerfaces*, 159:62-77.

Mhanna, R., Kashyap, A., Palazzolo, G., Vallmajo-Martin, Q., Becher, J., Möller, S., Schnabelrauch, M. & Zenobi-Wong, M. 2014. Chondrocyte culture in three dimensional alginate sulfate hydrogels promotes proliferation while maintaining expression of chondrogenic markers. *Tissue engineering,* 20:1454-1464.

Mills, E., Cooper, C., Seely, D. & Kanfer, I. 2005. African herbal medicines in the treatment of HIV: Hypoxis and Sutherlandia. An overview of evidence and pharmacology. *Nutrition journal*, 4:1-6.

Minocha, M., Mandava, N.K., Kwatra, D., Pal, D., Folk, W.R., Earla, R. & Mitra, A.K. 2011. Effect of short term and chronic administration of *Sutherlandia frutescens* on pharmacokinetics of nevirapine in rats. *International journal of pharmaceutics*, 413:44-50.

Mishra, J., Drummond, J., Quazi, S.H., Karanki, S.S., Shaw, J.J., Chen, B. & Kumar, N. 2013. Prospective of colon cancer treatments and scope for combinatorial approach to enhanced cancer cell apoptosis. *Critical reviews in oncology/hematology*, 86:232-250.

Mitri, C., Soustelle, L., Framery, B., Bockaert, J., Parmentier, M.L. & Grau, Y. 2009. Plant insecticide L-canavanine repels Drosophila via the insect orphan GPCR DmX. *PLoS biology*, 7:e1000147.

Moon, J.Y. & Gwak, H.S. 2015. Role of the nuclear pregnane X receptor in drug metabolism and the clinical response. *Receptors and clinical investigation*, 2:1-8.

Mouradov, D., Sloggett, C., Jorissen, R.N., Love, C.G., Li, S., Burgess, A.W., Arango, D., Strausberg, R.L., Buchanan, D., Wormald, S. & O'Connor, L. 2014. Colorectal cancer cell lines are representative models of the main molecular subtypes of primary cancer. *Cancer research*, 74:3238-3247.

Mukherjee, P.K., Ponnusankar, S., Pandit, S., Hazam, P.K., Ahmmed, M. & Mukherjee, K. 2011. Botanicals as medicinal food and their effects on drug metabolizing enzymes. *Food and chemical toxicology*, 49:3142-3153.

Murua, A., Portero, A., Orive, G., Hernández, R.M., de Castro, M. & Pedraz, J.L. 2008. Cell microencapsulation technology: towards clinical application. *Journal of controlled release*, 132:76-83.

Naghibalhossaini, F., Shefaghat, M., Mansouri, A., Jaberi, H., Tatar, M. & Eftekhar, E. 2017. The Impact of Thymidylate Synthase and Methylenetetrahydrofolate Reductase Genotypes on Sensitivity to 5-Fluorouracil Treatment in Colorectal Cancer Cells. *Acta medica iranica*, 55:751-758.

Negi, S., Akbarsha, M.A. & Tyagi, R.K. 2008. Clinical correlates in drug-herbal interaction mediated via nuclear receptor PXR activation and cytochrome P450 induction. J*ournal of endocrinology reproduction*, 12:1-12.

Oga, E.F., Sekine, S., Shitara, Y. & Horie, T. 2016. Pharmacokinetic herb-drug interactions: insight into mechanisms and consequences. *European journal of drug metabolism and pharmacokinetics*, 41:93-108.

Pappe, L. 1847. A list of South African indigenous plants, used as remedies by the colonists of the Cape of Good Hope. Cape Town.

Parkinson, A., Mudra, D.R., Johnson, C., Dwyer, A. & Carroll, K.M. 2004. The effects of gender, age, ethnicity and liver cirrhosis on cytochrome P450 enzyme activity in human liver microsomes and inducibility in cultured human hepatocytes. *Toxicology and applied pharmacology*, 199:193-209.

Partridge, J. & Flaherty, P. 2009. An *in vitro* FluoroBlok tumor invasion assay. *Journal of visualized experiments*, 29:e1475.

Patel, K., Patel, V., Patel, K. & Gandhi, T. 2010. Validated HPTLC method for quantification of myricetin in the stem bark of Myrica esculenta Buch. Ham. Ex D. Don, myricaceae. *Journal of planar chromatography-modern TLC*, 23:326-331.

Pelkonen, O., Turpeinen, M., Hakkola, J., Honkakoski, P., Hukkanen, J. & Raunio, H. 2008. Inhibition and induction of human cytochrome P450 enzymes: current status. *Archives of toxicology*, 82:667-715.

Pereira, R.F. & Bártolo, P.J. 2015. 3D photo-fabrication for tissue engineering and drug delivery. *Engineering*, 1:90-112.

Phulukdaree, A., Moodley, D. & Chuturgoon, A.A. 2010. The effects of *Sutherlandia frutescens* extracts in cultured renal proximal and distal tubule epithelial cells. *South African journal of science*, 106:54-58.

Preissner, S.C., Hoffmann, M.F., Preissner, R., Dunkel, M., Gewiess, A. & Preissner, S. 2013. Polymorphic cytochrome P450 enzymes (CYPs) and their role in personalized therapy. *PloS One*, 8:1-12.

Pond, S.M. & Tozer, T.N. 1984. First-pass elimination: Basic concepts and clinical consequences. *Clinical pharmacokinetics*, 9:1-25.

Ramaiahgari, S.C., Waidyanatha, S., Dixon, D., DeVito, M.J., Paules, R.S. & Ferguson, S.S. 2017. From the cover: three-dimensional (3D) HepaRG spheroid model with physiologically relevant xenobiotic metabolism competence and hepatocyte functionality for liver toxicity screening. *Toxicological Sciences*, 159:124-136.

Ramos-Esquivel, A., Víquez-Jaikel, Á. & Fernández, C. 2017. Potential drug-drug and herb-drug interactions in patients with cancer: A prospective study of medication surveillance. Jo*urnal of oncology practice*, 13:e613-e622.

Reid, K.A., Maes, J., Maes, A., Van Staden, J., De Kimpe, N., Mulholland, D.A. & Verschaeve, L. 2006. Evaluation of the mutagenic and antimutagenic effects of South African plants. *Journal of ethnopharmacology,* 106:44-50.

Rodriguez-Antona, C., Gomez, A., Karlgren, M., Sim, S.C. & Ingelman-Sundberg, M. 2010. Molecular genetics and epigenetics of the cytochrome P450 gene family and its relevance for cancer risk and treatment. *Human genetics*, 127:1-17.

Sasidharan, S., Chen, Y., Saravanan, D., Sundram, K.M. & Latha, L.Y. 2011. Extraction, isolation and characterization of bioactive compounds from plants' extracts. *African journal of traditional, complementary and alternative medicines*, 8:1-10.

Saeidnia, S., Manayi, A. & Abdollahi, M. 2015. From *in vitro* Experiments to *in vivo* and Clinical Studies; Pros and Cons. *Current drug discovery technologies*, 12:218-224.

Schmelzer, G.H. & Gurib-Fakim, A. 2011. *Xysmalobium undulatum* (L.) WT Aiton. Prota, 11(2).

Schuster-Bockler, B & Lehner, B. 2012. Chromatin organization is a major influence on regional mutation rates in human cancer cells. *Nature*, 488:504–507.

Seier, J.V., Mdhluli, M., Dhansay, M.A., Loza, J. & Laubscher, R. 2002. A toxicity study of Sutherlandia leaf powder (*Sutherlandia microphylla*) consumption. *Medical research council, National research foundation (NRF) of South Africa,* 1:35.

Sfaxi, I.H., Ferraro, D., Fasano, E., Pani, G., Limam, F. & Marzouki, M.N. 2009. Inhibitory effects of a manganese superoxide dismutase isolated from garlic (*Allium sativum L*.) on *in vitro* tumoral cell growth. *Biotechnology progress*, 25:257-264.

Shargel, L., Wu-Pong, S. & Yu, A. 2012. Applied biopharmaceutics & pharmakokineetics. 6th ed. New York: McGraw-Hill.

Sheeja, K., Shihab, P.K. & Kut- tan, G. 2006. Antioxidant and anti-inflammatory activities of the plant *Andrographis paniculata Nees*. *Immunopharmacology and immunotoxicology*, 28:129-140.

Simmonds, P.C. 2000. Palliative chemotherapy for advanced colorectal cancer: systematic review and meta-analysis. Colorectal cancer collaborative group, 321: 531-535.

Singh, A. 2011. Herbalism, phytochemistry and ethnopharmacology. London: CRC Press, Science Publishers.

Singh, S., Sharma, B., Kanwar, S.S. & Kumar, A. 2016. Lead phytochemicals for anticancer drug development. *Frontiers in plant science*, 7:1-13.

Smitskamp-Wilms, E., Pinedo, H.M., Veerman, G., Ruiz Van Haperen, V.W. & Peters, G.J. 1998. Postconfluent multilayered cell line cultures for selective screening of gemcitabine. *European journal of cancer*, 34:921–926.

Stander, A., Marais, S., Stivaktas, V., Vorster, C., Albrecht, C., Lottering, M-L. & Joubert, A.M. 2009. *In vitro* effects of *Sutherlandia frutescens* water extracts on cell numbers, morphology, cell cycle progression and cell death in a tumorigenic and a non-tumorigenic epithelial breast cell line. *Journal of ethnopharmacology*, 124:45-60.

Supek, F. & Lehner, B. 2015. Differential DNA mismatch repair underlies mutation rate variation across the human genome. *Nature,* 521:81–84.

Swaffar, D.S., Ang, C.Y., Desai, P.B., Rosenthal, G.A., Thomas, D.A., Crooks, P.A. & John, W.J. 1995. Combination therapy with 5-fluorouracil and L-canavanine: *in vitro* and *in vivo* studies. *Anti-cancer drugs*, 6:586-593.

Swanepoel, R.A. 2018. *In vitro* evaluation of the efficacy of selected medicinal plant extracts against multidrug resistant cancer cells. Potchefstroom:NWU. (Dissertation- MSc).

Tai, J., Cheung, S., Chan, E. & Hasman, D. 2004. *In vitro* culture studies of *Sutherlandia frutescens* on human tumor cell lines. *Journal of ethnopharmacology*, 93:9-19.

Tanaka, Y., Yamato, M., Okano, T., Kitamori, T. & Sato, K. 2006. Evaluation of effects of shear stress on hepatocytes by a microchip-based system. *Measurement science and technology*, 17:3167-3170.

Tan, W.H. & Takeuchi, S. 2007. Monodisperse alginate hydrogel microbeads for cell encapsulation. *Advanced materials*, 19:2696-2701.

Thring, T.S.A. & Weitz, F.M. 2006. Medicinal plant use in the Bredasdorp/Elim region of the Southern Overberg in the Western Cape Province of South Africa. *Journal of ethnopharmacology*, 103:261-275.

Thürmann, P.A., Neff, A. & Fleisch, J. 2004. Interference of Uzara glycosides in assays of digitalis glycosides. *International journal of clinical pharmacology and therapeutics*, 42:281-284.

Tomoda, Y., Katsura, M., Okajima, M., Hosoya, N., Kohno, N. & Miyagawa, K. 2009. Functional evidence for Eme1 as a marker of cisplatin resistance. *International journal of cancer*, 124:2997-3001.

Tsujimoto, M., Agawa, C., Ueda, S., Yamane, T., Kitayama, H., Terao, A., Fukuda, T., Minegaki, T. & Nishiguchi, K. 2017. Inhibitory effects of juices prepared from individual vegetables on CYP3A4 activity in recombinant CYP3A4 and LS180 cells. *Biological and pharmaceutical bulletin*, 40:1561-1565.

Tung, Y.C., Hsiao, A.Y., Allen, S.G., Torisawa, Y.S., Ho, M. & Takayama, S. 2011. High-throughput 3D spheroid culture and drug testing using a 384 hanging drop array. *Analyst*, 136:473-478.

Usuludin, S.B.M., Cao, X. & Lim, M. 2012. Co-culture of stromal and erythroleukemia cells in a perfused hollow fiber bioreactor system as an *in vitro* bone marrow model for myeloid leukemia. *Biotechnology and bioengineering*, 109:1248-1258.

Van Cutsem, E., Köhne, C.H., Hitre, E., Zaluski, J., Chang Chien, C.R., Makhson, A., D'Haens, G., Pintér, T., Lim, R., Bodoky, G. & Roh, J.K. 2009. Cetuximab and chemotherapy as initial treatment for metastatic colorectal cancer. *New England journal of medicine*, 360:1408-1417.

Van Cutsem, E., Cervantes, A., Nordlinger, B. & Arnold, D. 2014. Metastatic colorectal cancer: ESMO Clinical Practice Guidelines for diagnosis, treatment and follow-up. *Annals of oncology*, 25:iii1-iii9.

Van der Weide, J. & Steijns, L.S.W. 1999. Cytochrome P450 enzyme system: genetic polymorphisms and impact on clinical pharmacology. *Annals of clinical biochemistry*, 36:722-729.

Van Wyk, B.E. & Gericke, N. 2000. People's plants: A guide to useful plants of Southern Africa. Briza Publications, Pretoria South Africa.

Van Wyk, B.E. & Van Staden, J. 2002. A review of ethnobotanical research in southern Africa. *South African journal of botany*, 68:1-13.

Van Wyk, B.E. 2008. A broad review of commercially important southern African medicinal plants. *Journal of ethnopharmacology*, 119:342-355.

Van Wyk, B.E. & Albrecht, C. 2008. A review of the taxonomy, ethnobotany, chemistry and pharmacology of *Sutherlandia frutescens* (Fabaceae). *Journal of ethnopharmacology*, 119:620-629.

Van Wyk, B.-E., Van Oudtshoorn, B. & Gericke, N. 2009. Medicinal plants of South Africa. 2nd ed. Pretoria: Briza Publications.

Vermaak, I., Enslin, G.M., Idowu, T.O. & Viljoen, A.M. 2014. *Xysmalobium undulatum* (uzara) – review of an antidiarrhoeal traditional medicine. *Journal of ethnopharmacology*, 156:135-146.

Vermeulen, K., Van Bockstaele, D.R. & Berneman, Z.N. 2003. The cell cycle: a review of regulation, deregulation and therapeutic targets in cancer. *Cell proliferation*, 36:131-149.

Vorster, C., Stander, A. & Joubert, A. 2012. Differential signaling involved in *Sutherlandia frutescens*-induced cell death in MCF-7 and MCF-12A cells. *Journal of ethnopharmacology*, 140:123-130.

Wang, L., Shelton, R.M., Cooper, P.R., Lawson, M., Triffitt, J.T. & Barralet, J.E. 2003. Evaluation of sodium alginate for bone marrow cell tissue engineering. *Biomaterials*, 24:3475-3481.

Wang, W., Zhao, Y., Rayburn, E.R., Hill, D.L., Wang, H. & Zhang, R. 2007. *In vitro* anti-cancer activity and structure–activity relationships of natural products isolated from fruits of *Panax ginseng*. *Cancer chemotherapy and pharmacology*, 59:589-601.

Wen, S., Chen, Y., Lu, Y., Wang, Y., Ding, L. & Jiang, M. 2016. Cardenolides from the Apocynaceae family and their anticancer activity. *Fitoterapia*, 112:74-84.

White, C. 2016. Inhibitory effect of selected herbal supplements on CYP450-mediated metabolism: an *in vitro* approach. Stellenbosch: Stellenbosch University. (Thesis- PhD).

Wong, S.K., Lim, Y.Y., Abdullah, N.R. & Nordin, F.J. 2011. Assessment of antiproliferative and antiplasmodial activities of five selected Apocynaceae species. *BMC complementary and alternative medicine*, 11:1-8.

World Health Organization (WHO). 2012. The Regional Strategy for Traditional Medicine in the Western Pacific (2011-2020).

World Health Organization (WHO). 2013. Traditional medicine strategy 2014-2023. Geneva: WHO.

World Health Organization (WHO). 12 Sep. 2018. Cancer fact sheet. http://www.who.int/en/news-room/fact-sheets/detail/cancer, [Date of access: 6 February 2019].

Wrzesinski, K., Rogowska-Wrzesinska, A., Kanlaya, R., Borkowski, K., Schwämmle, V., Dai, J., Joensen, K.E., Wojdyla, K., Carvalho, V.B. & Fey, S.J. 2014. The cultural divide: exponential growth in classical 2D and metabolic equilibrium in 3D environments. *PloS one*, 9:e106973.

Wrzesinski, K. & Fey, S. 2018. MetaboliFEy reprogramming and the recovery of physiological functionality in 3D cultures in micro-bioreactors. *Bioengineering*, 5:1-25.

Wynendaele, E., Versbeke, F., D'Hondt, M., Hendrix, A., De Wiele, C.V., Burvenich, C., Peremans K., De Wever, O., Bracke, M. & Spiegeleer, M. 2015. Crosstalk between the microbiome and cancer cells by quorum sensing peptides. *Peptides,* 64:40–48.

Xu, X., Farach-Carson, M.C. & Jia, X. 2014. Three-dimensional *in vitro* tumor models for cancer research and drug evaluation. *Biotechnology advances*, 32:1256-1268.

Yan, Z. & Caldwell, G.W. 2001. Metabolism, profiling, and cytochrome P450 inhibition and induction in drug discovery. *Current topics in medicinal chemistry*, 1:403-425.

Yates, J.S., Mustian, K.M., Morrow, G.R., Gillies, L.J., Padmanaban, D., Atkins, J.N., Issell, B., Kirshner, J.J. & Colman, L.K. 2005. Prevalence of complementary and alternative medicine use in cancer patients during treatment. *Supportive care in cancer*, 13:806-811.

Zadoyan, G. & Fuhr, U. 2012. Phenotyping studies to assess the effects of phytopharmaceuticals on *in vivo* activity of main human cytochrome P450 enzymes. *Planta medica*, 78:1428-1457.

Zanger, U.M. & Schwab, M. 2013. Cytochrome P450 enzymes in drug metabolism: regulation of gene expression, enzyme activities, and impact of genetic variation. *Pharmacology and therapeutics*, 138:103-141.

Zhou, S.F. 2008. Drugs behave as substrates, inhibitors and inducers of human cytochrome P450 3A4. *Current drug metabolism*, 9:310-322.

CHAPTER 3

This chapter describes all materials and methods used during this study. This includes: basic cell culturing and cell seeding, the 3-(4,5-dimethylthiazol-2-yl)-2,5- diphenyl tetrazolium bromide assay, optimisation and characterisation of the three-dimensional sodium alginate encapsulated spheroid model, as well as validation and implementation of the model.

3.1. Introduction

The probability of success for drug development in oncology is extremely low, with only an estimated 3.4% of new agents progressing successfully through clinical trials (Wong *et al*., 2019). Clearly, there is a great need for more effective, accurate and cost-effective preclinical screening models (Breslin & O'Driscoll, 2013). While *in vivo* animal studies can provide fundamental knowledge, their high cost and poor translation to human subjects in predicting clinical outcomes causes a gap in the drug development channel (Waring *et al*., 2015).

For the past four decades, cells cultured in two dimensions on a flat surface have been routinely and persistently applied in thousands of laboratories worldwide. These two-dimensional (2D) cultures are, however, seen as primitive as they do not reproduce the anatomy and physiology of the *in vivo* situation (Haycock, 2011). This might be because the cells do not express the correct *in vivo* phenotype since the microenvironment has changed. The cell-cell and cell-matrix interaction of cells cultured in 2D are reduced dramatically because the cells lack the heterogeneity and three-dimensional (3D) architecture found *in vivo*. It is also evident that many hormonal and nutritional stimuli are absent (Freshney, 2015). Pre-clinical research to describe the molecular mechanisms that drive cancer growth and progression, or to determine the efficacy of therapeutics, are usually carried out in 2D *in vitro* models (Nyga *et al*., 2011). But, as mentioned above, the use of these models are clearly not sufficient. The use of next-generation 3D cell culture models is expected to improve the predictive capability and effectiveness of drug toxicological predictions (Astashkina & Grainger, 2014).

In this study, LS180 cells were cultured as sodium alginate encapsulated spheroids using rotating clinostat-based bioreactors. It is necessary to establish whether this model can be used for future anticancer activity screening, as well as drug-biotransformation studies. The standard chemotherapeutic drug, paclitaxel, was therefore used to validate the reactivity of the model for anticancer drug screening. To evaluate the potential use of the model for drug biotransformation research, gene expression was performed to relatively quantify the cytochrome P450 (CYP450) enzymes, *CYP3A4* and *CYP2D6.* Furthermore, the model was then implemented to study the anticancer effects of *Sutherlandia frutescens* and *Xysmalobium undulatum* in the treatment of colorectal cancer, as well as their effects on *CYP3A4* and *CYP2D6* gene expression.

3.2. General materials and reagents

The American Tissue Culture Collection (ATCC, Manassas, VA) was the authorised supplier of the LS180 cell line (cat. no. #CL-187™). Cells were grown in low-glucose Dulbecco's Modified Eagle's medium (DMEM) (Gibco; Thermo Fisher Scientific, Johannesburg, South Africa), supplemented with foetal bovine serum (FBS) (Gibco; Thermo Fisher Scientific, Johannesburg, South Africa), L-glutamine (200 mM; Lonza; Whitehead Scientific (Pty) Ltd, Cape Town, South Africa), non-essential amino acids (NEAA) (100 X; Sigma-Aldrich, Johannesburg, South Africa) and penicillin/streptomycin (10 000 penicillin U/ml/ 10 000 streptomycin U/ml; Lonza, Whitehead Scientific, Cape Town, South Africa). Other reagents and materials used included 0.1 µm sterile filtered phosphate buffered saline (PBS) (1 X; Hyclone; Separations, Johannesburg, South Africa) and trypsin-ethylenediaminetetraacetic acid (EDTA) (Lonza; Whitehead Scientific (Pty) Ltd, Cape Town, South Africa). Triton X-100, thiazolyl blue tetrazolium bromide powder, dimethyl sulfoxide (DMSO) and paclitaxel were purchased from Sigma-Aldrich (Johannesburg, South Africa).

Cells were cultured in 75 cm^2 cell culture flasks (Corning Inc., Ascendis medical, Johannesburg, South Africa) and Costar® flat bottom (clear and black) 96-well plates (Corning Inc., Ascendis medical, Johannesburg, South Africa). Raw powdered plant material of *S. frutescens* (SFFW) and *X. undulatum* (XU174) were purchased from Afrinatural holdings (Prestige Laboratory Supplies CC, KwaZulu-Natal, South Africa). Sodium alginate was purchased from Sigma-Aldrich (Johannesburg, South Africa), calcium chloride dihydrate ($CaCl_2.2H_2O$) and sodium chloride (NaCl) from UnivAR (SAARCHEM, Johannesburg, South Africa). The ToxiLight® BioAssay kit containing the adenylate kinase (AK) assay buffer and the AK detection reagent was purchased from Lonza (Whitehead Scientific (Pty) Ltd., Cape Town, South Africa). Adenosine triphosphate (ATP) disodium salt hydrate standard was purchased from Sigma Aldrich (Johannesburg, South Africa). The Quick Start™ Bradford Protein assay containing dye reagent concentrate and 2 mg/ml bovine serum albumin (BSA) standards were purchased from Bio-Rad (Lasec SA (Pty) Ltd., Midrand, South Africa). The lysis buffer was donated by Professor Krzysztof Wrzesinski from Celvivo® ApS (Odense, Denmark). The CellTiter-Glo® Luminescent Cell viability assay was supplied by Promega (Anatech Instruments (Pty) Ltd., Johannesburg, South Africa). Microgravity ProtoTissue™ bioreactors were purchased from Celvivo® ApS (Odense, Denmark).

3.3. Preparation and characterisation of the plant material aqueous extracts

3.3.1. Preparation of the *Sutherlandia frutescens* and *Xysmalobium undulatum* aqueous extracts

The *S. frutescens* and *X. undulatum* aqueous extracts were previously prepared by Mr. R.A. Swanepoel (Swanepoel, 2018). Briefly, both extracts were prepared at a 1:10 ratio in water (plant: liquid) followed by sonication at 45°C for 45 min (Eumax® ultrasonic cleaner, Labotec, Midrand, South Africa). The suspension was then centrifuged (5 000 x *g* for 10 min) in a Sigma 3-16 KL Laborzentrifugen (Germany) and the supernatant collected. The pellet was then re-suspended in water followed by sonication and centrifugation as mentioned above. The combined supernatants were once again centrifuged (1 218 *x g* for 5 min) followed by filtration of the supernatant through Whatman™ filtration paper with a pore diameter of 125 mm (Whatman™, Sigma, Johannesburg, South Africa). Second to last, the collected filtrate was frozen overnight at -80°C followed by lyophilisation in a Virtis freeze dryer (SP Scientific, Gardiner, New York, USA). Following lyophilisation, it was powdered with a mortar and pestle and stored in a desiccator until further use.

3.3.2. Chemical fingerprinting of all plant extracts

Chemical characterisation was done on all plant extracts following preparation to enable the identification, comparison and detection of the main active phytochemicals. The ultra-performance liquid chromatography (UPLC) analyses were performed by Prof A Viljoen (Tshwane University of Technology).

3.3.3. Chemical fingerprinting of *Sutherlandia frutescens* and *Xysmalobium undulatum*

Sample preparation for the UPLC analysis was done by adding 2 mg of freeze-dried powder of *S. frutescens* and *X. undulatum,* respectively, to 2 ml of methanol; followed by sonication (10 min) and filtration using a 0.2 µm syringe filter. After UPLC analysis of *S. frutescens*, a cycloartane-like triterpene glycoside (SU1) marker molecule was identified. Following UPLC analysis of *X. undulatum* the marker molecule Uzarin was also identified to be present in the extract. The UPLC analysis was performed on a Waters Acquity UPLC system, equipped with a photodiode array (PDA) detector (Waters, Milford, MA, USA) and an Acquity UPLC BEH C18 column (150 mm × 2.1 mm i.d., 1.7 µm particle size, Waters) maintained at 40ºC as previously described (Swanepoel, 2018).

3.4. Two-dimensional cell culturing and seeding

Cells were cultured in low glucose DMEM supplemented with 10% FBS, 1% NEAA, 1% L-glutamine and 1% penicillin/streptomycin in 75 cm^2 cell culture flasks. Cells were cultured under standard culturing conditions of 37ºC, 5% CO_2 and 95% humidified air in a Galaxy 170R incubator (Eppendorf Company, Stevenage, UK). Culture medium was replaced every second day. Upon reaching 80% confluence (assessed visually with a light microscopy) cells were sub-cultured by means of scraping (cells detach easily and no trypsinisation is necessary).

For seeding in 96-well plates to perform the 3- (4,5- dimethylthiazol- 2- yl)- 2,5- diphenyltetrazolium bromide (MTT) assay, cells were subjected to trypsinisation to reach a single cell suspension upon reaching 80% confluence. Cells were washed twice with 10 ml PBS to remove all culture medium residues. Trypsin (3 ml) was added and the flask was incubated at 37ºC for 5 min to allow cells to detach. After detachment, 1 ml FBS and 5 ml of culture medium was added to deactivate the trypsin and speed up the recovery process of the cells. The cell suspension was transferred to a 15 ml tube and centrifuged in a Sigma 3-16L benchtop centrifuge (Sigma, Osterode am Harz, Germany) at 140 x *g* for 5 min. The supernatant was removed and the cell pellet was resuspended in pre-warmed culture medium. The cell suspension was counted using the Scepter 2.0 automated cell counter (Millipore, Massachusetts, USA) with 60 µm sensors. The cell suspension was counted in triplicate following addition of 100 µl cell suspension to 900 µl PBS in a microcentrifuge tube.

The chosen seeding density for the LS180 cell line was 8 000 cells per well. This was predetermined to ensure that after 96 h, the cells would have reached 80% confluence. The cell suspension was diluted with culture medium to obtain the desired cell concentration and loaded at a volume of 200 µl per well. The seeded 96-well plates were incubated at 37ºC, 5% CO_2 and 95% humidified air for 24 h to allow cells to adhere. The empty outer wells were pre-filled with PBS to prevent the edge effect.

3.5. Two-dimensional anticancer activity pre-screening

3.5.1. Introduction

Since its development by Mosmann in the 1980's, MTT assay is seen by many as the gold standard to determine cell viability and proliferation (Mosmann, 1983). MTT is a colorimetric assay that measures a cell's metabolic activity (Bahuguna *et al.,* 2017). The MTT assay is a sensitive, quantitative and reliable high throughput assay to use when measuring cell viability

(Vega-Avila & Pugsley, 2011). In living cells, the mitochondria and other organelles (like the endoplasmic reticulum) produce many enzymes, such as nicotinamide adenine dinucleotide phosphate (NADP) hydrogen (H)-dependent oxidoreductases and dehydrogenases. These enzymes reduce the MTT salt to formazan crystals, and the absorption of dissolved formazan in the visible region correlates with the number of viable cells (Mueller *et al*., 2004). This assay can be used to determine the half-maximal inhibitory concentration (IC_{50}) of a compound. The IC_{50} value can be defined as the concentration of a compound needed to inhibit the biological activity of cells by 50%, compared to an untreated control (Cortés *et al*., 2001).

The biochemical mechanism behind the MTT assay is the enzymatic conversion of the yellow tetrazolium salt [3-(4,5-dimethylthiazol-2-yl)-2,5- diphenyl tetrazolium bromide] into insoluble formazan crystals [(E, Z)-5-(4,5-dimethylthiazol-2-yl)-1,3-diphenylformazan] by oxidoreductase enzymes, as shown in **Figure 3.1** (Lü *et al.,* 2012; Bahuguna *et al.,* 2017).

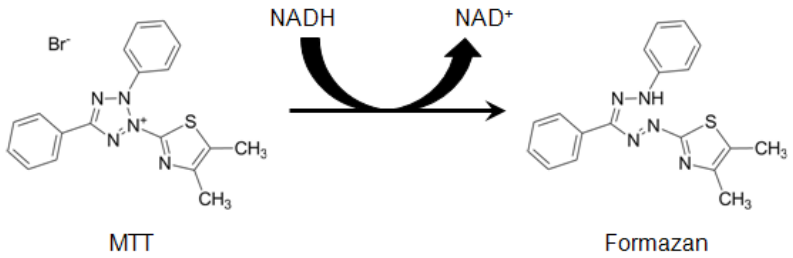

Figure 3.1. The enzymatic conversion of 3-(4,5-dimethylthiazol-2-yl)-2,5- diphenyl tetrazolium bromide into (E, Z)-5-(4,5-dimethylthiazol-2-yl)-1,3-diphenylformazan (formazan) by oxidoreductase enzymes (Riss *et al.,* 2016).

The formazan crystals accumulate as insoluble precipitate inside cells and near the cell surface in the culture medium (Riss *et al.,* 2016). The formation of these crystals could pose a problem, as the plasma membrane might be injured due to needle shaped formazan crystals (Lü *et al.*, 2012; Van Tonder *et al.*, 2015). The reduction of MTT salts have also been shown to differ from cell line to cell line, and this reduction decreases greatly as a cell line ages. There is also the possibility of non-mitochondrial enzymes potentially reducing tetrazolium salts (Sylvester, 2011). The formazan crystals must be solubilised before measuring, and many solubilisation methods exist. Some of these include: DMSO, acidic isopropanol, dimethylformamide and combinations

of detergent and organic solvent (Mossman, 1983; Denizot & Lang, 1986; Tada *et al.,* 1986; Hansen *et al.,* 1989; Riss *et al.,* 2016). The quantity of these formed and dissolved formazan crystals are then measured by recording the changes in absorbance at a wavelength of 560 nm with a reference wavelength of 630 nm, using a plate reading spectrophotometer (Riss *et al.,* 2016). These values can then be used to calculate relative inhibition values. The IC_{50} value represents the concentration of the inhibitor needed to inhibit the cancer cell growth by 50% (Burlingham & Widlanski, 2003).

Although the assay has some drawbacks, in this study the MTT assay was chosen as a fast and cost effective screening method to determine the IC_{50} ranges of *S. frutescens*, *X. undulatum* and paclitaxel in the LS180 cell line. These IC_{50} ranges will later be applied in validation and implementation of the 3D model.

3.5.2. Study design

The aim of this preliminary screening was to evaluate the anticancer activity of *S. frutescens*, *X. undulatum* aqueous extracts and paclitaxel (as a standard chemotherapeutic drug) after exposure of the cell line to different concentrations of the compounds for 96 h. The relative cell inhibition values were then used to statistically calculate the IC_{50} values, together with their 95% confidence limits.

3.5.3. Preparation of aqueous plant extracts

The crude aqueous extracts of *S. frutescens* and *X. undulatum* were prepared daily prior to commencing with the experiment. A stock solution of 8 mg/ml *S. frutescens* and 0.5 mg/ml *X. undulatum* were prepared in volumetric flasks, by dissolving the powder in pre-heated culture medium. The pH of the extracts was measured to ensure that they fall in the physiological range of normal pH (±7). The stock solutions were vortexed to ensure that a homogenous solution was formed, followed by sterilisation filtration using a 0.22 µm syringe filter. *S. frutescens* dilutions were prepared in culture medium in the range of 1 to 8 mg/ml, and *X. undulatum* from 0.05 to 0.5 mg/ml.

3.5.4. Preparation of the chemotherapeutic drug, paclitaxel

Paclitaxel is described as a white powder soluble in organic solvents such as DMSO. A stock solution of 1.171 mM was prepared on a weekly basis by dissolving paclitaxel powder in DMSO, and storing it as four separate aliquots at -20°C. These stock aliquots were covered with aluminium foil prior to freezing to prevent light exposure (Duggett *et al*., 2017). Prior to daily dosing the stock aliquots were removed from the freezer and thawed in a block heater at 37°C. The stock solution was then diluted to an intermediate concentration of 1.500 µM using culture medium, followed by further dilution in the range of 1.000 nM – 1.000 µM.

3.5.5. The 3-(4,5-dimethylthiazol-2-yl)-2,5- diphenyl tetrazolium bromide cytotoxicity assay

Cytotoxicity is one of the most common biological factors measured after experimental manipulation because it is easily measured (Cho *et al*., 2008). The MTT assay was used to determine the relative percentage cell viability inhibition, using the method adapted from Wentzel *et al.* (2017). Briefly, 24 h post-seeding, culture medium was removed and cells were treated with 200 µl of culture medium containing the various compounds at various concentrations (0 h). Medium containing treatment was replenished in 24 h intervals, until the assay was performed after 96 h exposure. Untreated wells (to indicate 100% cell viability), DMSO background control wells (cells treated with DMSO to eliminate background interference) and dead cells standard (cells treated with Triton X-100 to indicate 97 - 100% cell viability inhibition) received fresh supplemented medium during medium exchanges. A highest plant concentration control (8 mg/ml for *S. frutescens* and 0.5 mg/ml for *X. undulatum*) was included to ensure that the extract caused no interference with the MTT assay.

After 96 h exposure, medium was removed from all the wells and the cells were washed twice with 100 µl PBS. The dead cell standard cells were then treated with 200 µl of 0.2% Triton X-100 (dissolved in PBS) for 15 min, and subsequently carefully washed twice with 100 µl PBS. All wells (excluding the DMSO background standard) then received 180 µl non-additive medium. Fresh MTT stock of 5 mg/ml (dissolved in PBS) was prepared and wrapped in aluminium foil to prevent light exposure. A volume of 20 µl MTT stock solution was added to each well (excluding the DMSO background control wells) to achieve a final MTT solution concentration of 0.5 mg/ml (Shandiz *et al.*, 2017). The 96-well plate was then covered with aluminium foil and placed on a compact rocker for 5 min, followed by further incubation at 37ºC for 4 h. Following incubation, the

medium of each well (except that of the highest plant concentration wells) was carefully removed and replaced with 200 µl DMSO. The plate was then shaken on the compact rocker for 1 h. The amount of dye accumulated by the cells in each well was quantified by measuring the absorbance at 560 nm, with a reference wavelength of 630 nm (to eliminate the effect of bubbles, cell debris and light scattering) (Riss & Moravec, 2004) using a SpectraMax® plate reader (Paradigm® Multi-Mode Detection Platform; Molecular Devices®; Separations, Gauteng, South Africa).

3.5.6. Data analysis

The relative percentage viable cells were calculated using **Equation 1**, whereby the absorbance values for each group were expressed as percentage cell viability relative to the untreated control.

$$\%\ \text{Cell viability} = \frac{(\Delta\ \text{sample} - \Delta\ \text{blank})}{(\Delta\ \text{untreated control} - \Delta\ \text{blank})} \times 100 \qquad \textbf{Eq. 1}$$

Where Δ sample is the difference between the wavelength value 560 nm and that of the background wavelength 630 nm, measured for all the sample groups on the plate. Δ Blank is the difference between the wavelength value 560 nm and that of the background wavelength 630 nm of the DMSO control wells. Δ Untreated is the difference between the wavelength value 560 nm and that of the background wavelength 630 nm measured for the untreated control.

Equation 2 was subsequently used to determine the relative percentage cell viability inhibition (IC):

$$\%\ IC = 100\% - \%\ cell\ viability \qquad \textbf{Eq. 2}$$

3.5.7. Statistical data analysis

All MTT experiments were performed in six-fold. SPSS statistical analysis software (IBM Analytics, Version 25), in conjunction with the Probit Analysis Method, were used to calculate IC_{50} values and 95% confidence limit ranges for *S. frutescens*, *X. undulatum* and paclitaxel, using the data from the MTT analyses.

The IC_{50} values will then be divided by the measured soluble protein content (µg) of the 8 000 cells seeded per well. This will enable calculation of the approximate wet biomass of the cells in each well. The concentration of the various treatments can then be divided by the protein content in µg by to obtain a 2D IC_{50} value of the treatment per µg of soluble protein.

3.6. Culturing of the LS180 sodium alginate encapsulated spheroid model

During this study, the rotating clinostat-based bioreactors developed by Fey & Wrzesinski (2012) were used, as they provide a simple method for producing relatively large spheroids with better cell differentiation that more closely resembles the *in vivo* situation. The hydrogel, sodium alginate, which is obtained from brown seaweed is the biomaterial used to encapsulate the cells. Alginates are anionic polysaccharides composed of β-D-mannuronic acid and α-L-guluronic acid and they form hydrogels following cross-linking with Ca^{2+}, Ba^{2+} or Fe^{3+} (Tan & Takeuchi, 2007). Sodium alginate is biocompatible and has moderately high diffusion rates of macromolecules, as well as low toxicity. It is cost effective and biodegradable under normal physiological conditions, and it also mimics the extracellular matrix of body tissues fairly well (Gombotz & Wee, 2012; Lee & Mooney, 2012).

Calitz (2017) established the basic method for the LS180 sodium alginate encapsulated spheroid model, however, the model was not fully optimised or characterised in that study. During this study, the method was optimised and the model validated and implemented.

3.6.1. Preparation of sodium alginate and cross-linker

A sodium alginate solution of 2.5% w/v was prepared in PBS and autoclaved. The cross-linker solutions, which consisted of 50 mM $CaCl_2$ and 150 mM NaCl, were prepared in distilled water and filtered through a 0.8/0.2 µm Acrodisc® PF Supor® membrane syringe filter (PALL; Separations, Midrand, South Africa) to sterilise the solution.

3.6.2. Bioreactor setup

Bioreactors were prepared by filling the water chambers (**Figure 3.2 B**) with distilled, autoclaved water and adding approximately 8 ml culture medium to the cell chamber (**Figure 3.2 A**). The bioreactors were placed onto a drive-unit (BAM v4.6; CelVivo® ApS, Odense, Denmark) in an incubator to rotate and equilibrate overnight at 37°C and 5% CO_2. Prior to the addition of spheroids, all growth medium was removed from the cell chamber.

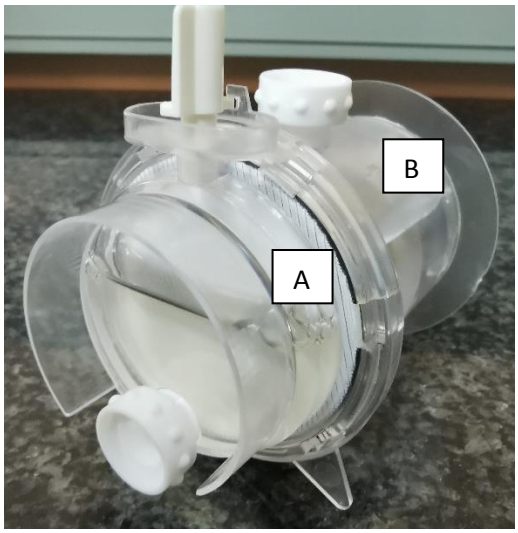

Figure 3.2. Photograph of an equilibrated bioreactor, with A indicating the cell chamber and B indicating the water chamber.

3.6.3. Preparation of a trypsinised LS180 cell suspension

A cell suspension was prepared from 80% confluent LS180 cells through trypsinisation. This was done, since scraping the cells made it difficult to obtain a single cell suspension. Cells were only trypsinised once before seeding. Cells were washed twice with 10 ml PBS followed by the addition of 3 ml Trypsin-EDTA for 5 min at 37°C. Following trypsinisation, the cell suspension was treated with 1 ml FBS and 5 ml warm culture medium. The cell suspension was centrifuged for 5 min at 140 x *g* to remove the trypsin-containing media. Culture medium (10 ml) was added and the pellet was re-suspended. The cell suspension was then counted using a Sceptre cell counter (Merck Millipore, Johannesburg, South Africa) and 60 µm sensor tips (Merck Millipore, Johannesburg, South Africa). After diluting the cell suspension to 2 000 cells/µl the cell suspension was again centrifuged at 140 x *g* for 5 min, the supernatant was removed and the pellet gently re-suspended in the prepared sodium alginate solution at 37°C.

3.6.4. Preparation of sodium alginate encapsulated spheroids

The LS180 cells, imbedded in the sodium alginate solution, were pipetted as 1 µl droplets onto square Perspex blocks covered with hydrophobic paraffin film, as illustrated in **Figure 3.3**. Distilled and autoclaved water was added to the bottom of the petri dish to ensure a humid environment. After the embedded cells were pipetted onto the blocks, a volume of 0.5 µl of the

50 mM $CaCl_2$, 150 mM NaCl cross-linker solution was added to each droplet. The petri dish was then covered and incubated at room temperature for 5 min. Spheroids were collected into culture medium after incubation and transferred to the bioreactors. Each bioreactor used during characterisation of the model contained 300 spheroids on day 0. The speed of each bioreactor was initially set at 16 rotations per minute (rpm).

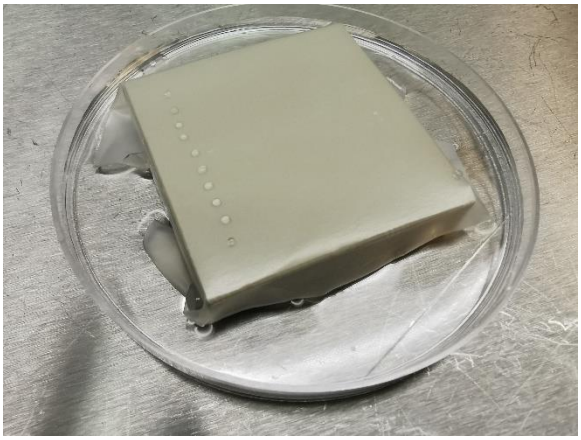

Figure 3.3. Ten 2.5% *w/v* sodium alginate encapsulated LS180 cell spheroids on a prepared block.

3.6.5. Encapsulated LS180 cell spheroid maintenance

The day the spheroids were transferred to the bioreactors, is referred to as day 0. The culture medium was exchanged after three days of culturing during the first week, followed by medium exchange every second day thereafter. Upon culture medium exchange, the bioreactor was removed from the drive unit and the spheroids were allowed to settle at the bottom of the bioreactor. The plug at the top of the cell chamber (see **Figure 3.2**) was removed. Approximately 90% of the spent culture medium was removed using a 10 ml syringe and 21'G needle. Culture medium was slowly replaced, taking care not to disrupt the spheroids, after which the plug at the top of the cell chamber was replaced. The plug cup was washed with 70% *v/v* ethanol and the bioreactor was placed back onto the drive unit in the incubator. Rotation speed was adjusted daily to keep the spheroids suspended in essentially a 'stationary orbit' (i.e. to prevent the spheroids from settling down). Photomicrographs of the developing spheroids were taken daily using a Nikon Eclipse TS100 light microscope (Nikon Instruments, Tokyo, Japan) and a DFK 72AUC02 USB 2.0 colour industrial camera (The Imaging Source, Bremen, Germany).

3.7. Characterisation of the sodium alginate encapsulated LS180 spheroid model

The optimised sodium alginate encapsulated LS180 spheroid model had to be fully characterised in terms of cell growth, cell viability, glucose consumption and CYP450 enzyme expression. This was done to determine if the cells would remain viable in the model, and for how long. Also, it was necessary to determine the normal behaviour of the model, prior to any interventions.

3.7.1. Study design

To establish the viability of the encapsulated cells, the model was characterized for a period of 20 days. The following parameters were measured: intracellular ATP, soluble protein content, extracellular AK, glucose consumption and CYP450 gene expression. During characterisation, samples were collected three times per week.

For the first ten days, sampling in microcentrifuge tubes were as follows: five spheroids for the CYP450 gene expression, five for the soluble protein assay and three for intracellular ATP assay.

From day 11 and onwards, sampling in microcentrifuge tubes was as follows: five spheroids for the CYP450 gene expression and one spheroid each for intracellular ATP and soluble protein assays. All experiments during this time consisted of three biological replicates with three technical replicates each.

For the duration of the characterisation, 200 µl spent medium was sampled for every biological replicate.

Following characterisation to establish spheroid viability in terms of soluble protein content, intracellular ATP, extracellular AK and glucose consumption, the ideal window in which to use the model for further assays could be established.

3.7.2. The Bradford soluble protein assay

This protein determination assay involves the binding of Coomassie Brilliant Blue G-250 dye to proteins. When this dye binds to protein, it is converted to its stable un-protonated blue form. This blue protein-dye form is then detectable at 595 nm using a spectrophotometer or a microplate reader. This assay is very reproducible and quick, with the dye binding process nearly complete in approximately 2 min with good colour stability for 1 h. Furthermore, there is little or no

interference from carbohydrates such as sucrose, nor from cations such as sodium or potassium (Bradford, 1976).

After sampling of the spheroids, all culture medium was removed from the microcentrifuge tubes and the dry spheroids flash frozen with liquid nitrogen. The microcentrifuge tubes were then stored in a -150°C freezer until sample analysis.

Finally, the protein content was expressed as an average soluble protein content per spheroid (µg).

The Bradford assay was used to determine the amount of soluble protein per spheroid. Samples were removed from the freezer and allowed to equilibrate to room temperature. Briefly, 450 µl water was added to each biological replicate and mixed vigorously to ensure that spheroids were broken. In a clear bottom 96-well plate, 150 µl of each biological replicate was then loaded as three technical replicates, followed by the addition of 10 µl lysis buffer to each well. The protein assay dye reagent (40 µl) was then added to all wells and mixed vigorously. The plate was centrifuged at 1 218 x *g* for 2 min to remove all bubbles. The absorbance was measured with a Spectramax® Paradigm plate reader at 595 nm and all samples were quantified relative to a BSA standard.

Table 3.1. Bovine Serum Albumin standard concentration series preparation for the Bradford soluble protein assay.

BSA concentration in µg/µl	Amount of water to be added (µl)	Amount of lysis buffer to be added (µl)	Amount of 0.1 mg/ml BSA to be added (µl)	Amount of colour reagent to be added (µl)
0.000	150	10	0	40
0.005	140	10	10	40
0.010	130	10	20	40
0.015	120	10	30	40
0.020	110	10	40	40
0.025	100	10	50	40
0.030	90	10	60	40

The BSA standard used in this assay was prepared as follows. Firstly, 40 µl of the standard was diluted with 760 µl of water to obtain a concentration of 0.1 mg/ml BSA. A standard concentration series was then prepared and loaded in triplicate according to **Table 3.1**.

3.7.3. Intracellular adenosine triphosphate cell viability assay

One of the most commonly used assays for 3D cell culture viability assessment, is the quantification of a luminescent signal that is generated by the conversion of luciferin by luciferase as a function of cytoplasmic ATP concentrations (Riss *et al*., 2014; Kijanska & Kelm, 2016). ATP is the primary energy unit for cells, and intracellular levels of this compound offer a potential marker for cell viability and growth (Ahmann *et al*., 1987).

The ATP assay was performed directly after sampling to ensure accurate results. The ATP standard was prepared by adding 1 ml of sterile water to the ATP standard vial and dividing it in 65 µl aliquots. These aliquots were then frozen at -20°C until needed for an assay.

Table 3.2. Adenosine triphosphate standard preparation for the intracellular adenosine triphosphate levels cell viability assay.

Standard number	Standard concentration (mM)	Standard concentration (mmol/L)	ATP standard (µl)	PBS buffer (µl)
Standard 1	0.1	0.2	50 stock	450
Standard 2	1.25×10^{-2}	2.50×10^{-2}	75 of standard 1	525
Standard 3	1.56×10^{-3}	3.12×10^{-3}	75 of standard 2	525
Standard 4	1.95×10^{-4}	3.91×10^{-4}	75 of standard 3	525
Standard 5	2.44×10^{-5}	4.88×10^{-5}	75 of standard 4	525
Standard 6	3.05×10^{-6}	6.10×10^{-6}	75 of standard 5	525
Standard 7	3.81×10^{-7}	7.63×10^{-7}	75 of standard 6	525
Standard 8	0	0	0	525

For the ATP assay, an ATP standard concentration series (provided in **Table 3.2**) was plated in triplicate (3 x 100 µl) and 100 µl CellTiter-Glo® luminescent lysis buffer was added in black, clear bottom 96-well plates. All culture medium was removed from the sampled spheroids in the microcentrifuge tubes. Following the addition of 300 µl PBS to each biological replicate, it was then mixed vigorously to ensure that spheroids were broken. Three technical replicates of each biological replicate were then plated in the 96-well plate. Finally, 100 µl of CellTiter-Glo® luminescent lysis buffer was added to all sample wells and mixed. The plate was covered and shaken in the dark for 40 min. The plate was then centrifuged at 1 218 x *g* to remove all bubbles. The luminescence was measured with a Spectramax® Paradigm plate reader and all samples were quantified relative to the known ATP standard.

Finally, the intracellular ATP content was expressed as an average ATP content per spheroid (µM).

3.7.4. Extracellular adenylate kinase cell death assay

AK is a universal intracellular enzyme that is released in the extracellular space upon cell lysis (Jacobs *et al*., 2013). It is therefore a useful marker of cell death.

Spent culture medium samples were collected in microcentrifuge tubes. The medium (3 biological replicates of 200 µl each) was centrifuged at 140 x *g* for 15 min, and 160 µl of the supernatant was then transferred to a new microcentrifuge tube. The transferred samples were once again centrifuged at 15 000 x *g* for 15 min and 140 µl of the supernatant transferred to a new tube. The samples were then flash frozen and stored at -150°C until further use.

All samples were removed from the freezer and equilibrated to room temperature. The three biological replicates were then plated with three technical replicates of each (20 µl per well) in black, clear bottom 96-well plates and 100 µl of AK detection reagent was added. The plate was covered and placed on a compact rocker for 20 min, followed by centrifugation at 1 218 x *g* for 2 min to remove bubbles. The luminescence was measured with a Spectramax® Paradigm plate reader and all samples were quantified relative to a known dead cell standard to determine the amount of dead cells per ml of culture medium.

The known dead cell standard was prepared by treating a known concentration of cells with Cyto-Tox Glo® digitonin lysis buffer (Promega; Anatech Instruments (Pty) Ltd., Johannesburg, South Africa). The cell concentration used was 1.117×10^6 cells/ml. The dead cell standard was then diluted with heat-treated medium and exposed to the same conditions as the samples.

3.7.5. Glucose consumption

Following the second centrifugation step of the AK samples and the removal of 140 µl of the spent medium, the remaining medium was used to measure the glucose content of the spent medium.

The OneTouch® Select™ blood glucose monitoring system and OneTouch® Select™ test strips were used for the assay. Firstly, a known glucose concentration standard was used to ensure that the strips and the machine were working and of good quality. The OneTouch Ultra™ control solution (Lifescan) was used. Subsequently, 3 µl of the spent medium was used from each biological replicate, and loaded on the test strips by means of a pipette. The glucose concentrations were read and noted. Deducting the remaining glucose content from the glucose content in unspent medium, provides an approximation of glucose consumption by the cells in culture.

3.7.6. Quantitative reverse transcription polymerase chain reaction relative cytochrome P450 gene expression

To confirm the presence of CYP3A4 and CYP2D6, and to investigate the potential changes due to 3D culture conditions, quantitative reverse transcription polymerase chain reaction (qRT-PCR) was performed. After sampling of the spheroids, all culture medium was removed from the microcentrifuge tubes and 200 µl RNAlater (Whitehead Scientific (Pty) Ltd., Cape Town, South Africa) solution was added to each sample tube. The microcentrifuge tubes were then stored in a -80°C freezer until further use.

Before ribonucleic acid (RNA) extraction, samples were thawed at room temperature followed by centrifugation (100 x *g* for 10 min). Total RNA was extracted using the PureLink™ RNA Mini Kit according to the manufacturer's guidelines, followed by RNA quantification using a NanoDrop™ One/OneC Ultraviolet-Vis spectrophotometer (Thermo Fisher, Wilmington, DE, USA). Complementary deoxyribonucleic acid (cDNA) was synthesized using 2 µg of total RNA and the High-Capacity cDNA reverse transcription kit, followed by real-time PCR using TaqMan™ Fast advanced Master Mix (Thermo Fisher Scientific, Johannesburg, South Africa), according to the manufacturer's guidelines, on the C1000Touch™ Thermal Cycler with 96-Well Fast Reaction Module (Bio-Rad, Singapore). FAM-labelled TaqMan™ Gene Expression Assays were used for the following genes: *CYP3A4* (Hs00604506_m1), *CYP2D6* (Hs00164385_m1), Glyceraldehyde 3-phosphate dehydrogenase (*GAPDH*) (Hs99999905_m1) and TATA-box binding protein (*TBP*) (Hs00427620_m1). *GAPDH* and *TBP* were used as housekeeping genes to normalise the data,

and to guarantee the comparability of the calculated mRNA (messenger RNA) expression in all samples analysed. All PCR analyses were performed in biological triplicates. Threshold cycle (Ct) values and data were further analysed with Bio-Rad CFX Maestro Software v1.1 (Bio-Rad CFX Maestro. Ink). Relative gene expression was calculated using the 2-ΔΔCt method (Livak & Schmittgen, 2001).

3.7.7. Statistical data analysis

Data collected following the assays performed in **Sections 3.7.2 - 3.7.6.** were analysed to determine statistical significance. Data analysis was performed with Statistica® software (TIBCO Software Inc. (2017). Statistica® (data analysis software system), version 13. http://statistica.io.). One-way ANOVA, followed by the Dunnett post-hoc test for comparison of multiple groups with a control group (time point 0), was used for analysis of model characterisation data. Real-time PCR data were analysed by means of one-way ANOVA with Bonferroni post-hoc test using Bio-Rad CFX Maestro 1.1 (4.1.2433.1219) software. Differences were considered statistically significant when $p < 0.05$.

3.8. Validation of the LS180 sodium alginate encapsulated spheroid model for anticancer treatment screening

Various cell-based assays can be used to evaluate compounds in terms of their potential effects on cell proliferation or cytotoxic effects which may lead to cell death (Riss *et al*., 2016). In this study cell viability was monitored through evaluation of soluble protein content, intracellular ATP levels, extracellular AK levels and glucose consumption.

The validation of the LS180 sodium alginate encapsulated spheroid model for anticancer treatment screening consisted of two separate experiments or biological replicates. During the first experiment 150 spheroids were seeded per bioreactor, and then reduced to 50 spheroids per bioreactor when the spheroids were 10 days old. During the second experiment, only 100 spheroids were seeded per bioreactor, and was then reduced to 50 spheroids per bioreactor on day 10.

The experiments commenced when the spheroids were 12 days of age. Sampling took place following 0 h, 24 h, 48 h, 72 h and 96 h of exposure to the model chemotherapeutic treatments.

3.8.1. Treatment groups

During this study, different bioreactors were set up for each of the various treatment groups. All experimental procedures were the same as described in **Sections 3.6.1. - 3.6.5.** Once the spheroids reached the age of 10 days, they were removed from the bioreactors and pooled together. This ensured homogenous distribution of spheroids for each treatment group. Subsequently, 50 spheroids were sampled for each of the following treatment groups:

- untreated control,
- paclitaxel [IC_{50}] (concentration paclitaxel per µg protein, based on the IC_{50} values obtained in the 2D cultures following the MTT assay),
- paclitaxel 2[IC_{50}] (two times the concentration paclitaxel per µg protein, based on the IC_{50} values obtained in the 2D cultures following the MTT assay).

Each treatment groups' spheroids were placed in their respective bioreactors, and the bioreactors were then filled with preheated culture medium as mentioned in **Section 3.6.5.** Bioreactors were returned to the drive unit, and speed was adjusted until they reached the age of 12 days.

3.8.2. Soluble protein content quantification

The total soluble protein content of each bioreactor needed to be determined daily, prior to the drug dosing. This quantification then enabled daily dosing of the spheroids per protein content of each bioreactor.

The soluble protein content was determined following sampling of one spheroid from each treatment group, as described in **Section 3.7.2**. The only exception was that the assay was conducted immediately, and not following storage at -80°C. Each spheroid sampled per treatment group were lysed and divided into three technical replicates.

3.8.3. Treatment dose calculations

The measured soluble protein content was then used to determine the dose per protein for the various treatment groups. The soluble protein content (µg) per spheroid was multiplied by the number of spheroids in each bioreactor per day to obtain a total protein mass (µg) for the bioreactor, and the doses were adapted accordingly. This adjustment ensured that the spheroids were constantly exposed to a constant amount of drug for the duration of the experiment. This

also better correlates with *in vivo* studies, where dosing is calculated according to body mass (Wrzesinski & Fey, 2013).

Following sampling for the soluble protein content, intracellular ATP, extracellular AK, as well as glucose content, the bioreactors were filled with the prepared treatments of the previous day. At time point 0 h, the bioreactors were filled with unspent medium.

Once the soluble protein content for each treatment group was determined and the new dose per bioreactor calculated, the new culture medium containing the treatments was prepared and the medium of each bioreactor changed.

For paclitaxel, a stock solution was prepared and stored as described in **Section 3.5.4.,** with the inclusion of an intermediate concentration of 2.0×10^{-5} M. The necessary dilutions were made in preheated culture medium.

3.8.4. Intracellular adenosine triphosphate cell viability assay

The intracellular ATP concentration for each treatment group, at each time point, was determined as described in **Section 3.7.3.** One spheroid was sampled per treatment group, per time point, and divided into three technical replicates.

3.8.5. Extracellular adenylate kinase cell death assay

An amount of 200 µl of spent culture medium was sampled from each treatment group at each time point, and processed as discussed in **Section 3.7.4.**

3.8.6. Glucose consumption

The amount of glucose (mmol/l) in the spent medium was measured for each of the treatment groups, at each time point, as described in **Section 3.7.5.** The glucose content in each treatment group culture medium sample was also measured before dosing to establish the unspent medium glucose content.

The glucose content was measured three times for each group, and the average calculated. This value was then subtracted from the unspent medium glucose content to estimate the glucose consumption (mmol/l) for the various treatment groups per time point.

3.8.7. Quantitative reverse transcription polymerase chain reaction relative cytochrome P450 gene expression

To establish the potential effect of each treatment group on the CYP450 enzyme family, the relative expression of P-glycoprotein (*P-gp), CYP3A4* and *CYP2D6* was measured by means of qRT-PCR. The relative gene expression was measured after 0 h and 96 h of exposure to the various treatments groups. Sampling and analysis of the various samples were performed as described in **Section 3.7.6.**, with the addition of the measurement of *P-gp* (ABCB1-Hs00184500_m1).

3.8.8. Statistical data analysis

Data collected following the assays performed in **Sections 3.8.2.** and **3.8.4.** - **3.8.7.** were analysed to measure statistical significance. Data analysis was performed with Statistica® software (TIBCO Software Inc. (2017). Statistica® (data analysis software system), version 13. http://statistica.io.). Repeated measurements ANOVA, followed by the Dunnett post-hoc test for comparison of multiple groups with a control group (untreated), was used for analysis of data before and after treatment. Real-time PCR data were analysed by means of one-way ANOVA with Bonferroni post-hoc test using Bio-Rad CFX Maestro 1.1 (4.1.2433.1219) software. Differences were considered statistically significant when $p < 0.05$.

3.9. Implementation of the LS180 sodium alginate encapsulated spheroid model for anticancer phytomedicine treatment screening

The potential anticancer properties of *S. frutescens* and *X. undulatum* were investigated in the characterised and validated LS180 sodium alginate encapsulated spheroid model. Once again, cell viability was monitored through evaluation of soluble protein content, intracellular ATP levels, extracellular AK levels and glucose consumption.

The phytomedicine treatment screening consisted of two separate experiments or biological replicates. During the first experiment 150 spheroids were seeded per bioreactor, and then reduced to 100 spheroids per bioreactor when the spheroids were 10 days old. During the second experiment, only 100 spheroids were seeded per bioreactor, and was then reduced to 50 spheroids per bioreactor on day 10.

The experiments commenced when the spheroids were 12 days of age. Sampling took place following 0 h, 24 h, 48 h, 72 h and 96 h of exposure to the phytomedicine treatments.

3.9.1. Treatment groups

Different bioreactors were again set up for each of the various treatment groups. All experimental procedures were the same as in **Sections 3.6.1.** - **3.6.5.** Once the spheroids reached 10 days, they were removed from the bioreactors and all pooled together. Subsequently, 50 spheroids were sampled for each of the following treatment groups:

- untreated control,
- *S. frutescens* [IC_{50}]/2 (half the concentration of *S. frutescens* per µg protein, based on the IC_{50} values obtained in the 2D cultures following the MTT assay. This concentration was added for only the second experiment, due to the high activity of the IC_{50} concentration observed in the first experiment),
- *S. frutescens* [IC_{50}] (the concentration of *S. frutescens* per µg protein, based on the IC_{50} values obtained in the 2D cultures following the MTT assay).
- *X. undulatum* [IC_{50}] (the concentration of *X. undulatum* per µg protein, based on the IC_{50} values obtained in the 2D cultures following the MTT assay).
- *X. undulatum* 2[IC_{50}] (two times the concentration of *X. undulatum* per µg protein, based on the IC_{50} values obtained in the 2D cultures following the MTT assay).

Due to the high 2D IC_{50} dose of *S. frutescens* it was determined that double the 2D IC_{50} per protein value, dosed for a bioreactor containing 50 spheroids, would not be able to dissolve. Each treatment groups' spheroids were placed in their respective bioreactors, and the bioreactors were then filled with preheated culture medium as mentioned in **Section 3.6.5.** Bioreactors were returned to the drive unit, and speed was adjusted until they reached the age of 12 days.

3.9.2. Soluble protein content quantification

The total soluble protein content of each bioreactor needed to be determined daily, prior to the drug dosing. This quantification then enabled daily dosing of the spheroids per protein content of each bioreactor.

The soluble protein content was determined following sampling of one spheroid from each treatment group, as described in **Section 3.7.2**. The only exception was that the assay was conducted immediately, and not following storage at -80°C. Each spheroid sampled per treatment group were lysed and divided into three technical replicates.

3.9.3. Treatment dose calculations

The measured soluble protein content was then used to determine the dose per protein for the various treatment groups. The soluble protein content (µg) per spheroid was multiplied by the number of spheroids in each bioreactor per day to obtain a total protein mass (µg) for the bioreactor, and the doses were adapted accordingly.

Following sampling for the soluble protein content, intracellular ATP, extracellular AK, as well as glucose content, the bioreactors were filled with the prepared treatments of the previous day. At time point 0 h, the bioreactors were filled with unspent medium.

Once the soluble protein content for each treatment group was determined and the new dose per bioreactor calculated, the new culture medium containing the treatments was prepared and the medium of each bioreactor changed.

A stock solution (25 ml) equal to the concentration of *S. frutescens* [IC_{50}] was prepared as described in **Section 3.5.3.** Dilutions were made for *S. frutescens* [IC_{50}]/2 using the stock solution of *S. frutescens* [IC_{50}]. Spent medium was removed and replaced (as discussed in **Section 3.6.5.**) with the fresh *S. frutescens* treatment for the day.

A stock solution (25 ml) equal to the concentration of *X. undulatum* 2[IC_{50}] was prepared as described in **Section 3.5.3.** Dilutions were made for *X. undulatum* [IC_{50}] using the stock solution of *X. undulatum* 2[IC_{50}]. Spent medium was removed and replaced (as discussed in **Section 3.6.5.**) with the fresh *X. undulatum* treatment for the day.

3.9.4. Intracellular adenosine triphosphate cell viability assay

The intracellular ATP concentration for each treatment group, at each time point, was determined as described in **Section 3.7.3**. One spheroid was sampled per treatment group, per time point, and divided into three technical replicates.

3.9.5. Extracellular adenylate kinase cell death assay

An amount of 200 µl of spent culture medium was sampled from each treatment group at each time point, and processed as discussed in **Section 3.7.4.**

3.9.6. Glucose consumption

The amount of glucose (mmol/L) in the spent medium was measured for each of the treatment groups, at each time point, as described in **Section 3.7.5.** The glucose content in each treatment group culture medium sample was also measured before dosing to establish the unspent medium glucose content.

The glucose content was measured three times for each group, and the average calculated. This value was then subtracted from the unspent medium glucose content to estimate the glucose consumption (mmol/l) for the various treatment groups per time point.

3.9.7. Quantitative reverse transcription polymerase chain reaction relative cytochrome P450 gene expression

To establish the potential effect of each treatment group on the CYP450 enzyme family, the relative expression of *CYP3A4* and *CYP2D6* was measured by means of qRT-PCR. The relative gene expression was measured after 0 h and 96 h of exposure to the various treatments groups. Sampling and analysis of the various samples were performed as described in **Section 3.7.6.**

3.9.8. Statistical data analysis

After the assays performed in **Sections 3.9.2.** and **3.9.4. - 3.9.6.,** the data were analysed to measure statistical significance. Data analysis was performed with Statistica® software (TIBCO Software Inc. (2017). Statistica® (data analysis software system), version 13. http://statistica.io.). Repeated measurements ANOVA, followed by the Dunnett post-hoc test for comparison of multiple groups with a control group (untreated), was used for analysis of data before and after treatment. Real-time PCR data were analysed by means of one-way ANOVA with Bonferroni post-hoc test using Bio-Rad CFX Maestro 1.1 (4.1.2433.1219) software. Differences were considered statistically significant when $p < 0.05$.

3.10. Summary

In order to establish the well-being of the 3D colorectal cell model, the soluble protein content, intracellular ATP levels, extracellular AK levels and glucose consumption of the spheroids needed to be assessed for a period of at least 20 days.

Furthermore, to determine the potential of the established model for future anticancer research the model was tested with a standard chemotherapeutic compound, namely paclitaxel. The validated model was subsequently used to evaluate two phytomedicines for possible anticancer activity. This was done through evaluation of the soluble protein content, intracellular ATP levels, extracellular AK levels and glucose consumption.

Lastly, to consider the use of the model for biotransformation evaluation, the relative gene expression of *CYP3A4* and *CYP2D6* were evaluated for 20 days during the characterisation of the model, as well as during the 96 h of treatment with paclitaxel, *S. frutescens* and *X. undulatum*.

References:

Ahmann, F.R., Garewal, H.S., Schifman, R., Celniker, A. & Rodney, S. 1987. Intracellular adenosine triphosphate as a measure of human tumor cell viability and drug modulated growth. *In vitro cellular & developmental biology*, 23:474-480.

Astashkina, A. & Grainger, D.W. 2014. Critical analysis of 3-D organoid *in vitro* cell culture models for high-throughput drug candidate toxicity assessments. *Advanced drug delivery reviews*, 69:1-18.

Bahuguna, A., Khan, I., Bajpai, V.K. & Kang, S.C. 2017. MTT assay to evaluate the cytotoxic potential of a drug. *Bangladesh journal of pharmacology*, 12:116-118.

Bradford, M.M. 1976. A rapid and sensitive method for the quantitation of microgram quantities of protein utilizing the principle of protein-dye binding. *Analytical biochemistry*, 72:248-254.

Breslin, S. & O'Driscoll, L. 2013. Three-dimensional cell culture: the missing link in drug discovery. *Drug discovery today*, 18:240-249.

Burlingham, B.T. & Widlanski, T.S. 2003. An intuitive look at the relationship of K_i and IC_{50}: a more general use for the Dixon plot. *Journal of chemical education*, 80:214-218.

Calitz, C. 2017. Establishing three-dimensional cell culture models to measure biotransformation and toxicity. Potchefstroom:NWU. (Thesis- PhD).

Cho, M.H., Niles, A., Huang, R., Inglese, J., Austin, C.P., Riss, T. & Xia, M. 2008. A bioluminescent cytotoxicity assay for assessment of membrane integrity using a proteolytic biomarker. *Toxicology in vitro*, 22:1099-1106.

Cortés, A., Cascante, M., Cárdenas, M.L. & Cornish-Bowden, A. 2001. Relationships between inhibition constants, inhibitor concentrations for 50% inhibition and types of inhibition: new ways of analysing data. *Biochemical journal*, 357:263-268.

Denizot, F. & Lang, R. 1986. Rapid colorimetric assay for cell growth and survival: modifications to the tetrazolium dye procedure giving improved sensitivity and reliability. *Journal of immunological methods*, 89:271-277.

Duggett, N.A., Griffiths, L.A. & Flatters, S.J.L. 2017. Paclitaxel-induced painful neuropathy is associated with changes in mitochondrial bioenergetics, glycolysis, and an energy deficit in dorsal root ganglia neurons. *Pain*, 158:1499-1508.

Fey, S.J. & Wrzesinski, K. 2012. Bioreactor with lid for easy access to incubation cavity. USA PA 61/423, 145, 2010; DK PCT/DK2011/050466.

Freshney, R.I. 2015. Culture of animal cells: a manual of basic technique and specialized applications. 7th ed. New Jersey: Wiley-Blackwell.

Gombotz, W.R & Wee, S.F. 2012. Protein release from alginate matrices. *Advanced drug delivery reviews*, 64:194-205.

Hansen, M.B., Nielsen, S.E. & Berg, K. 1989. Re-examination and further development of a precise and rapid dye method for measuring cell growth/cell kill. *Journal of immunological methods*, 119:203-210.

Haycock, J.W. 2011. 3D cell culture: a review of current approaches and techniques. (*In* Methods in molecular biology. Heidelberg: Springer Science and Business Media. 1-15).

Jacobs, A.C., DiDone, L., Jobson, J., Sofia, M.K., Krysan, D. & Dunman, P.M. 2013. Adenylate kinase release as a high-throughput-screening-compatible reporter of bacterial lysis for identification of antibacterial agents. *Antimicrobial agents and chemotherapy*, 57:26-36.

Kijanska, M. & Kelm, J. 2016. *In vitro* 3D spheroids and microtissues: ATP-based cell viability and toxicity assays. (In Sittampalam, G.S., Coussens, N.P., Brimacombe, K., Grossman, A., Arkin, M., Auld, A., Austin, C., Baell, J., Bejcek, B., Chung, T.D.Y., Dahlin, J.L., Devanaryan, V., Foley, T.L., Glicksman, M., Hall, M.D., Hass, J.V., Inglese, J., Iversen, P.W., Kahl, S.D., Kales, S.C., Lal-Nag, M., Li, Z., McGee, J., McManus, O., Riss, T., Trask, O.J., Weidner, J.R., Xia, M., Xu, X. ed. Assay Guidance Manual. Bethesda: Eli Lilly & Company and the National Center for Advancing Translational Sciences. p.355-385).

Lee, K.Y. & Mooney, D.J. 2012. Alginate: Properties and biomedical applications. *Progress in polymer science*, 37:106-126.

Livak K.J. & Schmittgen T.D. 2001. Analysis of relative gene expression data using real-time quantitative PCR and the 2(-Delta Delta C(T)) method. *Methods*, 25:402-408.

Lü, L., Zhang, L., Wai, M.S.M., Yew, D.T.W. Xu, J. 2012. Exocytosis of MTT formazan could exacerbate cell injury. *Toxicology in vitro*, 26:636-644.

Mosmann, T. 1983. Rapid colorimetric assay for cellular growth and survival: application to proliferation and cytotoxicity assays. *Journal of immunological methods*, 65:55-63.

Mueller, H., Kassack, M.U. & Wiese, M. 2004. Comparison of the usefulness of the MTT, ATP, and calcein assays to predict the potency of cytotoxic agents in various human cancer cell lines. *Journal of biomolecular screening*, 9:506-515.

Nyga, A., Cheema, U. & Loizidou, M. 2011. 3D tumour models: novel *in vitro* approaches to cancer studies. *Journal of cell communication and signaling*, 5:239-248.

Riss, T.L. & Moravec, R.A. 2004. Use of multiple assay endpoints to investigate the effects of incubation time, dose of toxin, and plating density in cell-based cytotoxicity assays. *Assay and drug development technologies*, 2: 51-62.

Riss, T., Valley, M., Kupcho, K., Zimprich, C., Leippe, D., Niles, A., Vidugiriene, J., Cali, J., Kelm, J., Moritz, W. & Lazar, D. 2014. Validation of *in vitro* assays to measure cytotoxicity in 3D cell cultures. *Toxicology letters*, 229:S145.

Riss, T., Moravec, R.A., Niles, A.L., Duellman, S., Benink, H.A., Worzella, T.J. & Minor, L. 2016. Cell Viability Assays. (*In* Sittampalam, G.S., Coussens, N.P., Brimacombe, K., Grossman, A., Arkin, M., Auld, A., Austin, C., Baell, J., Bejcek, B., Chung, T.D.Y., Dahlin, J.L., Devanaryan, V., Foley, T.L., Glicksman, M., Hall, M.D., Hass, J.V., Inglese, J., Iversen, P.W., Kahl, S.D., Kales, S.C., Lal-Nag, M., Li, Z., McGee, J., McManus, O., Riss, T., Trask, O.J., Weidner, J.R., Xia, M., Xu, X. *ed.* Assay Guidance Manual. Bethesda: Eli Lilly & Company and the National Center for Advancing Translational Sciences. p.355-385).

Shandiz, S.A.S., Salehzadeh, A., Ahmadzadeh, M. & Khalatbari, K. 2017. Evaluation of cytotoxicity activity and NM23 gene expression in T47D breast cancer cell line treated with *Glycyrrhiza glabra* extract. *Journal of genetic resources*, 3:47-53.

Swanepoel, R.A. 2018. *In vitro* evaluation of the efficacy of selected medicinal plant extracts against multidrug resistant cancer cells. Potchefstroom:NWU. (Dissertation- MSc).

Sylvester, P.W. 2011. Optimization of the tetrazolium dye (MTT) colorimetric assay for cellular growth and viability. *Drug design and discovery*, 157-168.

Tada, H., Shiho, O., Kuroshima, K.I., Koyama, M. & Tsukamoto, K. 1986. An improved colorimetric assay for interleukin 2. *Journal of immunological methods*, 93:157-165.

Tan, W.H. & Takeuchi, S. 2007. Monodisperse alginate hydrogel microbeads for cell encapsulation. *Advanced materials*, 19:2696-2701.

Van Tonder, A., Joubert, A.M. & Cromarty, A.D. 2015. Limitations of the 3-(4, 5-dimethylthiazol-2-yl)-2, 5-diphenyl-2H-tetrazolium bromide (MTT) assay when compared to three commonly used cell enumeration assays. *Biomed central research notes*, 8:1-10.

Vega-Avila, E. & Pugsley, M.K. 2011. An overview of colorimetric assay methods used to assess survival or proliferation of mammalian cells. *Proceedings of the Western pharmacology society,* 54:10-14.

Waring, M.J., Arrowsmith, J., Leach, A.R., Leeson, P.D., Mandrell, S., Owen, R.M., Pairaudeau, G., Pennie, W.D., Pickett, S.D., Wang, J. & Wallace, O. 2015. An analysis of the attrition of drug candidates from four major pharmaceutical companies. *Nature reviews drug discovery*, 14:475-486.

Wentzel, J.F., Lewies, A., Bronkhorst, A.J., Van Dyk, E., Du Plessis, L.H. & Pretorius, P.J. 2017. Exposure to high levels of fumarate and succinate leads to apoptotic cytotoxicity and altered global DNA methylation profiles *in vitro*. *Biochimie*, 135:28-34.

Wong, C.H., Siah, K.W. & Lo, A.W. 2019. Estimation of clinical trial success rates and related parameters. *Biostatistics*, 20:273-286.

Wrzesinski, K. & Fey, S.J. 2013. After trypsinisation, 3D spheroids of C3A hepatocytes need 18 days to re-establish similar levels of key physiological functions to those seen in the liver. *Toxicology research*, 2:123-135.

CHAPTER 4

This chapter presents the results and discussion following the preliminary anticancer activity screening with the 3-(4,5-dimethylthiazol-2-yl)-2,5- diphenyl tetrazolium bromide assay, as well as the optimisation and characterisation of the LS180 three-dimensional sodium alginate encapsulated spheroid model, validation of this model for anticancer treatment screening, induction of the cytochrome P450 enzyme family and, finally, implementation of the model to evaluate the potential use of *Sutherlandia frutescens* and *Xysmalobium undulatum* in the treatment of colorectal cancer.

4.1. Introduction

In this study a sodium alginate encapsulated colorectal cancer cell spheroid model was optimised and characterised in terms of growth and viability, to serve as a potential model for drug biotransformation and anticancer activity screening of new compounds and phytomedicines. The following parameters were measured as an indication of cell viability: intracellular adenosine triphosphate (ATP) content, extracellular adenylate kinase (AK) release and glucose consumption. The growth in terms of soluble protein content was also measured. Relative gene expression of the cytochrome P450 (CYP450) enzymes CYP3A4 and CYP2D6 was measured using a real-time polymerase chain reaction-based (qRT-PCR) gene expression assay. This provided an indication of the feasibility of the model for drug biotransformation studies.

To validate use of the model for anticancer treatment activity screening, the standard chemotherapeutic drug paclitaxel was used as a model drug. The effects of the drug on the growth and viability of cells were investigated in terms of soluble protein content, intracellular ATP content, extracellular AK release and glucose consumption. Lastly, the effects of exposure to paclitaxel in terms of *P-glycoprotein* (*P-gp*), *CYP3A4* and *CYP2D6* gene expression were determined.

The model was then used to study the anticancer and drug biotransformation effects of the phytomedicines, *S. frutescens* and *X. undulatum.* These effects were studied in terms of soluble protein content, intracellular ATP content, extracellular AK release, glucose consumption and *CYP3A4* and *CYP2D6* gene expression following exposure for 96 h.

4.2. Preparation and characterisation of crude aqueous plant extracts

Crude aqueous extracts were previously prepared from dried *S. frutescence* and *X. undulatum* plant material. These extracts were subsequently characterised through chemical profiling. These characterised extracts were then used again in this study.

4.2.1. Characterisation of *Sutherlandia frutescens* extract

Following liquid chromatography-mass spectrometry (LC-MS), the presence of the known marker molecule, SU1, was confirmed (See **Appendix B**) and quantified as 10.11 µg/mg (n = 2) (Swanepoel, 2018).

4.2.2. Characterisation of *Xysmalobium undulatum* extract

The chemical characterisation of the *X. undulatum* crude aqueous extract via ultra-high pressure liquid chromatography (UPLC) analysis confirmed the presence of the marker molecule, Uzarin, in the extract (See **Appendix C**) (Swanepoel, 2018).

4.3. Pre-screening of anticancer activity

Anticancer activity of the chemotherapeutic drug and the plant extracts were first evaluated in two-dimensional (2D) cultures of the LS180 cell line, employing the 3- (4,5- dimethylthiazol- 2-yl)- 2,5- diphenyltetrazolium bromide (MTT) assay. This was done to estimate the 50% inhibitory concentration (IC_{50}) per protein content of each treatment for the LS180 cell line, relative to an untreated control. The cells were treated with a concentration series of each treatment for 96 h, and the viability then assessed via MTT. The data was subsequently analysed with the Probit analysis to calculate the IC_{50} concentrations.

The Probit analysis is a type of regression used to analyse binominal response variables. Data obtained from bioassays are generally expressed as percentage response at the corresponding dose. The response is always binominal (death or no death) and the response is always sigmoid. The Probit analysis acts as a transformation from sigmoid to linear, and then runs a regression on the relationship. Once the regression is run, the output can be used to compare the amount of chemicals required to compare differences in dose and response (Akcay, 2013). In this study, the data was used to produce inhibition concentrations (IC_{25}, IC_{50} and IC_{75}) and their 95% confidence limits.

According to McDonald (2014), confidence limits are the numbers at the upper and lower end of a confidence interval. Having 95% confidence limits mean that if you took repeated random samples and calculated the mean and confidence limits for each sample, the confidence limit for 95% of your samples would include the parametric mean.

4.3.1. Paclitaxel inhibitory concentrations

The paclitaxel IC_{25}, IC_{50} and IC_{75} values were determined by means of Probit analysis (using SPSS statistical analysis software) of the MTT data. The calculated concentrations and their 95% confidence intervals are presented in **Table 4.1.** The MTT data used to obtain these values are presented in **Appendix D**.

Table 4.1. Cell viability inhibition concentrations (IC) of paclitaxel, relative to an untreated control, in LS180 cells as determined with Probit analysis.

Inhibitory Concentration percentage	Calculated concentration (nM)	95% confidence limits (nM)	
IC_{25}	14.579	11.057	18.485
IC_{50}	94.595	81.467	108.910
IC_{75}	613.773	516.078	746.375

The LS180 colorectal cell line demonstrated reduced cell viability relative to the untreated control at concentrations exceeding 9 nM of paclitaxel for 96 h (**Appendix D**). The IC_{75} concentrations was calculated to be 613.77 nM of paclitaxel resulted. However, treatment with 1 µM paclitaxel resulted in a lower percentage of cell viability inhibition (73.86%). This is indicative of drug resistance to paclitaxel in this cell line at high concentrations. The IC_{50} concentration for paclitaxel was also calculated as 94.595 nM for this cell line.

In a study by Rossouw (2018) the effects of paclitaxel were tested on various cell lines. The effects were tested in a non-cancerous porcine kidney cell line (LLC-PK1), and the IC_{50} concentration calculated following 96 h exposure in this cell line was 29.73 nM. Furthermore, the cytotoxic effects were evaluated in a chemosensitive small cell lung cancer (SCLC) cell line (HCI-H69V), with the estimated IC_{50} concentration being 2.84 nM. Lastly, the paclitaxel was tested on drug resistant SCLC cell lines (H69AR and NCI-H69/LX4), with their IC_{50} concentrations estimated at 4.75 nM and 613.05 nM, respectively. Rossouw (2018) also indicated that SCLC cells undergo adaptive mechanisms as a coping mechanism after exposure to paclitaxel. These cellular models can eventually reach a threshold of cytotoxicity, and then a rebound of multidrug resistance will emerge. This emergence of resistance correlates with the findings of this study, where the relative percentage cell viability inhibition decreases as the dose reached 1 mM.

4.3.2. *Sutherlandia frutescens* inhibitory concentrations

The *S. frutescens* IC_{25}, IC_{50} and IC_{75} values following treatment of LS180 cells in 2D for 96 h were determined by means of Probit analysis of the MTT data. These concentrations and their 95%

confidence intervals are presented in **Table 4.2**. These concentration correlates with the experimental MTT findings (as shown in **Appendix E**).

Table 4.2. Cell viability inhibition concentrations (IC) of *Sutherlandia frutescens*, relative to an untreated control, in LS180 cells as determined with Probit analysis.

Inhibitory Concentration percentage	Calculated concentration (mg/ml)	95% confidence limits (mg/ml)	
IC_{25}	2.007	1.824	2.168
IC_{50}	2.625	2.461	2.772
IC_{75}	3.434	3.286	3.582

The LS180 colorectal cell line demonstrated reduced cell viability at concentrations exceeding 2 mg/ml when exposed to *S. frutescens* extracts for 96 h. Concentrations lower than this inversely caused an increase in cell growth when compared to the untreated control. These effects are, however, suggested to be influenced by the period of exposure (Swanepoel, 2018). In this study the cytotoxic effects of the extract reached a plateau at 5 mg/ml, and exceeding concentrations did not cause further reduction in cell viability.

In a study by Omoruyi *et al*. (2018), they tested the effects of aqueous extracts of *S. frutescens* on human malignant neuroblastoma cell lines SKNBE(2) and SHSY5Y for 48 h. They determined the IC_{50} values to be 2.3 mg/ml and 2.2 mg/ml, respectively. They also treated a non-tumorigenic cell line (KMST6) and established the IC_{50} value of 5 mg/ml. This suggested *S. frutescens* aqueous extracts to be less toxic in the non-tumorigenic cell line than effective in the neuroblastoma cell lines. The results of the study also indicated that *S. frutescens* extracts induced apoptosis, and that the reduction in cell viability was dose dependant.

The results of the study by Omoruyi *et al*. (2018) correlate well with the current study, as this study also indicated dose dependant cell viability inhibition.

4.3.3. *Xysmalobium undulatum* inhibitory concentrations

Probit analysis of the MTT data following treatment of LS180 cells in 2D for 96 h with *X. undulatum,* determined IC_{25}, IC_{50} and IC_{75} values and their 95% limits. These concentrations are presented in **Table 4.3**, and correlates with the experimental MTT findings (as shown in **Appendix F**).

Table 4.3. Cell viability inhibition concentrations (IC) of *Xysmalobium undulatum*, relative to an untreated control, in LS180 cells as determined with Probit analysis.

Inhibitory Concentration percentage	Calculated concentration (mg/ml)	95% confidence limits (mg/ml)	
IC_{25}	0.063	0.055	0.069
IC_{50}	0.098	0.090	0.105
IC_{75}	0.153	0.143	0.164

The LS180 colorectal cancer cell line demonstrated reduced cell viability at concentrations exceeding 0.05 mg/ml when exposed to crude *X. undulatum* aqueous extracts for 96 h. *X. undulatum* had anticancer activity at very low doses when compared to *S. frutescens*. Treatment with a concentration of 0.35 mg/ml, and higher, induces a near complete (97.28%) inhibition of cell viability. The IC_{50} concentration was calculated as 0.098 mg/ml.

In the study by Swanepoel (2018), it was suggested that *X. undulatum* has possible cytotoxic effects. The cytotoxicity of *X. undulatum* was tested on a drug sensitive SCLC cell line (H69V) and an IC_{50} concentration of 0.004 mg/ml was determined. The cytotoxicity of *X. undulatum* was also tested on SCLC cell lines which hyper-expressed efflux transporters, namely H69AR and NCI-H69/LX4, and the IC_{50} values was indicated as 0.020 mg/ml and 0.015 mg/ml respectively. Lastly, the cytotoxic effects were tested on the non-cancerous cell line, LLC-PK1, and the IC_{50} concentration was determined as 0.010 mg/ml. These results suggest a risk of toxicity to non-cancerous cell lines, as higher concentrations of *X. undulatum* extract are needed to inhibit cell viability in the cancerous cell lines than in the non-cancerous cell lines.

4.3.4. Summary for the two-dimensional anticancer activity pre-screening

In this study, preliminary anticancer screening of paclitaxel, *S. frutescens* and *X. undulatum* resulted in the estimation of the IC_{50} values and their 95% confidence limits. These values were then used to validate and implement the LS180 sodium alginate encapsulated spheroid model for anticancer and drug biotransformation screening (see **Section 4.6 - 4.8**).

The effects of paclitaxel were tested during this study as paclitaxel is a standard chemotherapeutic drug used in the treatment of colorectal cancer and treatment resulted in a reduction in cell viability. Treatment with certain concentrations of *S. frutescens, X. undulatum* aqueous extracts for 96 h also resulted in a reduction in cell viability in comparison to the untreated control group. It is thus evident that the two phytomedicines have anticancer potential as they inhibit the cell viability.

4.4. Optimised culturing of the LS180 sodium alginate encapsulated spheroid model

The sodium alginate encapsulation of LS180 cells was previously performed by Calitz (2017). This method was further optimised and applied in this study. The cells were cultured as three-dimensional (3D) sodium alginate encapsulated spheroids using 2.5% sodium alginate cross-linked with 50 mM $CaCl_2$ and 150 mM NaCl. Each spheroid was 1 µl in volume and contained 2 000 cells. After spheroid encapsulation, they were transferred to rotating bioreactors. Speed was adjusted according to spheroid growth to ensure that spheroids remained in a stationary orbit.

Growth medium was exchanged every second or third day, and the spheroid population was split into more bioreactors on days 10 and 15.

4.5. Characterisation of the LS180 sodium alginate encapsulated spheroid model

During the development and maintenance of multicellular organisms, there must be a balance between cell division and cell death (Bröker *et al*. 2005). According to Ahmann *et al*. (1987), ATP levels are linearly related to the number of viable cells and will increase with time, correlating to growth kinetics. When a cell loses membrane integrity it loses the ability to synthesize ATP, resulting in the rapid depletion of any remaining ATP from the cytoplasm by ATPase (Riss *et al*., 2016). It is thus important for the 3D cell culture system to maintain adequate levels op ATP during the culturing period.

Cell death is an important variable in cancer development (Kanduc *et al*., 2002). The process of programmed cell death or apoptosis occurs normally during development and aging and serves as a homeostatic mechanism to maintain cell populations in tissues (Elmore, 2007). One parameter that can serve as a determinant of cell death, is AK. AK is a universal intracellular enzyme that is released into the extracellular space upon cell lysis (Jacobs *et al*., 2013).

To evaluate the viability and growth of the established model, intracellular ATP and extracellular AK levels were measured, and the data was normalised per µg soluble protein to correct for changes in cell numbers.

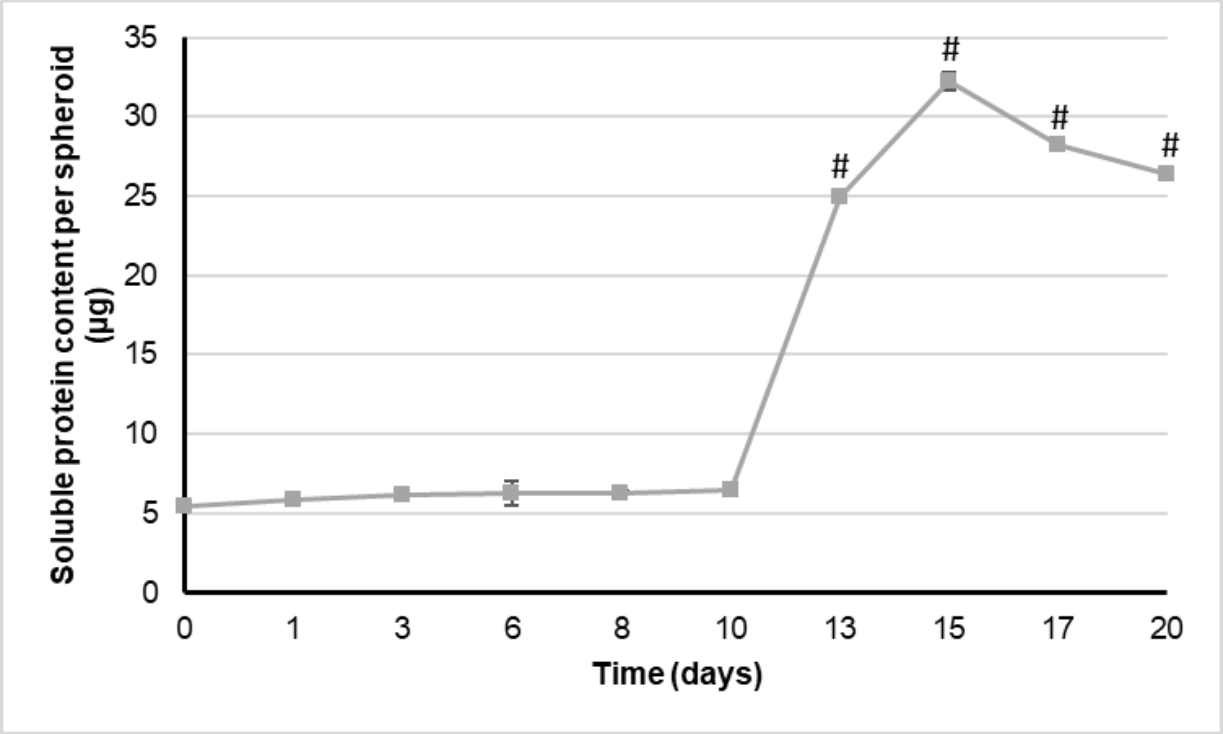

Figure 4.1. Soluble protein content per spheroid (µg) of the sodium alginate encapsulated LS180 spheroid model (*n* = 3, error bars = standard deviation; # = statistically significant compared to time point 0, $p < 0.001$ (one-way ANOVA followed by the Dunnett post-hoc test for comparison with time point 0)).

4.5.1. Soluble protein content

To determine the growth rate of the spheroid culture, the soluble protein content was determined. This data was subsequently used to express the intracellular ATP content, as well as the

extracellular AK release per µg protein. After conducting the Bradford soluble protein assay for the duration of the experiment, the following data was obtained.

There was a constant increase in soluble protein content in the spheroids over time, although the increase was very small until day 10. In **Figure 4.1.** it is evident that there was a substantial increase in the soluble protein content per spheroid after day 10. All bioreactors contained 300 spheroids from day 0 - 10. This amount of spheroids was reduced to 150 spheroids per bioreactor following sampling on day 10. This resulted in a greater abundance of nutrients per cell, as the density of the spheroids was reduced. This may have induced the increase in soluble protein content from day 10 - 13. It was also evident that the growth increase from day 13 - 20 was statistically significant with $p < 0.001$. On day 15 the population was still deemed too dense, and further reductions were made to 50 spheroids per bioreactor. In **Figure 4.2.** it is evident that there was a substantial difference in the density of the spheroids from day 8 - 16. Following this second reduction there was a slight decline in soluble protein content per spheroid, possibly due to the increased handling or stabilization of the model. During the characterisation period the standard deviation between the biological replicates remained small.

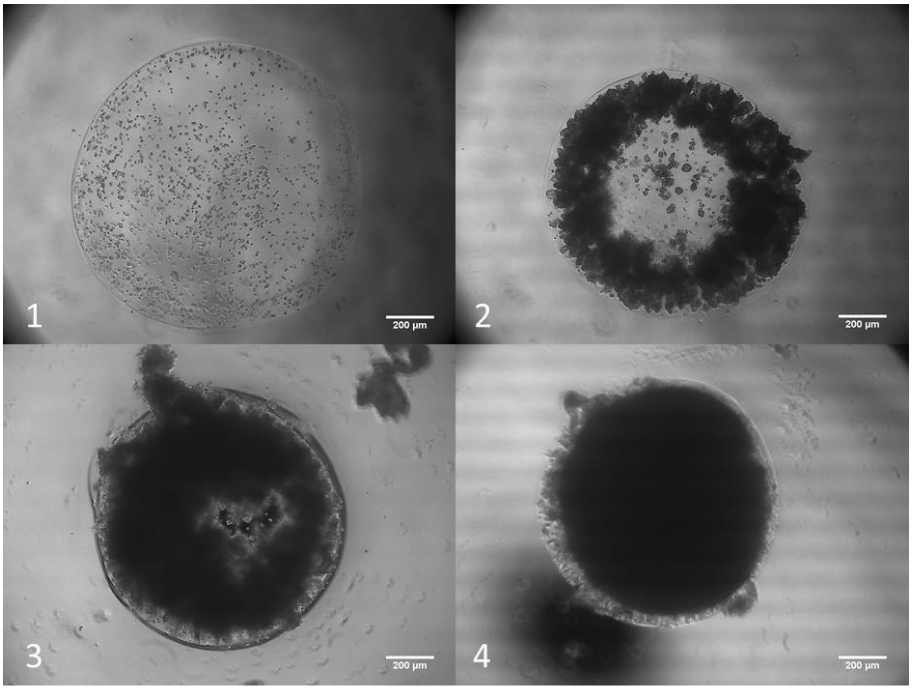

Figure 4.2. Photomicrographs depicting spheroid growth. Image 1 illustrates a spheroid after encapsulation before transfer to a bioreactor. Images 2, 3 and 4 show spheroids 8, 16 and 20 days following encapsulation.

4.5.2. Intracellular adenosine triphosphate content

Intracellular ATP was measured for 20 days during characterisation of the model, as an indicator of cell viability. The ATP content per spheroid was then divided by the amount of soluble protein per spheroid to obtain the intracellular ATP content per µg protein. This data is displayed in **Figure 4.3**.

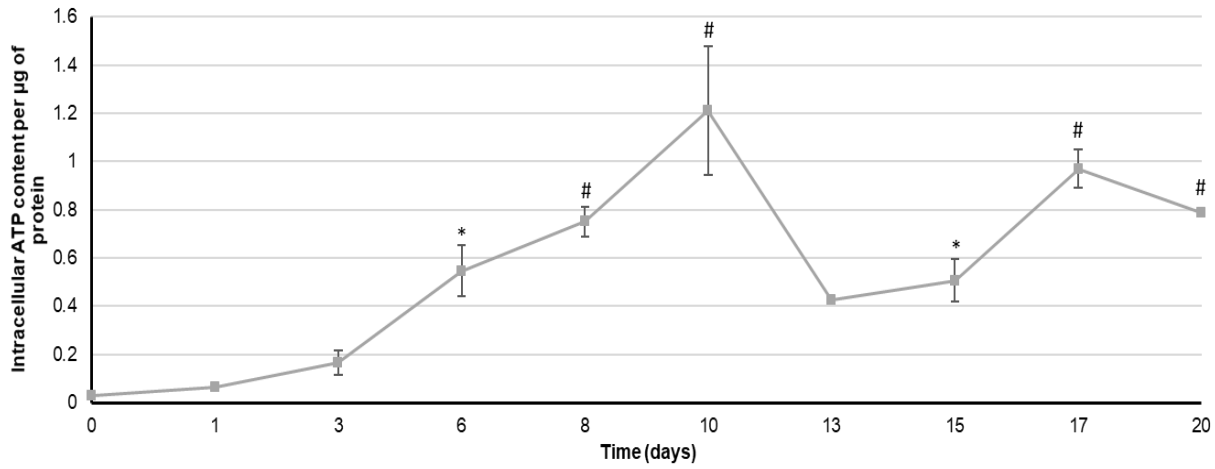

Figure 4.3. Intracellular adenosine triphosphate content per soluble protein (µM/µg) of the sodium alginate encapsulated LS180 spheroid model (n = 3, error bars = standard deviation; * = statistically significant, $p < 0.05$; # = statistically significant, $p < 0.001$ (one-way ANOVA followed by Dunnett post-hoc test for comparison with time point 0)).

A steady increase in the intracellular ATP content per µg protein could be observed for the first ten days of the characterisation. On day 10, the spheroids were subjected to a large amount of handling as the number of spheroids were reduced. This handling resulted in the decrease of intracellular ATP content per µg protein on day 13. After this, the spheroids started to recover and an increase was visible, with days 17 and 20 being very significantly increased compared to day 0 ($p < 0.001$). Once again the standard deviation between the biological replicates remained small throughout the experiment.

4.5.3. Extracellular adenylate kinase content

The extracellular AK content was measured as an indicator of cell death for the duration of the characterisation of the sodium alginate encapsulated LS180 spheroid model. The extracellular AK release per spheroid was divided by the amount of soluble protein per spheroid to obtain the extracellular AK release per µg protein. The data is presented in **Figure 4.4.**

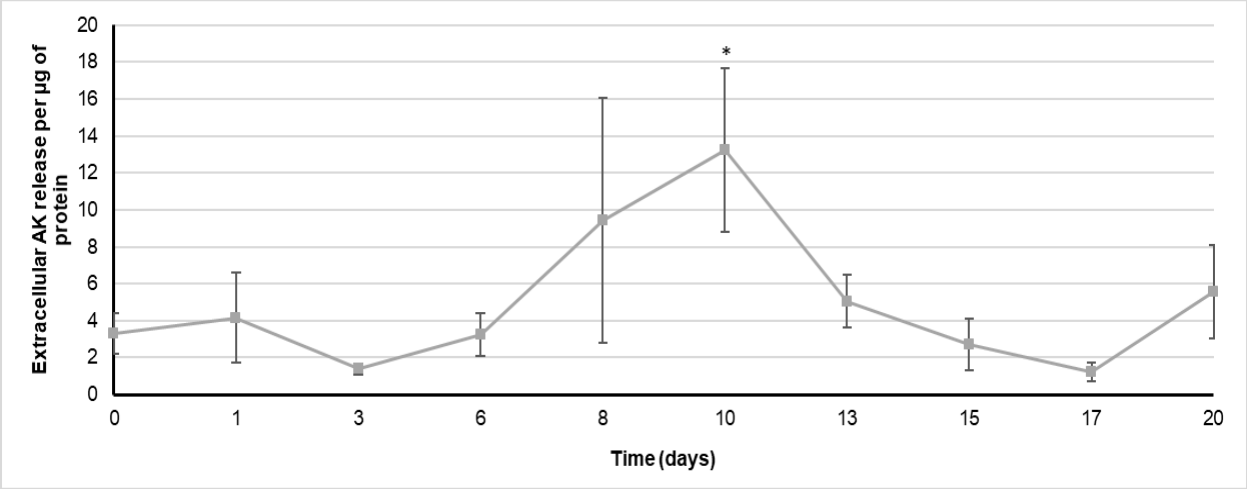

Figure 4.4. The extracellular adenylate kinase release per microgram protein of the sodium alginate encapsulated LS180 spheroid model ($n = 3$, error bars = standard deviation; * = statistically significant, $p < 0.05$ (one-way ANOVA followed by the Dunnett post-hoc test for comparison with time point 0)).

During the characterisation of the LS180 model, the extracellular AK release per µg protein remained low for the first 6 days of culturing, with a subsequent steady increase until day 10 when the AK release per µg protein was significantly higher than at time point 0 ($p < 0.05$). Following sampling on day 10, the spheroid numbers per bioreactor were reduced. This reduction in the amount of spheroids resulted in a decrease in the extracellular AK release per µg protein from day 10 - 17, with a slight increase on day 20. It is evident that 300 spheroids per bioreactor was too dense of a population as the AK release per µg protein was very high.

4.5.4. Glucose consumption

Glucose consumption as an indicator of metabolic activity was estimated through quantification of glucose disappearance from the culture medium during spheroid growth. The average glucose content of unspent medium was 6.8 mmol/L. After one day of culturing the average glucose content in the spent medium decreased to 3.9 mmol/L, and after three days the glucose content was below 1.1 mmol/L. From day 6 to 10 the glucose content was below detection limits. Even following the reduction in spheroid density on days 10 and 15, the glucose was still depleted in the culture medium. This indicated that all the glucose in the culture medium was consumed between the medium change intervals, and that cells in the spheroids were metabolically active.

In a study by Khoo *et al*. (2005), they examined the effects of medium glucose content on the growth and differentiation of embryoid bodies. They questioned why these embryoid bodies were grown in high glucose-containing medium, and thus evaluated the growth in medium containing 25 mM, 5.5 mM and 0 mM of glucose. Their results indicated that cell growth was not detrimentally affected by reduced, but not absent, glucose concentrations. The cells grew optimal in medium containing 5.5 mM of glucose, and although the cells receiving 0 mM glucose still showed growth, this was reduced drastically in comparison with the other groups. According to Wrzesinski and Fey (2018), the lack of glucose appeared to play a minimal role in the metabolic reprogramming of cells as it causes little stress after prolonged starvation. The small effects that were present appeared to stabilise cellular metabolism and were anti-apoptotic.

4.5.5. Relative cytochrome P450 gene expression

Since the CYP450 superfamily is the largest and most important phase I enzymes, and the CYP3A, CYP2D and CYP2C families are responsible for respectively 50%, 25% and 20% of the biotransformation of all drugs, it is of utmost importance to study the effects of drug on these enzymes *in vitro* (Smith & Jones, 1991; Wrighton & Stevens, 1992; Brandon *et al*., 2006).

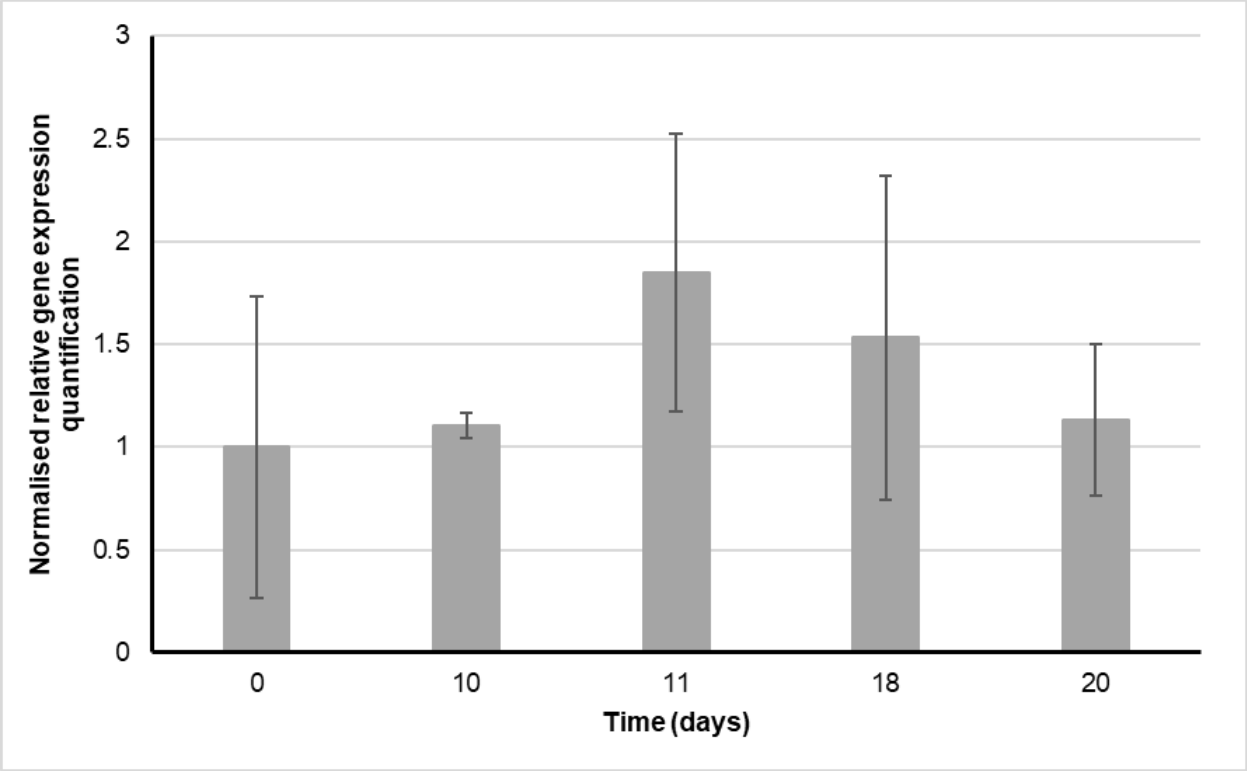

Figure 4.5. Relative *CYP3A4* gene expression of the sodium alginate encapsulated LS180 spheroid model. All data was relative to the gene expression on day 0 ($n = 3$; error bars = standard deviation).

In **Figure 4.5.** it is evident that growth in 3D induced an increase in the relative *CYP3A4* gene expression on day 11. The relative *CYP3A4* expression peaked on day 11, making this the optimal timeframe for drug biotransformation experiments. The expression was, however, slightly decreased on day 18, and even lower on day 20. Therefore, use of the model after 18 days of culturing would be sub-optimal for drug biotransformation, making days 11 to 18 the ideal window in which to perform further experiments.

As shown in **Figure 4.6.**, the relative *CYP2D6* gene expression decreased as a result of the spheroid culture, it is also noteworthy that this was statistically significant on days 18 and 20.

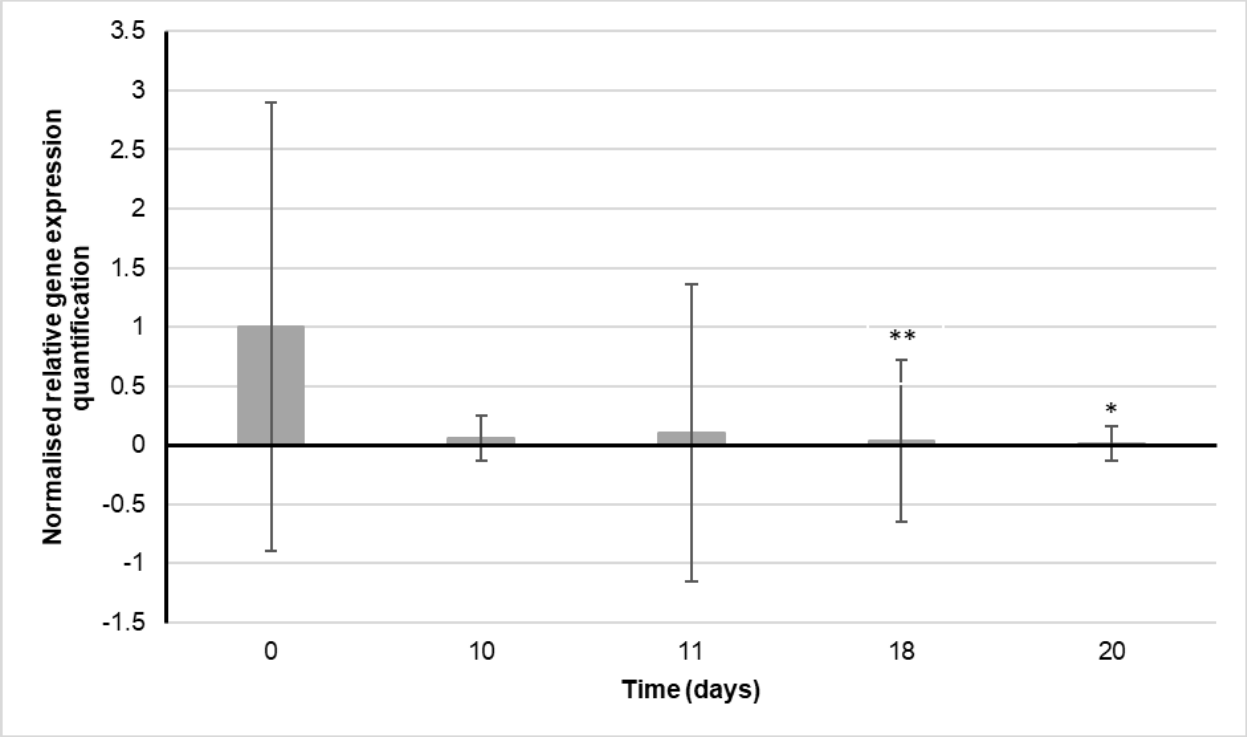

Figure 4.6. Relative *CYP2D6* gene expression of the sodium alginate encapsulated LS180 spheroid model. All data was relative to the gene expression on day 0 ($n = 3$; error bars = standard deviation; * = statistically significant, $p < 0.05$; ** = statistically significant, $p < 0.01$ (one-way ANOVA followed by Bonferroni post-hoc test for comparison with time point 0)).

4.5.6. Model characterisation summary

During the first 10 days of characterisation the increase in soluble protein content was slow, as the number of spheroids per bioreactor was high. However, following the reduction in spheroid numbers, rapid growth was indicated. Furthermore, the slower growth from day 0 to 10 could have been a result of recovery from trypsinisation. During this recovery the cells in the spheroids are engaged in the restoration of their key functions and this causes their growth rate to be reduced (Wrzesinski *et al*., 2013).

The interplay between cell growth and cell death is an important factor to take into consideration when evaluating cell viability. During the characterisation of the model, there was a steady increase in the intracellular ATP per protein content. The extracellular AK release per protein content also slowly increased as the spheroids aged, possibly indicating apoptosis. However, the intracellular ATP per protein content indicated that cells inside the spheroids were viable, even

though the extracellular AK release also increased. This was supported by the increase and extent of glucose consumption observed over time. The interplay between these parameters indicated that spheroids were actively growing and dying, suggesting that the sodium alginate encapsulated spheroids were viable until at least 20 days of culturing.

Following characterisation of the model in terms of growth, cell viability and relative gene expression, the optimal experimental window needed to be identified for further experiments. The first ten days were automatically ruled out because of the slow increase in soluble protein content, and the expected recovery from trypsinisation. After day 17, there was a slight decrease in the intracellular ATP content per µg protein, with a corresponding increase in the extracellular AK release per µg protein. Although these findings could be attributed to the depletion of nutrients which could be alleviated by a greater reduction of spheroid numbers, it was decided not to use the model after day 17 for this study. The relative *CYP3A4* gene expression also indicated days 11 - 18 being optimal.

4.6. Validation of the LS180 sodium alginate encapsulated spheroid model for anticancer treatment screening and drug biotransformation evaluation

To validate the use of the model for future anticancer treatment screening, the standard chemotherapeutic drug paclitaxel was used as a model drug. The reactivity of the LS180 sodium alginate encapsulated spheroid model to treatment with paclitaxel was investigated. The following parameters were investigated: soluble protein content, intracellular ATP content, extracellular AK release, glucose consumption, as well as the relative quantification of *CYP3A4*, *CYP2D6* and *P-gp* gene expression. For the model to be useful in future anticancer research, it is expected that standard chemotherapeutic drugs used to treat colon cancer will have a negative effect on the viability of the cells. Thus, during this study it was expected that treatment with paclitaxel would decrease the intracellular ATP content per spheroid, increase the extracellular AK release per spheroid and cause a reduction in the glucose consumed over time. Furthermore, it was expected that treatment with paclitaxel would increase the relative *CYP3A4* gene expression as the drug is metabolically inactivated by the enzyme, it was also expected that the relative *P-gp* gene expression will increase as paclitaxel is subjected to efflux by means of P-gp (Synold *et al*., 2001).

4.6.1. Soluble protein content

Following exposure to paclitaxel [IC_{50}] and paclitaxel 2[IC_{50}] for 96 h, the soluble protein content per spheroid was measured using the Bradford assay. All data was normalised to the untreated control group, as can be seen in **Figure 4.7.**

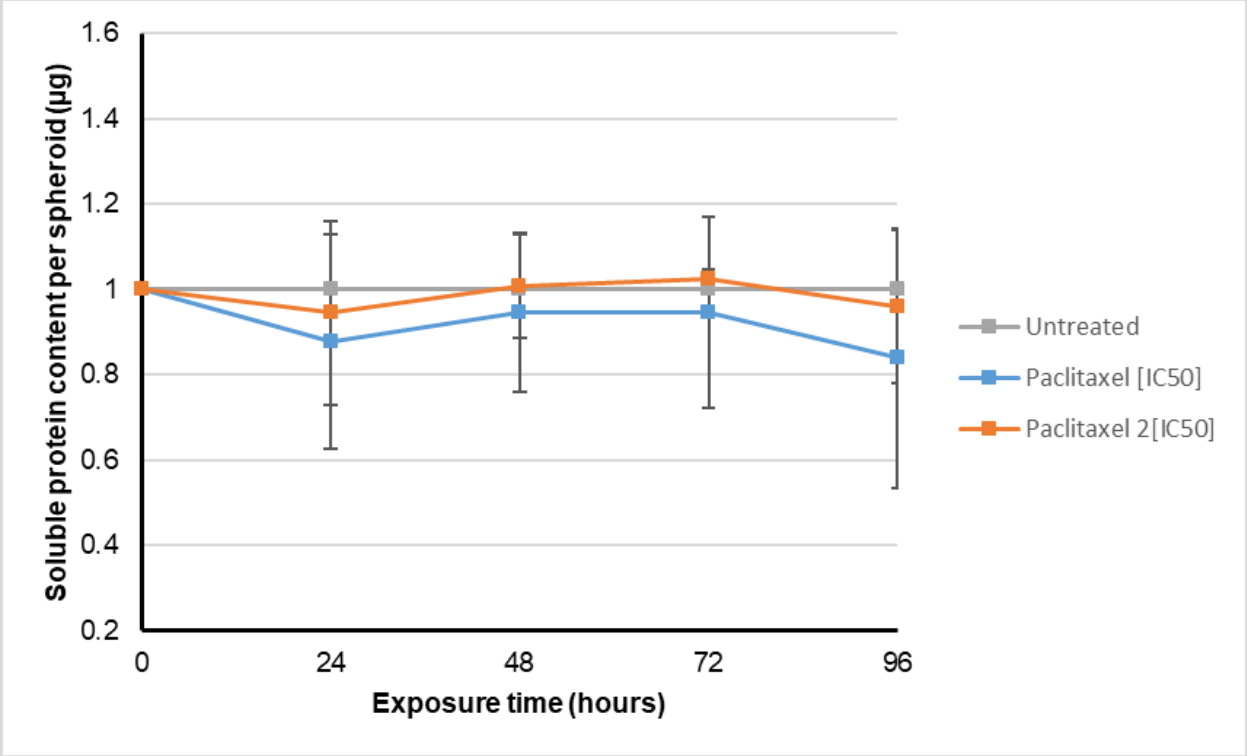

Figure 4.7. Normalised soluble protein content per spheroid (µg) of the sodium alginate encapsulated LS180 spheroid model, following 96 h exposure to paclitaxel. All data was normalised to the untreated control group (*n* = 2, error bars = standard deviation).

In **Figure 4.7.** it is evident that the soluble protein content per spheroid of the paclitaxel treated groups were lower than that of the untreated spheroids. It is also notable that there was not a substantial difference between the paclitaxel [IC_{50}] treatment group and that of paclitaxel 2[IC_{50}], although after 96 h of exposure the soluble protein content per spheroid of the higher dose of paclitaxel was slightly higher than that of the spheroids treated with the lower paclitaxel dose. None of these changes were, however, statistically significant.

4.6.2. Treatment dose calculations

To ensure constant exposure of all spheroids to the same amount of paclitaxel, the total soluble protein content per bioreactor was determined before each new dosing. The initial dosages were based on the IC_{50} concentration for paclitaxel determined in 2D cultured LS180 cells.

To establish the 2D IC_{50} concentration per protein, the determined 2D IC_{50} dose was divided by the measured soluble protein content per well containing 8 000 seeded cells. The soluble protein content was established as 2.606 µg soluble protein per well (*n* = 6; standard deviation = 0.233).

Thus the IC_{50} dosages per protein was established as:

- Paclitaxel [IC_{50}] = 0.006 mg/ml/µg protein
- Paclitaxel 2[IC_{50}] = 0.012 mg/ml/µg protein

These values were then multiplied by the amount of soluble protein per spheroid based on the amount of spheroids left in the bioreactor for the specific day. This then gave the dosage per bioreactor per day.

4.6.3. Intracellular adenosine triphosphate content

When looking at **Figure 4.8**, a slight reduction in the intracellular ATP levels per protein for both groups treated with paclitaxel could be observed, after only 4 h of exposure. Thereafter, there was a steady increase in the intracellular ATP levels per protein for both the paclitaxel treatment groups relative to the untreated control, reaching a peak at 24 h of exposure. The paclitaxel [IC_{50}] treatment group had a steady decrease in intracellular ATP levels per protein for the remainder of the experiment. The paclitaxel 2[IC_{50}] treatment group, however, had a very slight increase in intracellular ATP levels at 72 h of exposure, but this was once again followed by a decrease. After 96 h of exposure the intracellular ATP levels per protein for both treatment groups were reduced to almost half of the untreated group's ATP, with paclitaxel 2[IC_{50}] being statistically significantly decreased relative to the untreated control ($p < 0.05$). This indicated that the treatment with paclitaxel affected the health, growth and energy status of the LS180 spheroids.

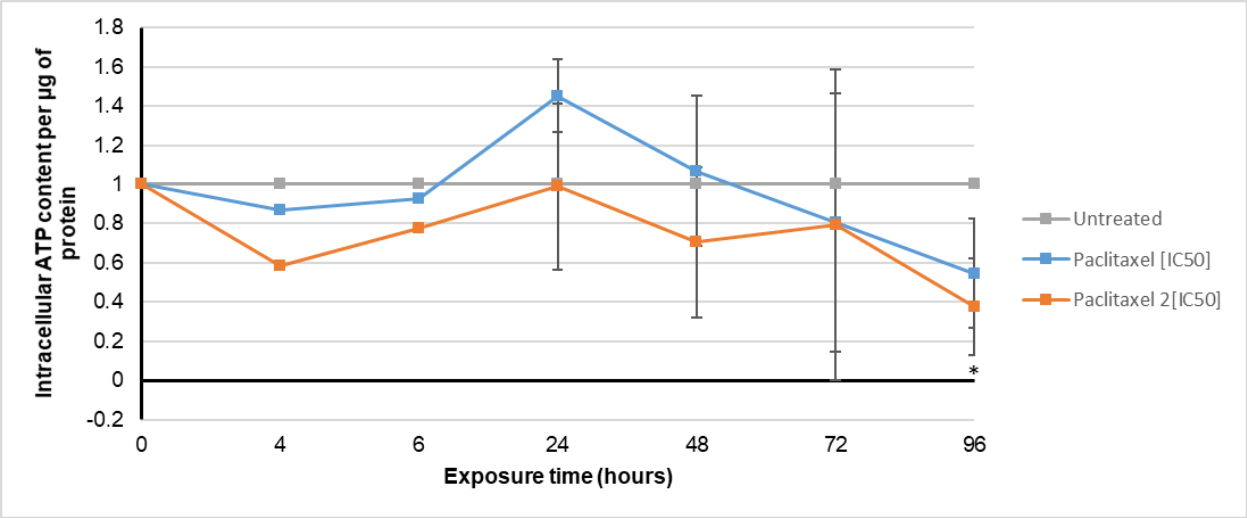

Figure 4.8. Normalised intracellular adenosine triphosphate content per soluble protein (µM/µg) following exposure of the sodium alginate encapsulated LS180 spheroid model to paclitaxel. All data was normalised to the untreated control group (n = 2, error bars = standard deviation; * = statistically significant, $p < 0.05$ (one-way ANOVA followed by the Dunnett post-hoc test for comparison with the untreated control)).

4.6.4. Extracellular adenylate kinase content

Following 96 h exposure to paclitaxel [IC_{50}] and paclitaxel 2[IC_{50}], the extracellular AK release was measured and data was expressed as intracellular ATP content per µg protein. Data was then expressed relative to the untreated control group and is illustrated in **Figure 4.9**.

The AK released per µg protein for both paclitaxel treated groups were not substantially different from the untreated group for the first 48 h of exposure (see **Figure 4.9.**). The paclitaxel [IC_{50}] treatment group then had a sharp increase in AK release per µg protein at the 72 h time point, followed by a decrease to below the untreated control at 96 h. It was notable that the AK release per µg protein following exposure to the higher concentration paclitaxel did not reach the high levels seen for the lower concentration. The paclitaxel 2[IC_{50}] concentration rather had a steady increase in the AK release per µg protein after 48 h of exposure. This suggests that cell death took place at a slower pace in the higher concentration group than in the lower concentration group.

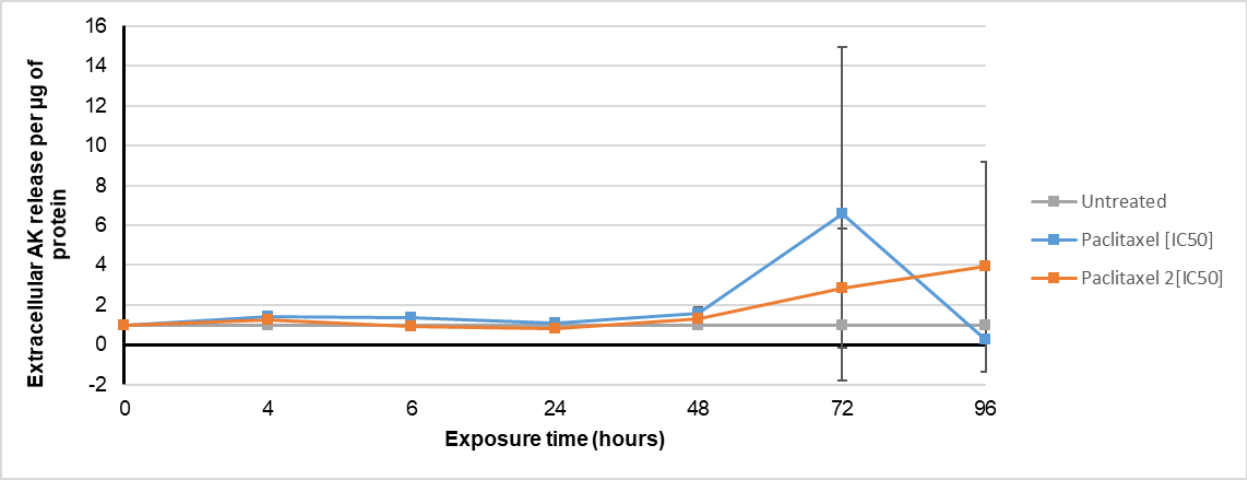

Figure 4.9. Normalised extracellular adenylate kinase release per microgram protein following exposure of the sodium alginate encapsulated LS180 spheroid model to paclitaxel. All data was normalised to the untreated control group (*n* =2, error bars = standard deviation).

4.6.5. Glucose consumption

The approximate quantities of glucose consumed by cells in each treatment group (mmol/L) were estimated from the glucose disappearance from the culture medium, and was expressed as glucose consumption per µg protein (see **Figure 4.10**). The data was then normalised to the glucose consumption per µg protein of the untreated control group.

Following 6 h of exposure to paclitaxel [IC_{50}], there was a marked increase in the quantity of glucose consumed by the treatment group in comparison to the untreated control group. This treatment group therefore appear to have consumed more glucose than the untreated control for the first 24 h of exposure. After 24 h of exposure there was a strong and steady decline in the glucose consumed by this group, with very little glucose consumed after 72 h and 96 h of exposure. It also notable that at time points, 48 h, 72 h and 96 h after exposure, the decrease was of statistical significance when compared to the untreated control ($p < 0.05$).

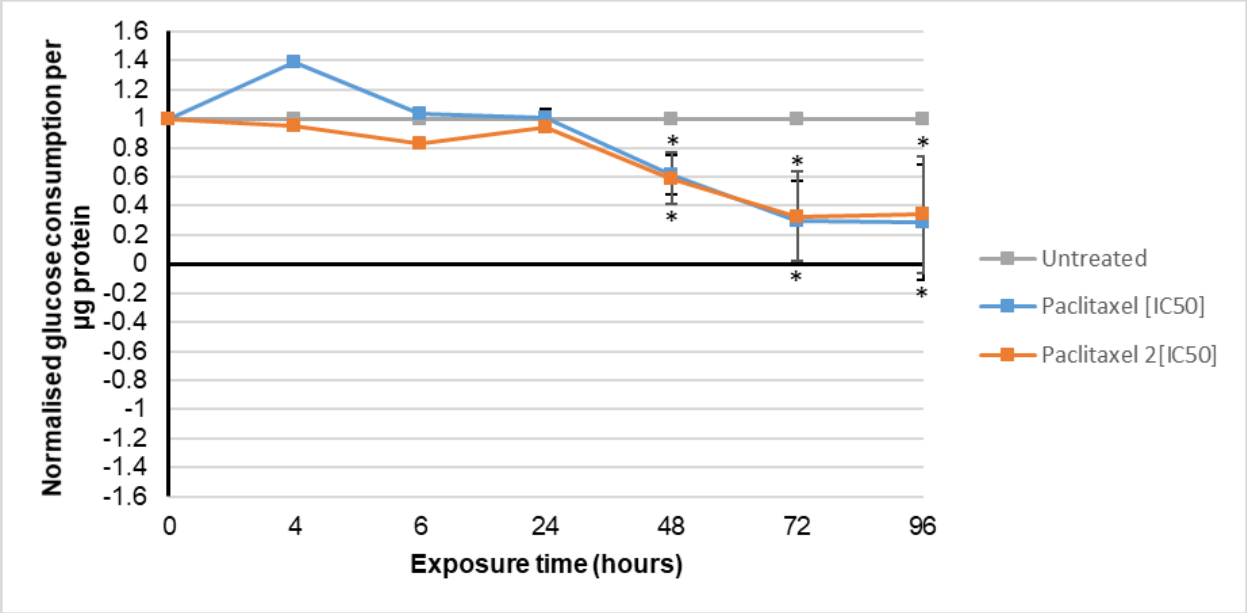

Figure 4.10. Normalised glucose consumption per microgram protein following exposure of the sodium alginate encapsulated LS180 spheroid model to paclitaxel. All data was normalised to the untreated control group (n = 2, error bars = standard deviation, * = statistically significant, $p < 0.05$ (one-way ANOVA followed by the Dunnett post-hoc test for comparison to the untreated control)).

The paclitaxel 2[IC_{50}] treatment group did not show the same increase in glucose consumption at 24 h as was seen with the lower dose. Instead, the paclitaxel 2[IC_{50}] treatment group showed a decline in glucose consumption for the first four hours, with a slight increase after 24 h of exposure. This was followed to a decrease in consumption similar to that of the paclitaxel [IC_{50}] group. It is clear that this group also had a strong and steady decline in glucose consumption for the duration of the experiment, with the same notable statistical significance.

4.6.6. Relative cytochrome P450 and P-glycoprotein gene expression

According to Synold *et al*. (2001), paclitaxel is one of the most commonly used antineoplastic agents and is subject to metabolic inactivation by CYP3A4 and CYP2C8. These enzymes hydroxylate the drug and thereby abolishes its antimitotic properties. Furthermore, paclitaxel is also excreted from the cells via P-gp, a broad-specificity efflux pump protein encoded by the gene MDR1.

The relative expression of the *CYP3A4* and *CYP2D6* genes were therefore measured before and after exposure by means of the qRT-PCR. This would indicate whether the expression of these

key phase I oxidation enzymes were affected by the paclitaxel exposure. The relative expression of the efflux protein, P-gp, was also measured following exposure, as P-gp plays a vital role in the development of drug resistance. All 96 h data was expressed relative to the untreated control group at time point 0 h.

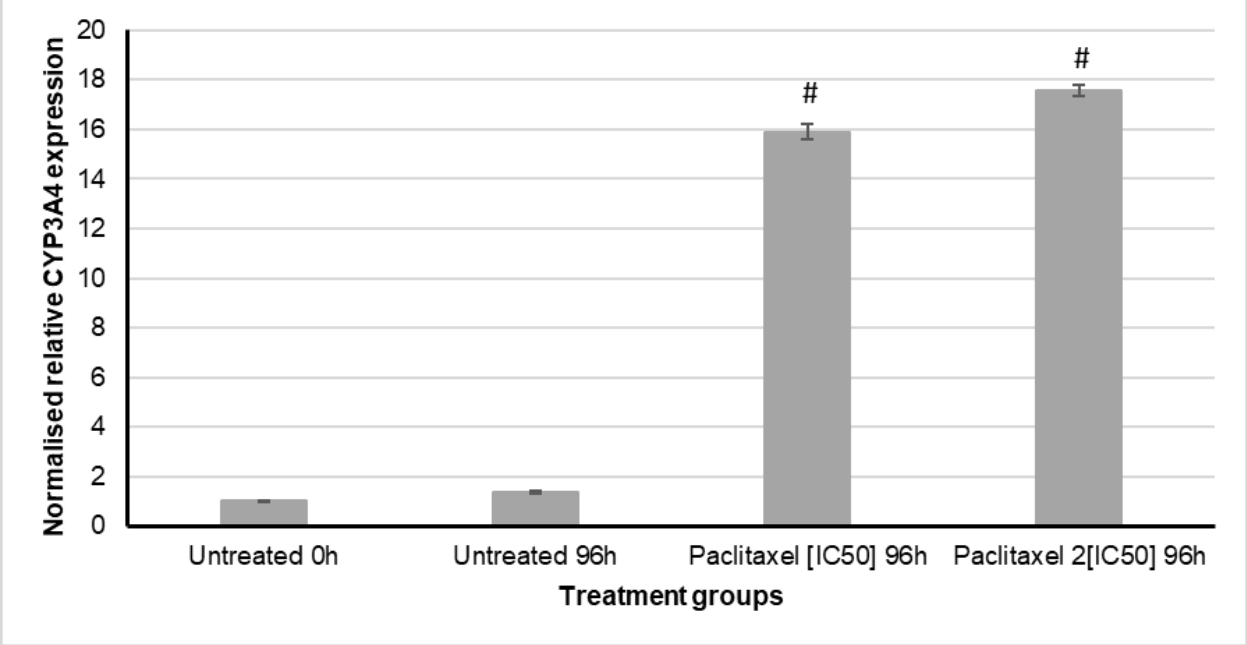

Figure 4.11. Relative *CYP3A4* gene expression following exposure of the sodium alginate encapsulated LS180 spheroid model to paclitaxel. All data was expressed relative to the untreated control group at time point 0 h (*n* = 3; error bars = standard deviation; # = statistically very significant, $p < 0.001$ (one-way ANOVA followed by the Bonferroni post-hoc test for comparison with the untreated control)).

In **Figure 4.11.**, the relative *CYP3A4* expression clearly indicated that the spheroids treated with paclitaxel had significantly increased expression of *CYP3A4* ($p < 0.001$) for both paclitaxel treatment concentrations. Synold *et al*. (2001) indicated in their study that paclitaxel was an effective activator of *CYP3A4*. Treatment with paclitaxel [IC_{50}] resulted in a sixteen-fold increase in the relative *CYP3A4* gene expression, while treatment with paclitaxel 2[IC_{50}] resulted in a seventeen-fold increase in relative *CYP3A4* gene expression.

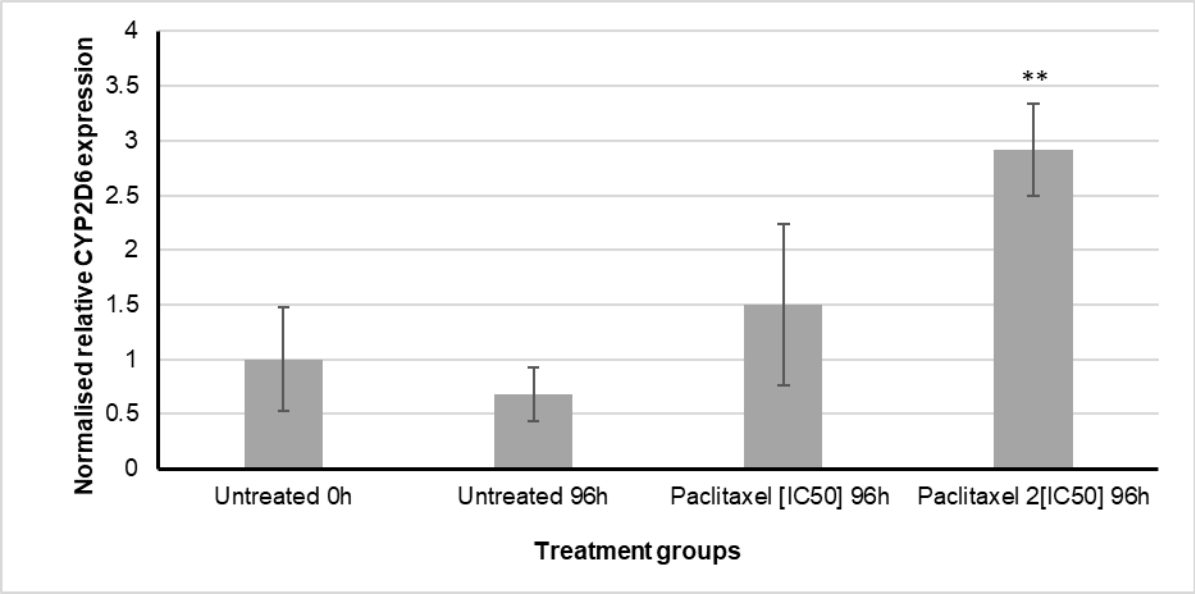

Figure 4.12. Relative *CYP2D6* gene expression following exposure of the sodium alginate encapsulated LS180 spheroid model to paclitaxel. All data was expressed relative to the untreated control group at time point 0 h (*n* = 3; error bars = standard deviation; ** = statistically very significant, $p < 0.01$ (one-way ANOVA followed by the Bonferroni post-hoc test for comparison with the untreated control)).

In **Figure 4.12.**, the relative *CYP2D6* gene expression was increase by treatment with paclitaxel. This increase was not as significant as the increase seen in the expression of *CYP3A4*. The treatment with paclitaxel [IC_{50}] resulted in a slight increase in expression. Treatment with paclitaxel 2[IC_{50}], on the other hand, resulted in almost a three-fold increase in the expression and this increase was indicated as statistically significant ($p < 0.01$).

Treatment with paclitaxel resulted in the increased expression of the P-gp efflux pump (see **Figure 4.13.**). Synold *et al*. (2001) also indicated in their study in 2D cultured LS180 cells, that paclitaxel induced its own efflux from the cells. The data presented in this study indicated that this efflux was dose dependant, as the treatment with the higher dose of paclitaxel showed a statistically significant increase in the expression of *P-gp* ($p < 0.01$).

Li and colleagues (2003) also confirmed that treatment with paclitaxel resulted in the upregulation of *P-gp*, as well as *CYP3A4*. P-gp and CYP3A4 are simultaneously increased by various xenobiotics and clinically administered drugs which are substrates of P-gp and CYP3A4. Therefore, drug interactions can occur via alterations in the expression of transporters and the

metabolic enzymes, and this should be considered as a possible cause of pharmacokinetic interactions.

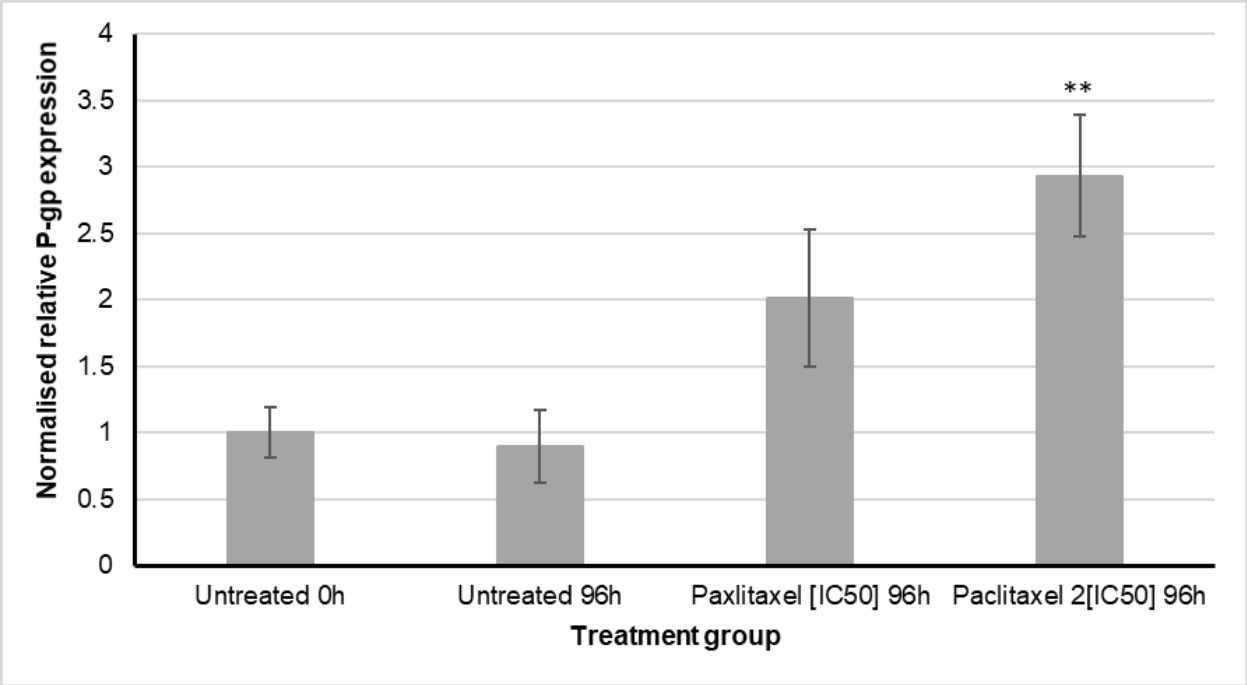

Figure 4.13. Relative P-glycoprotein gene expression following exposure of the sodium alginate encapsulated LS180 spheroid model to paclitaxel. All data was expressed relative to the untreated control group at time point 0 h (*n* = 3; error bars = standard deviation; ** = statistically significant, $p < 0.01$ (one-way ANOVA followed by the Bonferroni post-hoc test for comparison with the untreated control)).

4.6.7. Validation of the LS180 sodium alginate encapsulated spheroid model for anticancer treatment screening and drug biotransformation studies summary

To summarise, the LS180 sodium alginate encapsulated spheroid model may be used for anticancer treatment screening and drug biotransformation studies, for the following reasons:

1. Treatment with paclitaxel caused the interplay between intracellular ATP and extracellular AK per spheroid to change, when compared to the untreated control. This change indicated a reduction in cell viability and a possible increase in cell death.

2. Following treatment with paclitaxel for 96 h, there was a marked reduction in glucose consumption for both treatment groups when compared to the untreated control. This was a possible indication of decreased cell growth and function.
3. Paclitaxel treatment also resulted in a significant change in relative gene expression of *CYP3A4*, *CYP2D6* and *P-gp* in comparison to the untreated control, indicating reactivity of the model and the ability to represent efflux- or metabolism-based drug resistance.

4.7. *Sutherlandia frutescens* anticancer activity screening in the LS180 sodium alginate encapsulated spheroid model

To establish the anticancer treatment potential of *S. frutescens,* the LS180 sodium alginate model was implemented. The following parameters were investigated as indicators of cell growth and viability: soluble protein content, intracellular ATP content, extracellular AK release and the relative quantification of *CYP3A4* and *CYP2D6* gene expression.

4.7.1. Soluble protein content

The soluble protein content of the LS180 model was determined before and after exposure to *S. frutescens* treatment as an indicator of cell growth (see **Figure 4.14**). This protein content was also used to determine the exact dosages for each day, since treatment was calculated per soluble protein content. The first biological repeat of the treatment only included [IC_{50}] of *S. frutescence*, as determined in 2D, since 2[IC_{50}] of this crude aqueous extract was not soluble. Following the results obtained in the first experiment, [IC_{50}]/2 was included for the second biological repeat, but was only evaluated once.

After 24 h of exposure to the *S. frutescens* treatment, there was a reduction in soluble protein content per spheroid in comparison to the untreated control for both treatment groups. After 48 h of exposure, the soluble protein content per spheroid for both groups increased again. That of *S. frutescens* [IC_{50}]/2 was higher than for the untreated group, while for [IC_{50}] the protein content only increased slightly. Beyond 48 h of exposure, the soluble protein content per spheroid of the *S. frutescens* [IC_{50}]/2 treatment group continuously decreased, and at the 96 h time point the soluble protein content per spheroid of the *S. frutescens* [IC_{50}]/2 treatment group was 0.4 µg lower than the untreated group.

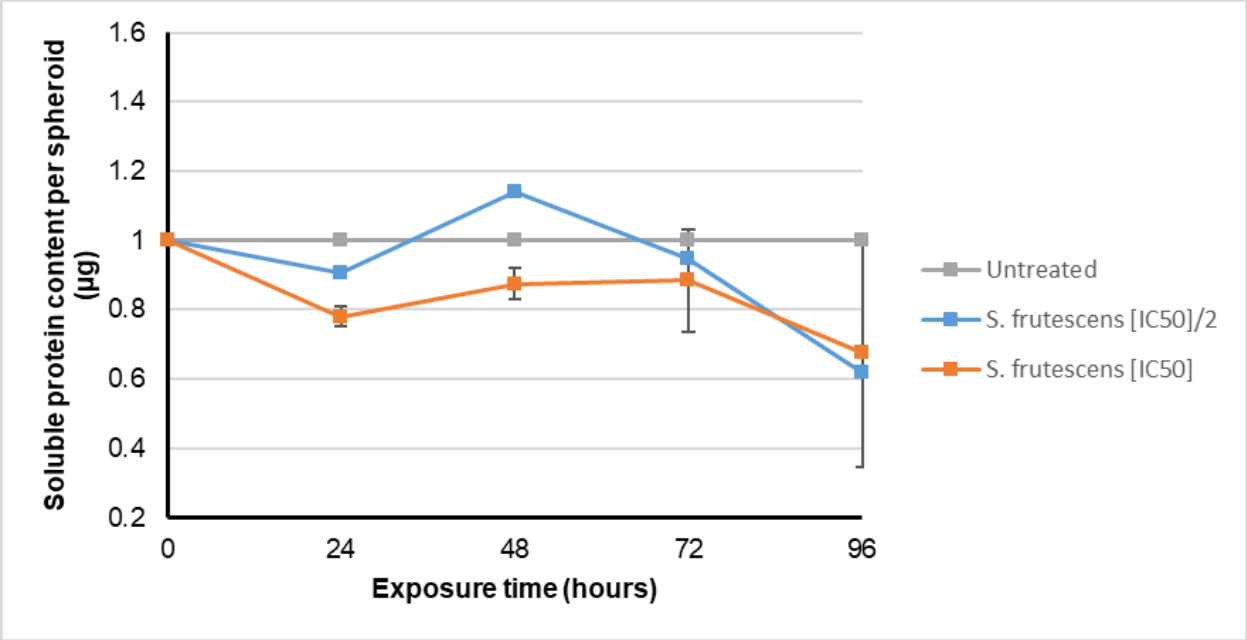

Figure 4.14. Normalised soluble protein content per spheroid (µg) of the sodium alginate encapsulated LS180 spheroid model, following 96 h exposure to *Sutherlandia frutescens* aqueous extract. All data was normalised to the untreated control group (error bars = standard deviation, n = 1 for the *S. frutescens* [IC_{50}]/2, n = 2 for *S. frutescens* [IC_{50}]).

The soluble protein content per spheroid for the *S. frutescens* [IC_{50}] treatment group remained lower than the untreated control throughout the experiment, but the decrease was not as marked as for the [IC_{50}] group. The soluble protein content per spheroid for the *S. frutescens* [IC_{50}] treatment group was only 0.3 µg lower than the untreated control. None of the changes were of statistical significance.

4.7.2. Treatment dose calculations

To ensure constant exposure of all spheroids to the same amount of *S. frutescens*, the total soluble protein content per bioreactor was determined before each new dosing. The initial dosages were based on the IC_{50} concentration for *S. frutescens* determined in 2D cultured LS180 cells.

To establish the 2D IC_{50} concentration per protein, the determined 2D IC_{50} dose was divided by the measured soluble protein content per well containing 8 000 seeded cells. The soluble protein content was established as 2.606 µg soluble protein per well (n = 6; standard deviation = 0.233).

Thus the IC_{50} dosages per protein was established as:

- *S. frutescens* [IC_{50}]/2 was 0.201 mg/ml/µg protein
- *S. frutescens* [IC_{50}] was 0.403 mg/ml/µg protein

These values were then multiplied by the amount of soluble protein per spheroid based on the amount of spheroids left in the bioreactor for the specific day. This then gave the dosage per bioreactor per day.

4.7.3. Intracellular adenosine triphosphate content

Following 96 h exposure to *S. frutescens* [IC_{50}]/2 and *S. frutescens* [IC_{50}], the intracellular ATP content was measured and data was expressed as intracellular ATP content per µg protein. Data was then expressed relative to the untreated control group and is illustrated in **Figure 4.15.**

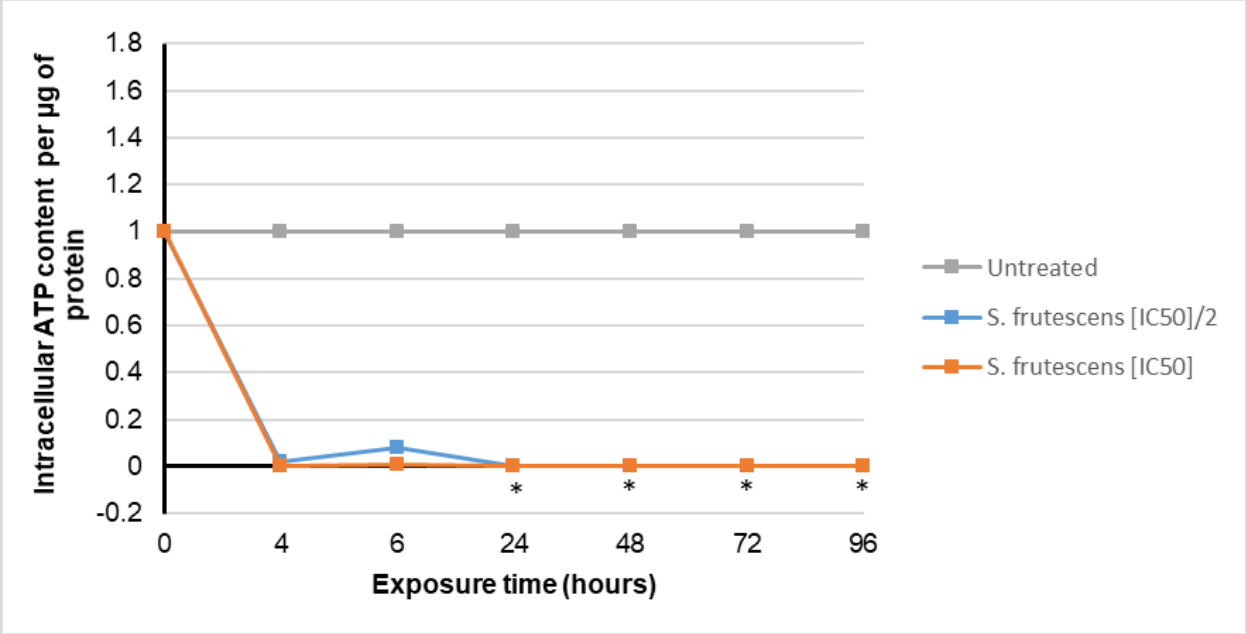

Figure 4.15. Normalised intracellular adenosine triphosphate content per soluble protein (µM/µg) following exposure of the sodium alginate encapsulated LS180 spheroid model to *Sutherlandia frutescens* aqueous extract. All data was normalised to the untreated control group (error bars = standard deviation; $n = 1$ for *S. frutescens* [IC_{50}]; $n = 2$ for *S. frutescens* [IC_{50}]; * = statistically significant, $p < 0.05$ (one-way ANOVA followed by the Dunnett post-hoc test for comparison with the untreated control)).

After only 4 h of treatment, no ATP could be detected in the spheroids treated with either concentration *S. frutescens,* resulting in significantly decreased intracellular ATP content per protein of 0 µM/µg ($p < 0.05$). This remained the case for the *S. frutescens* [IC_{50}] treatment group for the duration of the experiment. The *S. frutescens* [IC_{50}]/2 group had a slight increase in the intracellular ATP content per protein after 6 h of exposure, but the 24 h exposure time point, the ATP content per protein was also near 0 µM/µg and remained significantly decreased for the duration of the experiment ($p < 0.05$).

This was indicative of a loss of cell viability following treatment with the *S. frutescens* [IC_{50}] and [IC_{50}]/2 concentrations. Following a recovery period of 96 h with no treatment, the ATP content remained below detectable limits (results not shown).

4.7.4. Extracellular adenylate kinase content

Following 96 h exposure to *S. frutescens* [IC_{50}]/2 and *S. frutescens* [IC_{50}], the extracellular AK release was measured and data was expressed as intracellular ATP content per µg protein. Data was then expressed relative to the untreated control group and is illustrated in **Figure 4.16**.

Exposure to the *S. frutescens* aqueous extract for only 4 h, also resulted in extracellular AK release below detectable limits in both treatment groups ($p < 0.05$). The extracellular AK per µg protein for the *S. frutescens* [IC_{50}] group remained below detectable limits for the duration of the experiment. The *S. frutescens* [IC_{50}]/2 group showed an increase in AK per µg protein between the 6 h and 48 h time points. This was still markedly lower than the AK released by the untreated control group. The AK released then also decreased below detectable limits.

The results suggest that if AK was released in the *S. frutescens* [IC_{50}] group, this would have had to take place within the first 4 h of treatment.

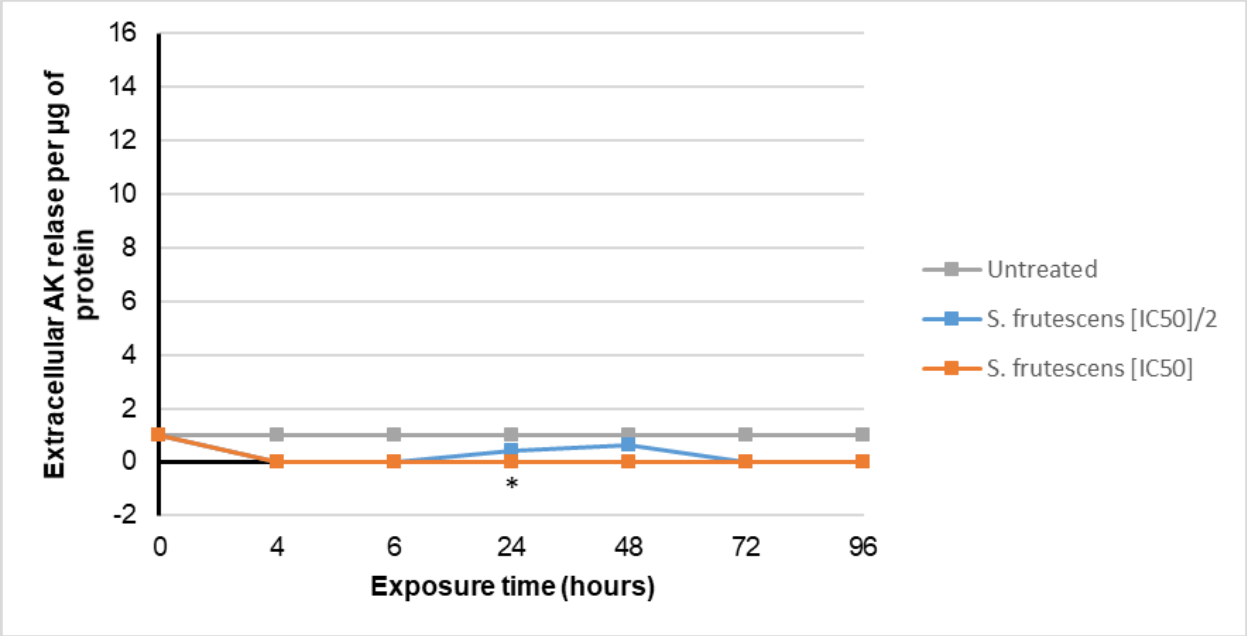

Figure 4.16. Normalised extracellular adenylate kinase release per microgram protein following exposure of the sodium alginate encapsulated LS180 spheroid model to *Sutherlandia frutescens*. All data was normalised to the untreated control group (error bars = standard deviation; *n* = 1 for *S. frutescens* [IC_{50}]/2; *n* = 2 for *S. frutescens* [IC_{50}]; * = statistically significant, $p < 0.05$ (one-way ANOVA followed by the Dunnett post-hoc test for comparison with the untreated control)).

4.7.5. Glucose consumption

The approximate quantities of glucose consumed by cells in each treatment group (mmol/L) were estimated from the glucose disappearance from the culture medium, and was expressed as glucose consumption per µg protein (see **Figure 4.17**). The data was then normalised to the glucose consumption per µg protein of the untreated control group.

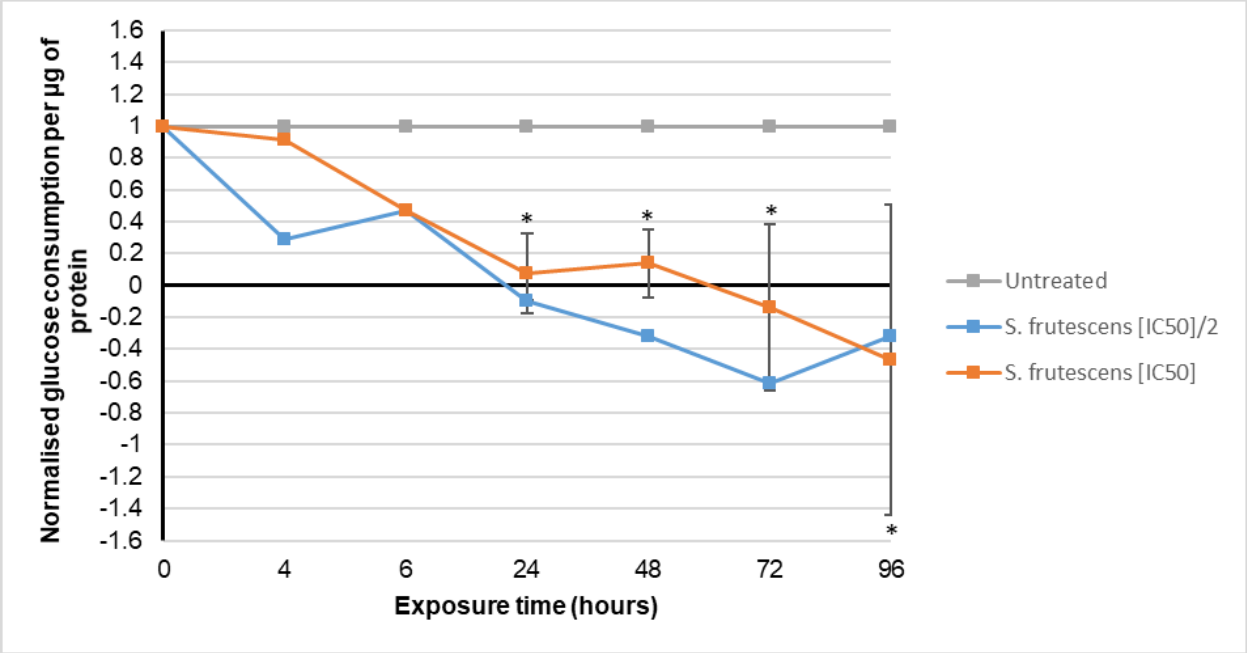

Figure 4.17. Normalised glucose consumption per microgram protein following exposure of the sodium alginate encapsulated LS180 spheroid model to *Sutherlandia frutescens*. All data was normalised to the untreated control group (error bars = standard deviation; n = 1 for *S. frutescens* [IC_{50}]/2; n = 2 for *S. frutescens* [IC_{50}]; * = statistically significant, $p < 0.05$ (one-way ANOVA followed by the Dunnett post-hoc test for comparison with the untreated control)).

The measured glucose content of the *S. frutescens* [IC_{50}]/2 treatment was very high (±10.9 mmol/L), and the content of the *S. frutescens* [IC_{50}] treatment was even higher (15.1 - 16.8 mmol/L). The normal unspent medium had a glucose content of only 6.4 - 6.8 mmol/L, which is much lower.

When considering glucose consumption in terms of the protein content it is, however, clear from **Figure 4.17** that both treatment groups consumed much less glucose relative to the untreated control. The glucose consumption for after 24 h of exposure to *S. frutescens* [IC_{50}] was significance reduced ($p < 0.05$), and it remained so for the duration of the experiment. After 24 h of exposure, the *S. frutescens* [IC_{50}]/2 consumed no glucose at all, and the glucose content of the spent medium was even higher than that of the unspent extract-containing medium. The same was also observed for the *S. frutescens* [IC_{50}] treatment group after 72 h of exposure.

According to Nakashima *et al*. (1984), some tumour cells produce as much as 60% of their ATP through glycolysis under aerobic conditions (Chen *et al*., 2007). After only 4 h of exposure to

S. frutescens, the intracellular ATP levels per µg protein were below detectable limits, indicating that no glucose was needed to be converted to pyruvate in order to produce ATP. This could serve as a possible explanation for the decline in glucose consumption. Many cancer cells, however, do not exclusively rely on glycolysis as the sole pathway to generate ATP and this should be kept in mind (Chen *et al*., 2007).

It is also possible that the high glucose content of the treatment-containing medium resulted in apoptosis, as demonstrated in a study by Ho *et al*. (2000). They indicated that high-glucose medium content induced apoptosis in human umbilical vein endothelial cells. To clarify this, further investigation is required.

4.7.6. Relative cytochrome P450 gene expression

In a study by Katerere (2018), it was established that *S. frutescens* aqueous and organic extracts showed no potential for inhibiting CYP450 enzymes.

In the current study, the qRT-PCR assay was performed following 96 h of exposure to *S. frutescens* crude aqueous extract, and the housekeeping genes glyceraldehyde 3-phosphate dehydrogenase (*GADPH*) and TATA-box binding protein (*TBP*) was indicated and present. Expression of the *CYP3A4* and *CYP2D6* genes were, however, not detected in either the *S. frutescens* [IC_{50}]/2 or the *S. frutescens* [IC_{50}] treatment samples (please see **Appendix G** for qRT-PCR amplification results).

It is possible that treatment with this plant extract resulted in the suppression of these genes below detectable limits in the LS180 model. This contradicts the findings by Katerere (2018), but this may be a result of the specific cell type used in the two studies, and the 3D nature of the LS180 model.

4.7.7. Summary for the anticancer screening of *Sutherlandia frutescence*

The results of this study suggest very good potential anticancer activity for the *S. frutescence* crude aqueous extract, specifically in colon cancer. This activity even appears to surpass that of the model chemotherapeutic drug, paclitaxel.

However, there are some questions which remain unanswered and further studies are needed to understand the full extent of this activity.

4.8. *Xysmalobium undulatum* anticancer activity screening in the LS180 sodium alginate encapsulated spheroid model

To establish the anticancer treatment potential of *X. undulatum,* the LS180 sodium alginate model was implemented. The following parameters were investigated as indicators of cell growth and viability: soluble protein content, intracellular ATP content, extracellular AK release and the relative quantification of *CYP3A4* and *CYP2D6* gene expression.

4.8.1. Soluble protein content

The soluble protein content of the LS180 model was determined before and after exposure to *X. undulatum* treatment as an indicator of cell growth (see **Figure 4.18**). This protein content was also used to determine the exact doses for each day, since treatment was calculated per soluble protein content.

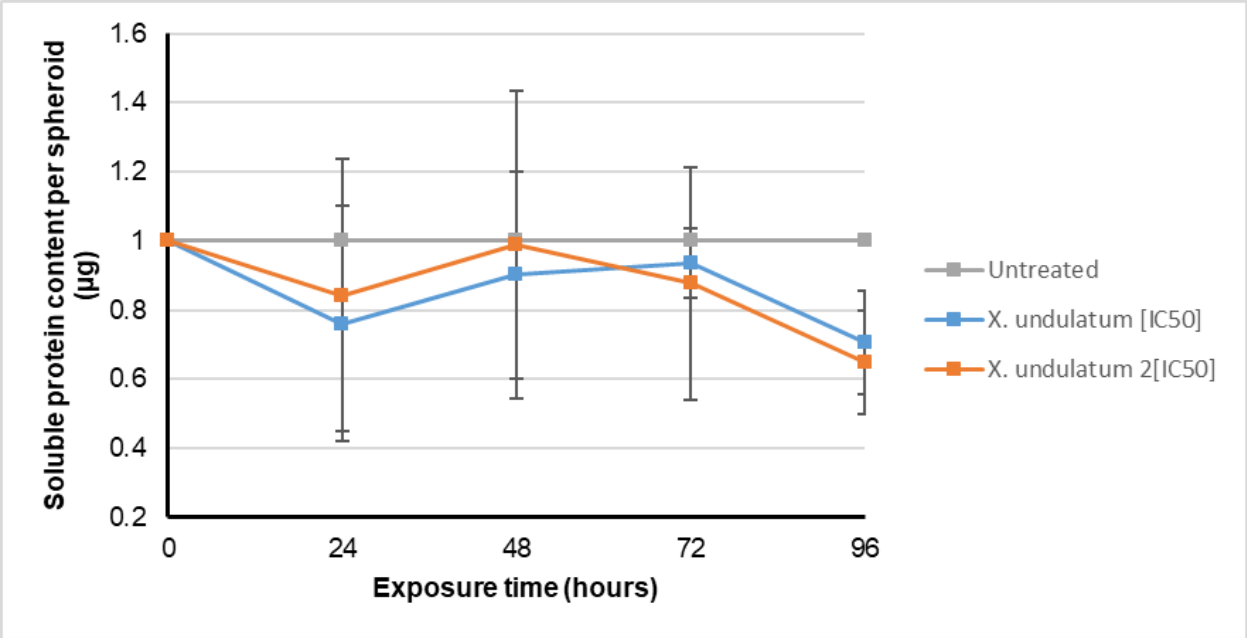

Figure 4.18. Normalised soluble protein content per spheroid (µg) of the sodium alginate encapsulated LS180 spheroid model, following 96 h exposure to *Xysmalobium undulatum* aqueous extract. All data was normalised to the untreated control group (n = 2, error bars = standard deviation).

The soluble protein content per spheroid for both *X. undulatum* treatment groups showed a slight decrease after only 24 h of exposure. The soluble protein content per spheroid for both treatment groups then remained lower than the untreated group throughout the experiment, although the decrease appeared slower for the *X. undulatum* [IC_{50}] group than for the *X. undulatum* 2[IC_{50}] group.

4.8.2. Treatment dose calculations

To ensure constant exposure of all spheroids to the same amount of *X. undulatum*, the total soluble protein content per bioreactor was determined before each new dosing. The initial dosages were based on the IC_{50} concentration for *X. undulatum* determined in 2D cultured LS180 cells.

To establish the 2D IC_{50} concentration per protein, the determined 2D IC_{50} dose was divided by the measured soluble protein content per well containing 8 000 seeded cells. The soluble protein content was established as 2.606 µg soluble protein per well (n = 6; standard deviation = 0.233).

Thus the IC_{50} dosages per protein was established as:

- *X. undulatum* [IC_{50}] was 0.008 mg/ml/µg protein
- *X. undulatum* 2[IC_{50}] was 0.015 mg/ml/µg protein

These values were then multiplied by the amount of soluble protein per spheroid based on the amount of spheroids left in the bioreactor for the specific day. This then gave the dosage per bioreactor per day.

4.8.3. Intracellular adenosine triphosphate content

Following 96 h exposure to *X. undulatum* 2[IC_{50}] and *X. undulatum* [IC_{50}], the intracellular ATP content was measured and data was expressed as intracellular ATP content per µg protein. Data was then expressed relative to the untreated control group and is illustrated in **Figure 4.19.**

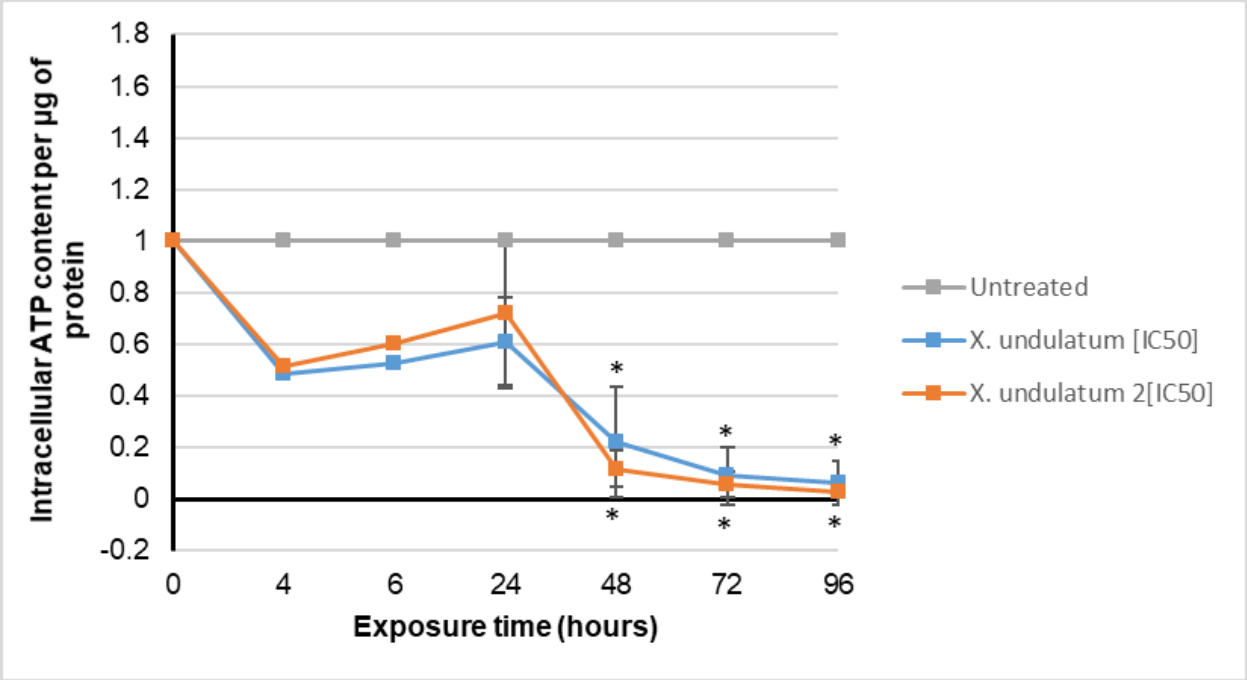

Figure 4.19. Normalised intracellular adenosine triphosphate content per soluble protein (µM/µg) following exposure of the sodium alginate encapsulated LS180 spheroid model to *Xysmalobium undulatum* aqueous extract. All data was normalised to the untreated control group (n = 2, error bars = standard deviation; * = statistically significant, $p < 0.05$ (one-way ANOVA followed by the Dunnett post-hoc test for comparison with the untreated control)).

Treatment with *X. undulatum* resulted in a dramatic decrease in intracellular ATP content per protein after only 4 h exposure. After that, followed by a slight increase in ATP content for the next 20 hours. The *X. undulatum* [IC_{50}] treatment group then showed a steady decrease in intracellular ATP content per protein, with the ATP content being 0.032 µM/µg (significantly reduced relative to the untreated control group, $p < 0.05$) at the end of the experiment. The intracellular ATP content per protein for the *X. undulatum* 2[IC_{50}] also reached a climax after 24 h of exposure. After this increase, the intracellular ATP content per spheroid had a significant decline to levels almost equal to those of the *X. undulatum* [IC_{50}] treatment group. The *X. undulatum* 2[IC_{50}] had a slightly lower intracellular ATP content per spheroid than that of *X. undulatum* [IC_{50}] after 96 h of exposure (0.021 µM/µg relative to the untreated control, $p < 0.05$).

This decrease in intracellular ATP content, combined with the decreased protein content of the treated spheroids, suggests that treatment with *X. undulatum* reduced viability and growth of the LS180 cells.

4.8.4. Extracellular adenylate kinase content

Following 96 h of exposure to *X. undulatum* 2[IC_{50}] and *X. undulatum* [IC_{50}], the extracellular AK release was measured and data was expressed as extracellular AK per µg protein. Data was then expressed relative to the untreated control group and is illustrated in **Figure 4.20.**

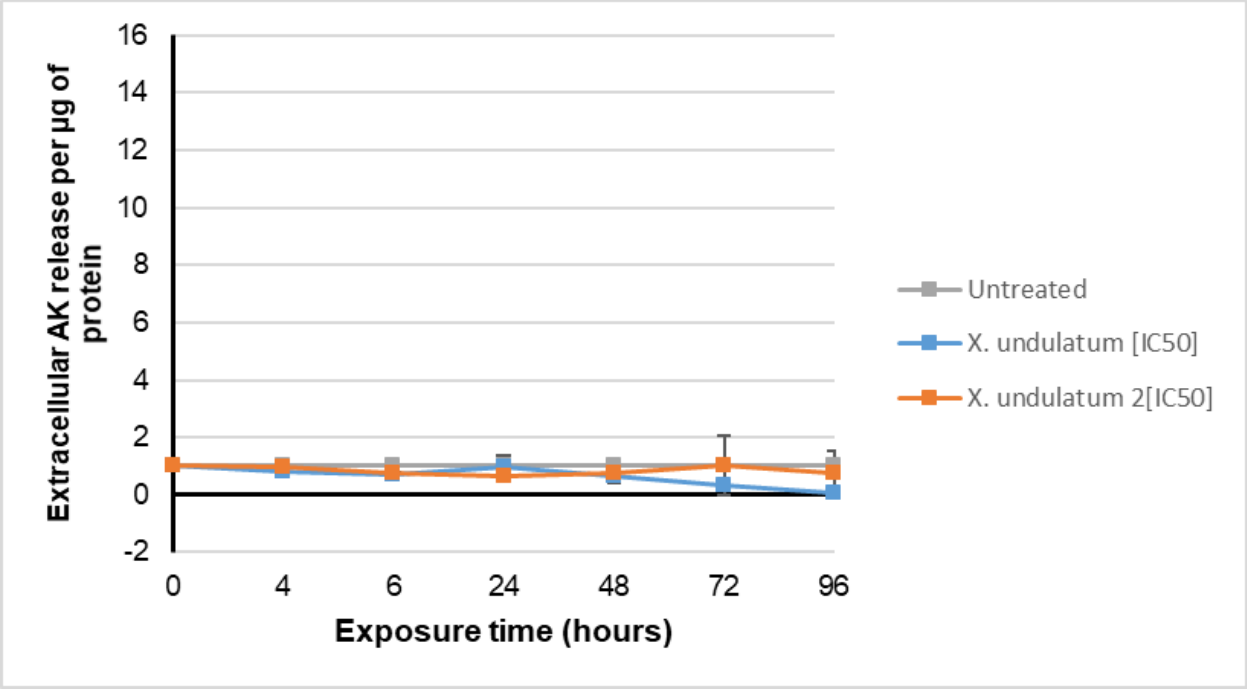

Figure 4.20. Normalised extracellular adenylate kinase release per microgram protein following exposure of the sodium alginate encapsulated LS180 spheroid model to *Xysmalobium undulatum*. All data was normalised to the untreated control group (*n* = 2; error bars = standard deviation).

When evaluating the AK release for the *X. undulatum* [IC_{50}] group, the AK release had a decline for the first few hours, but after 24 h the value was almost the same as that of the untreated group. After 24 h exposure there was a steady decline in AK release for the remainder of the experiment, being close to 0 after 96 h exposure. The *X. undulatum* 2[IC_{50}] group had no noteworthy changes in AK release after the first 4 h of exposure. Following the first 4 h, the AK release had a decline, with a slight increase after 48 h of exposure. All this was, however, still below that of the untreated

control group. After 72 h of exposure the AK release of the *X. undulatum* 2[IC_{50}] group was almost the same as the untreated control group. This was then followed by a decrease after 96 h of exposure. Following the completion of the experiment, the AK release per µg protein for *X. undulatum* 2[IC_{50}] was much higher than that of the *X. undulatum* [IC_{50}] group. The results once again suggest that the increased release of AK may have occurred at time points not evaluated in this study.

4.8.5. Glucose consumption

The approximate quantities of glucose consumed by cells in each treatment group (mmol/L) were estimated from the glucose disappearance from the culture medium, and was expressed as glucose consumption per µg protein (see **Figure 4.21**).

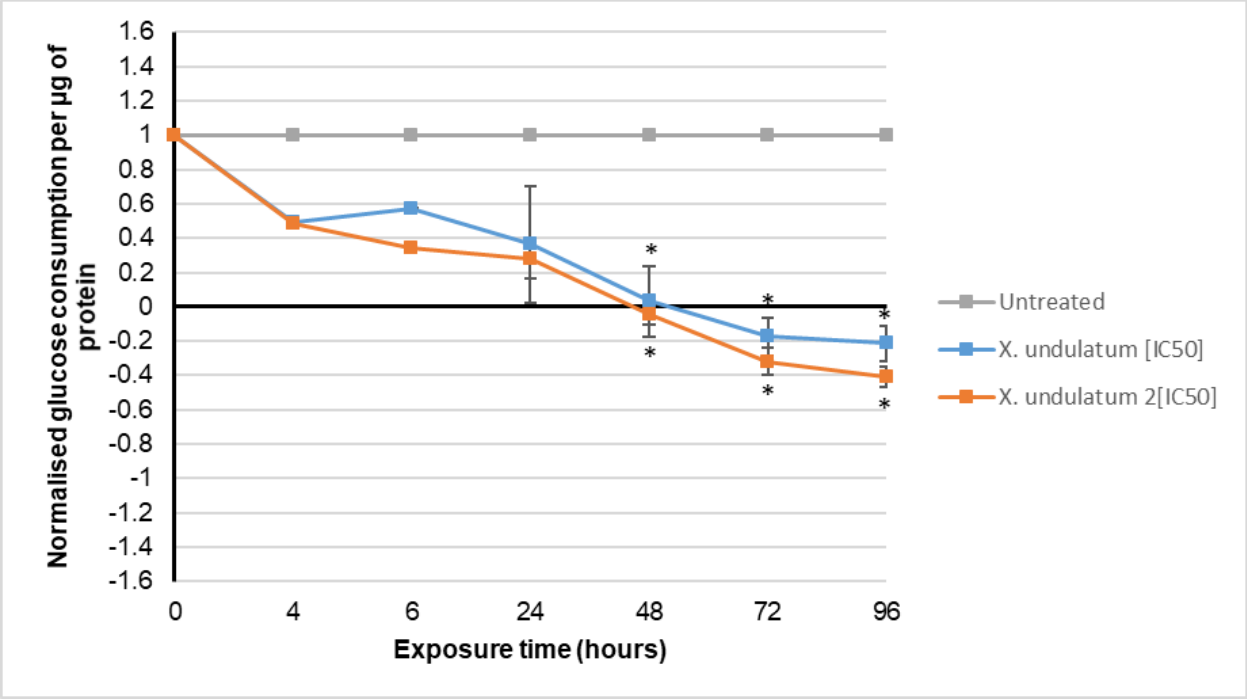

Figure 4.21. Normalised glucose consumption per microgram protein following exposure of the sodium alginate encapsulated LS180 spheroid model to *Xysmalobium undulatum*. All data was normalised to the untreated control group (n = 2, error bars = standard deviation; * = statistically significant, $p < 0.05$ (one-way ANOVA followed by the Dunnett post-hoc test for comparison with the untreated control)).

The data was then normalised to the glucose consumption per µg protein of the untreated control group.

As shown in **Figure 4.21.** treatment with *X. undulatum* aqueous extract resulted in a decrease in glucose consumption after only 4 h of exposure. Both *X. undulatum* treatment groups had a steady decline in glucose consumption per µg protein for the duration of the treatment. The decrease was slightly slower for the lower dose of *X. undulatum*.

The decrease in glucose consumption corresponds very well with the decreased soluble protein content and intracellular ATP content observed following treatment with *X. undulatum*, and the results suggests reduced cell viability and growth. The decrease in glucose consumption during this experiment was of statistical significance after 48 h, 72 h and 96 h of exposure for both groups, with $p < 0.05$.

4.8.6. Relative cytochrome P450 gene expression

Following 96 h of exposure to *X. undulatum,* the qRT-PCR assay was performed and the housekeeping genes *GADPH* and *TBP* was indicated and present. Expression of the *CYP3A4* and *CYP2D6* genes were, however, not detected in any of the *X. undulatum* treated samples (please see **Appendix G** for qRT-PCR amplification results). It is a possibility that treatment with the plant extract resulted in the suppression of these genes below detectable limits.

4.8.7. Summary for the anticancer screening of *Xysmalobium undulatum*

The results of this study suggest good potential anticancer activity for the *X. undulatum* crude aqueous extract, specifically in colon cancer. This activity appears to also surpass that of the model chemotherapeutic drug, paclitaxel. However, the activity seems to be less pronounced than observed for *S. frutescence*.

Further studies are needed to further investigate this activity, and to evaluate the significance of the activity relative to the potential for cytotoxicity.

4.9. Summary

The LS180 sodium alginate encapsulated spheroid model was successfully cultured and maintained for 20 days during this study. The model was subsequently characterised in terms of

growth, viability and relative gene expression of *CYP3A4* and *CYP2D6*, confirming viability of the model for the duration of the culturing.

The established model was then successfully validated in terms of its use an *in vitro* model for future anticancer treatment screening and drug biotransformation evaluations by using the standard chemotherapeutic drug, paclitaxel. The model clearly showed reactivity to the treatment, as well as the development of resistance to the treatment in the same way previously observed in patients, with upregulation of metabolic enzymes and efflux transporters.

Lastly, the model was implemented to evaluate the potential of *S. frutescens* and *X. undulatum* aqueous extracts to be used as anticancer treatments for colorectal cancer. Results of this study indicated that the model could indeed be used for future anticancer treatment screening. Furthermore, the results of the phytomedicine treatment of the LS180 spheroid model with *S. frutescens* and *X. undulatum* indicated that these extracts could indeed have potential as anticancer treatments for colorectal cancer, with more pronounced activity than the standard chemotherapeutic drug, paclitaxel.

References:

Akcay, A. 2013. The calculation of LD50 using probit analysis. *Federation of American societies for experimental biology*, 27:1217-1218.

Ahmann, F.R., Garewal, H.S., Schifman, R., Celniker, A. & Rodney, S. 1987. Intracellular adenosine triphosphate as a measure of human tumor cell viability and drug modulated growth. *In vitro cellular & developmental biology*, 23:474-480.

Brandon, E.F.A., Bosch, T.M., Deenena, M.J., Levinka, R., Van der Wal, E., Van Meerveld, J.B.M., Bijl, M., Beijnen, J.H., Schellens, J.H.M. & Meijerman, I. 2006. Validation of *in vitro* cell models used in drug metabolism and transport studies; genotyping of cytochrome P450, phase II enzymes and drug transporter polymorphisms in the human hepatoma (HepG2), ovarian carcinoma (IGROV-1) and colon carcinoma (CaCo-2, LS180) cell lines. *Toxicology and applied pharmacology*, 211:1-10.

Bröker, L.E., Kruyt, F.A. & Giaccone, G. 2005. Cell death independent of caspases: a review. *Clinical cancer research*, 11:3155-3162.

Elmore, S. 2007. Apoptosis: a review of programmed cell death. *Toxicologic pathology*, 35:495-516.

Calitz, C. 2017. Establishing three-dimensional cell culture models to measure biotransformation and toxicity. Potchefstroom:NWU. (Thesis- PhD).

Chen, Z., Lu, W., Garcia-Prieto, C. & Huang, P. 2007. The Warburg effect and its cancer therapeutic implications. *Journal of bioenergetics and biomembranes*, 39:267-274.

Ho, F.M., Liu, S.H., Liau, C.S., Huang, P.J. & Lin-Shiau, S.Y. 2000. High glucose–induced apoptosis in human endothelial cells is mediated by sequential activations of c-Jun NH2-terminal kinase and caspase-3. *Circulation*, 101:2618-2624.

Jacobs, A.C., DiDone, L., Jobson, J., Sofia, M.K., Krysan, D. & Dunman, P.M. 2013. Adenylate kinase release as a high-throughput-screening-compatible reporter of bacterial lysis for identification of antibacterial agents. *Antimicrobial agents and chemotherapy*, 57:26-36.

Kanduc, D., Mittelman, A., Serpico, R., Sinigaglia, E., Sinha, A.A., Natale, C., Santacroce, R., Di Corcia, M.G., Lucchese, A., Dini, L., Pani, P., Santacroce, S., Simone, S., Bucci, R. & Farber, E. 2002. Cell death: apoptosis versus necrosis. *International journal of oncology*, 21:165-170.

Katerere, D.R. 2018. Effects of extracts of *Sutherlandia frutescens* on drug transport and drug metabolising enzymes. *South African journal for science and technology*, 37:1-5

Khoo, M.L., McQuade, L.R., Smith, M.S., Lees, J.G., Sidhu, K.S. & Tuch, B.E. 2005. Growth and differentiation of embryoid bodies derived from human embryonic stem cells: effect of glucose and basic fibroblast growth factor. *Biology of reproduction*, 73:1147-1156.

Li, Q., Sai, Y., Kato, Y., Tamai, I. & Tsuji, A. 2003. Influence of drugs and nutrients on transporter gene expression levels in Caco-2 and LS180 intestinal epithelial cell lines. *Pharmaceutical research*, 20:1119-1124.

McDonald, J.H. 2014. Handbook of biological statistics. 3rd ed. Baltimore: Sparky House Publishing.

Nakashima, R.A., Paggi, M.G. & Pedersen, P.L. 1984. Contributions of glycolysis and oxidative phosphorylation to adenosine 5′-triphosphate production in AS-30D hepatoma cells. *Cancer research*, 44:5702-5706.

Omoruyi, S.I., Enogieru, A.B. & Ekpo, O.E. 2018. Cytotoxic and apoptosis-inducing effects of *Sutherlandia frutescens* in neuroblastoma cells. *Journal of African association of physiological sciences*, 6:136-144.

Swanepoel, R.A. 2018. *In vitro* evaluation of the efficacy of selected medicinal plant extracts against multidrug resistant cancer cells. Potchefstroom:NWU. (Dissertation- MSc).

Smith, D.A.& Jones, B.C. 1991. Commentary: speculations on the structure-activity relationship (SSAR) of cytochrome P450 enzymes. *Biochemical pharmacology*., 44:2089-2098.

Riss, T., Moravec, R.A., Niles, A.L., Duellman, S., Benink, H.A., Worzella, T.J. & Minor, L. 2016. Cell Viability Assays. (In Sittampalam, G.S., Coussens, N.P., Brimacombe, K., Grossman, A., Arkin, M., Auld, A., Austin, C., Baell, J., Bejcek, B., Chung, T.D.Y., Dahlin, J.L., Devanaryan, V., Foley, T.L., Glicksman, M., Hall, M.D., Hass, J.V., Inglese, J., Iversen, P.W., Kahl, S.D., Kales, S.C., Lal-Nag, M., Li, Z., McGee, J., McManus, O., Riss, T., Trask, O.J., Weidner, J.R., Xia, M., Xu, X. ed. Assay Guidance Manual. Bethesda: Eli Lilly & Company and the National Center for Advancing Translational Sciences. p.355-385).

Rossouw, M.J. 2018. Evaluation of the efficacy of selected anticancer compounds in multidrug resistant cell culture models. Potchefstroom:NWU. (Dissertation- MSc).

Synold, T.W., Dussault, I. & Forman, B.M. 2001. The orphan nuclear receptor SXR coordinately regulates drug metabolism and efflux. *Nature medicine*, 7:584-590.

Wrighton, S.A. & Stevens, J.C. 1992. The human hepatic cytochromes P450 involved in drug metabolism. *Critical reviews in toxicology*, 22:1-21.

Wrzesinski, K., Magnone, M.C., Hansen, L.V., Kruse, M.E., Bergauer, T., Bobadilla, M., Gubler, M., Mizrahi, J., Zhang, K., Andreasen, C.M. & Joensen, K.E. 2013. HepG2/C3A 3D spheroids exhibit stable physiological functionality for at least 24 days after recovering from trypsinisation. *Toxicology research*, 2:163-172.

Wrzesinski, K. & Fey, S. 2018. Metabolic reprogramming and the recovery of physiological functionality in 3D cultures in micro-bioreactors. *Bioengineering*, 5:1-25.

CHAPTER 5

This chapter presents concluding remarks on the LS180 three-dimensional sodium alginate encapsulated spheroid model, its characterization and its validation for use in anticancer treatment screening and drug biotransformation evaluations. Furthermore, the potential use of *Sutherlandia frutescence* and *Xysmalobium undulatum* in the treatment of colorectal cancer is reflected on, and future recommendations are also presented.

5.1. Introduction

The potential use of African phytomedicines to address the burden of cancer on the continent requires thorough study in suitable models. New, more physiologically relevant models are needed to increase the success rate of new treatments in clinical trials, and three-dimensional (3D) cell culture models have been proposed as a viable option for such models.

The general aim of this project was to optimise and characterise the LS180 sodium alginate encapsulated 3D spheroid model as a potential model for drug biotransformation studies and anticancer treatment screening of new compounds and phytomedicines.

5.2. Pre-screening of the chemotherapeutic drug and the phytomedicines

The 3-(4,5-dimethylthiazol-2-yl)-2,5- diphenyl tetrazolium bromide (MTT) assay was used in this study to serve as a predictive tool for possible anticancer activity. LS180 cells cultured two-dimensionally (2D) were exposed to different concentrations of the drug and the plant extracts for 96 h. The subsequent cell viability was assessed with the MTT assay. The Probit analysis was applied to the data to generate 50% inhibition concentrations (IC_{50}) concentrations for paclitaxel (a standard chemotherapeutic drug), *S. frutescens* and *X. undulatum*, as indicators of anticancer activity.

The IC_{50} values were determined to be:

- Paclitaxel: 94.595 nM,
- *S. frutescens*: 2.625 mg/ml,
- *X. undulatum*: 0.098 mg/ml.

These values were then used to calculate the dosage per soluble protein content for each treatment group in 3D, to ensure cells in subsequent assays were constantly exposed to the same concentration of the compound. This would also allow better comparison to *in vivo* and clinical studies, since dosing in these studies works on the same principle.

5.3. Characterisation of the LS180 sodium alginate encapsulated 3D model

The LS180 sodium alginate encapsulated spheroid model was cultured, maintained and characterised for 20 days. The model was fully characterised to ensure adequate cell growth and

viability during this period. The following parameters were measured: soluble protein content, intracellular adenosine triphosphate (ATP), extracellular adenylate kinase (AK), as well as glucose consumption. The CYP3A4 and CYP2D6 enzyme gene expression were also measured to evaluate the potential of the model for future drug biotransformation studies.

The spent medium glucose content remained low for the duration of the characterisation, indicating glucose consumption by the cells. It is, however, possible that the low levels of glucose could have impacted the growth of the spheroids. This should be closely monitored.

When evaluating the soluble protein content, the following conclusions were made. Firstly, the soluble protein content per spheroid (µg) remained stable, with no rapid increase in the first 10 days. This was probably due to the high concentration of spheroids per bioreactor, resulting in nutrient depletion. When the spheroid numbers were reduced on day 10, rapid growth occurred as indicated by the increase in protein content. The average protein content per spheroid increased from 5.398 µg on day 0 to 26.394 µg on day 20. All data collected after day10 showed statistical significant increases with $p < 0.001$.

Secondly, when evaluating the ATP content per µg soluble protein, the following was observed. During the first 10 days of characterisation, there was a steady increase in the ATP content per µg of soluble protein and reaching a peak on day 10. The changes in the data seen of day 10 was also statistically significant with $p < 0.001$. The average ATP content per µg of soluble protein was 0.027 µM/µg on day 0 and on day 20 it was 2.368 µM/µg.

Thirdly, the extracellular AK release per µg of soluble protein remained low for the first 6 days, with a slow increase that reached a peak on day 10. This can possibly be explained by the dense number of spheroids per bioreactor. After a reduction in spheroid numbers, there was a visible decrease in the extracellular AK release per µg of soluble protein, which remained low for the duration of the experiment.

Lastly, the gene expression data for *CYP3A4* and *CYP2D6* yielded interesting results. Expression of *CYP3A4* increased as a result of culturing in 3D. This data suggests the ideal time in which to perform experiments that could affect *CYP3A4* gene expression, would be between days 11 and 18. When evaluating the *CYP2D6* gene expression, it was noted that the gene expression decreased slightly as the spheroids aged.

All these results indicated that the model had adequate growth and viability during the characterisation period, with cells actively living and dying. Thus it could be concluded that the model was viable and useful for a period of 20 days.

5.4. Validation of the LS180 sodium alginate encapsulated 3D model

The ATP content of 3D cell culture models is a powerful tool to predict health, growth and energy status with high confidence (Kijanska & Kelm, 2016). When a cell dies, ATP levels fall rapidly, followed by the cessation of energy producing metabolic pathways and the presence of ATPase which rapidly degrade ATP (Ahmann *et al*., 1987). Studies have indicated that in order for cells to undergo apoptosis, maintenance of adequate amounts of intracellular ATP levels are required. If ATP depletion occurs, it affects various steps in the apoptotic program. Cells will still die under these circumstances, but their demise will be necrotic (Leist *et al*., 1999).

According to Leist & Jaattela (2001), when mammalian cells interact with toxins they undergo a series of dramatic structural and morphological changes which can lead to loss of membrane integrity. Cytotoxicity can therefore be indicated by the presence of extracellular AK due to the cytoplasmic membrane rupture, and this serves as an important marker of cell death (Squirrell & Murphy, 1997).

During validation of the model, the standard chemotherapeutic drug, paclitaxel, was employed to evaluate the potential of the model for cancer treatment screening and drug biotransformation studies. During the validation experiments soluble protein content, intracellular ATP, extracellular AK as well as glucose consumption were measured. P-glycoprotein (*P-gp*), *CYP3A4* and *CYP2D6* gene expression were also measured.

During this experiment two concentrations of paclitaxel were used, and spheroids were exposed for 96 h with treatment every 24 h. The doses were determined by dividing the 2D IC_{50} concentration by the soluble protein content per well. This resulted in a dose concentration per µg protein and the treatment groups consisted of 0.000 mg/ml/µg protein (Untreated), 0.006 mg/ml/µg protein (paclitaxel [IC_{50}]) and 0.012 mg/ml/µg protein (paclitaxel 2[IC_{50}]).

When evaluating the effects of treatment with paclitaxel [IC_{50}], the following findings were made. Treatment resulted in a decrease in soluble protein content in comparison to the untreated control group. Following 24 h exposure, there was a marked increase in the intracellular ATP per µg soluble protein, followed by a decrease. After 96 h exposure, the intracellular ATP per µg soluble protein was less than that of the untreated control. The extracellular AK per µg soluble protein remained very similar to the AK of the untreated control group during the first 48 h. There was a notable spike at time point 72 h, followed by rapid decline. It was also noted that the glucose consumption after 96 h exposure was far below that of the untreated control group. All of these

results suggested that treatment with paclitaxel [IC_{50}] resulted in a decrease in cell growth, as well as cell viability.

Treatment with paclitaxel 2[IC_{50}] resulted in decreased soluble protein content relative to the untreated control group. The soluble protein content following treatment with paclitaxel 2[IC_{50}] and paclitaxel [IC_{50}] followed very similar trends during the experiment. Once again, the ATP per µg soluble protein of the paclitaxel 2[IC_{50}] treatment group followed the same trend as treatment with the lower concertation. The extracellular AK per µg soluble protein also remained closely relatable to that of the untreated control group during the first 48 h. Thereafter, there was an increase in AK for the next 48 h. It was also noted that the glucose consumption after 96 h exposure was decidedly decreased. The results proposed that treatment with paclitaxel 2[IC_{50}] resulted in a decrease in cell growth and cell viability. It is noteworthy that the higher concentration was not significantly more active than the lower concentration, suggesting an upper limit of treatment activity.

Treatment with paclitaxel [IC_{50}] and paclitaxel 2[IC_{50}] resulted in a statistically significant increase in the relative *CYP3A4* gene expression. This was to be expected, as it was previously established by Li *et al* (2003) that paclitaxel treatment resulted in the upregulation of the enzyme. Treatment with paclitaxel [IC_{50}] and paclitaxel 2[IC_{50}] also resulted in increased relative *CYP2D6* gene expression. Treatment with paclitaxel 2[IC_{50}] caused a statistically significant increase in expression of the gene. Treatment with paclitaxel also resulted in increased relative *P-gp* gene expression. This upregulation of *P-gp* was also observed by Li *et al*. (2003).

The results indicated that the model could indeed be used for future anticancer efficacy screening as treatment with a standard chemotherapeutic drug resulted in a decrease in cellular growth. There was also a decrease in the ATP produced by the cells and according to Ahmann *et al*. (1987) this could possibly indicate cell death. The gene expression findings also indicated that the LS180 sodium alginate encapsulated spheroid model was reactive to treatment, and could be used for future drug biotransformation research.

5.5. Phytomedicine screening in the LS180 sodium alginate encapsulated spheroid model

During this study, the LS180 sodium alginate encapsulated spheroid model was implemented to evaluate the anticancer potential of *S. frutescens* and *X. undulatum*. To evaluate the anticancer activity of the crude aqueous extracts, soluble protein content, intracellular ATP, extracellular AK

as well as glucose consumption were measured. The potential effect of these plants on biotransformation was also evaluated by measuring relative *CYP3A4* and *CYP2D6* gene expression.

5.5.1. Anticancer potential of *Sutherlandia frutescens*

During this experiment, two different concentrations were used and spheroids were exposed for 96 h, with treatment every 24 h. The spheroids were treated with 0.000 mg/ml/µg protein (Untreated), 0.201 mg/ml/µg protein (*S. frutescens* [IC_{50}]/2) and 0.403 mg/ml/µg protein (*S. frutescens* [IC_{50}]).

Exposure to *S. frutescens* [IC_{50}]/2 for 96 h led to a decreased soluble protein content relative to the untreated control. After a mere 4 h of exposure, the ATP content per µg soluble protein decreased below detectable limits, and mostly remained this way. The same was observed for AK release per µg soluble protein, with the exception of a slight increase between 24 h and 72 h. The glucose consumption of this group was also far less than that of the untreated group for the duration of the treatment.

Following treatment with *S. frutescens* [IC_{50}] for 96 h, decreased soluble protein content per spheroid was again observed, in comparison to the untreated group. Similar to the *S. frutescens* [IC_{50}]/2 group, this treatment group also showed ATP content per µg soluble protein below detectable limits after 4 h treatment, and it again persisted this low. The AK release per µg soluble protein was also below detectable limits for the duration of the experiment. The glucose consumption of this group was also reduced relative to the untreated group.

The results suggested that *S. frutescens* aqueous extract could have cancer treatment potential. This was supported by the decrease in cell growth and viability following treatment. The fact that almost no ATP could be detected after four hours could possibly indicate cell death, because as a cell dies the ATP levels fall (Ahmann *et al*., 1987). In this case, ATP depletion probably occurred, and in combination with the lack of AK suggests possible necrosis (Leist *et al*. 1999). Swanepoel (2018) also indicated anticancer potential for *S. frutescens,* and supported its use in cancer management, since *S. frutescens* extracts are claimed to be both cytotoxic and tumoricidal.

5.5.2. Anticancer potential of *Xysmalobium undulatum*

Spheroids were exposed to two concentrations *X. undulatum* for 96 h, and the groups consisted of an Untreated (0.000 mg/ml/µg protein), an *X. undulatum* [IC_{50}] (0.008 mg/ml/µg protein) treated and an *X. undulatum* 2[IC_{50}] (0.015 mg/ml/µg protein) treated.

Treatment with *X. undulatum* [IC_{50}] for 96 h resulted in a decrease in soluble protein content when compared to the untreated control. Secondly, treatment resulted in a decrease in ATP content per µg soluble protein. After 96 h of treatment, the ATP content was almost 0 µM/µg. Interestingly, the AK release per µg soluble protein was similar to that of the untreated group for the first 48 h of exposure. Thereafter, a decrease in the AK release was observer, and after 96 h the AK was nearly undetectable. The glucose consumption of this group also rapidly decreased after only 4 h exposure. This group consumed much less glucose in comparison to the untreated control.

Treatment with *X. undulatum* 2[IC_{50}] once again resulted in decreased soluble protein content. As for *X. undulatum* [IC_{50}], treatment also resulted in decreased in ATP content per µg soluble protein. The ATP was also nearing 0 µM/µg after 96 h exposure. The AK release per µg soluble protein of this treatment group also followed the same trend as the *X. undulatum* [IC_{50}] group, but with a slightly higher AK release. The glucose consumption results were also consistent with the *X. undulatum* [IC_{50}] treatment group.

The results indicated that *X. undulatum* crude aqueous extract could also have anticancer potential. This statement was supported by the decrease in cell growth and viability. According to Calitz *et al*. (2018), crude aqueous extracts of *X. undulatum* had anti-proliferating effects and this was confirmed in the current study.

5.5.3. Influence of *Sutherlandia frutescens* and *Xysmalobium undulatum* on biotransformation

Following 96 h exposure to the different plant extracts, the relative *CYP3A4* and *CYP2D6* gene expression was evaluated. Although all housekeeping genes could be detected in all samples, the presence of *CYP3A4* and *CYP2D6* could not be detected. It is possible that treatment with *S. frutescens* and *X. undulatum,* respectively, resulted in the suppression of these genes below detectable limits. If this was indeed the case, it would be warranted to further study potential phytomedicine-drug interactions with these aqueous extracts as they may possibly interfere with the normal metabolism of co-administered drugs.

5.6. Final conclusion

It can be concluded that the established 3D LS180 sodium alginate encapsulated spheroid model is viable for up to at least 20 days. 3D models have been shown by various sources to be better models than its 2D counterparts, as it more closely resembles the *in vivo* situation (Hoarau-Véchot *et al*., 2018; Kapałczyńska *et al*. 2018). This model can serve as a new platform for future colorectal cancer treatment screening, as well as drug biotransformation studies. This use was successfully validated using the standard chemotherapeutic drug, paclitaxel.

The model was also successfully implemented to evaluate the anticancer potential and drug biotransformation effects of two South African phytomedicines, *S. frutescens* and *X. undulatum*. It was concluded that both phytomedicines have potential for use during treatment of colorectal cancer. It is, however, necessary to establish what the effects of the same concentrations of these phytomedicines would be on non-cancerous cells, although they are presumed to be non-toxic due to their frequent use as traditional medicines.

Lastly, this study did not give conclusive results on the potential of *S. frutescens* and *X. undulatum* aqueous extracts to influence *CYP3A4* and *CYP2D6* gene expression, although an inhibiting effect was suggested. Potential phytomedicine-drug interactions between these plants and commercially used drugs cannot be excluded, but should be considered.

5.7. Future recommendations

The LS180 sodium alginate encapsulated spheroid model can be implemented in various future studies. It would be advisable to characterise the model for longer than 20 days. Proteomic analysis of this model could also be of value to establish what specific protein changes there are in the LS180 cells when grown in 2D or 3D. In terms of the implementation and validation of the model, sampling should be done more regularly during the first six hours, for instance after one, two and three hours of exposure. This will ensure no data on possible cell response will be missed. It is also essential to elucidate the exact mechanism of cell death following treatment with the phytomedicines. Once the exact mechanism is known, combination studies with other compounds with different mechanism of cell death could be considered.

It would also be of interest to evaluate the effects of *S. frutescens* and *X. undulatum* on more cancer types to establish whether it can only be used for colorectal cancer treatment or various types of cancer. Further studies are also needed to identify at least which fractions of the extracts are most active, or even which specific phytoconstituents.

References:

Ahmann, F.R., Garewal, H.S., Schifman, R., Celniker, A. & Rodney, S. 1987. Intracellular adenosine triphosphate as a measure of human tumor cell viability and drug modulated growth. *In vitro cellular & developmental biology*, 23:474-480.

Calitz, C., Hamman, J.H., Viljoen, A.M., Fey, S.J., Wrzesinski, K. & Gouws, C. 2018. Toxicity and anti-prolific properties of *Xysmalobium undulatum* water extract during short-term exposure to two-dimensional and three-dimensional spheroid cell cultures. *Toxicology mechanisms and methods*, 28:641-652.

Hoarau-Véchot, J., Rafii, A., Touboul, C. & Pasquier, J. 2018. Halfway between 2D and animal models: are 3D cultures the ideal tool to study cancer-microenvironment interactions? *International journal of molecular sciences*, 19:181.

Kijanska, M. & Kelm, J. 2016. *In vitro* 3D spheroids and microtissues: ATP-based cell viability and toxicity assays. (*In* Sittampalam, G.S., Coussens, N.P., Brimacombe, K., Grossman, A., Arkin, M., Auld, A., Austin, C., Baell, J., Bejcek, B., Chung, T.D.Y., Dahlin, J.L., Devanaryan, V., Foley, T.L., Glicksman, M., Hall, M.D., Hass, J.V., Inglese, J., Iversen, P.W., Kahl, S.D., Kales, S.C., Lal-Nag, M., Li, Z., McGee, J., McManus, O., Riss, T., Trask, O.J., Weidner, J.R., Xia, M., Xu, X. *ed.* Assay Guidance Manual. Bethesda: Eli Lilly & Company and the National Center for Advancing Translational Sciences. p. 355-385).

Kapałczyńska, M., Kolenda, T., Przybyła, W., Zajączkowska, M., Teresiak, A., Filas, V., Ibbs, M., Bliźniak, R., Łuczewski, Ł. & Lamperska, K. 2018. 2D and 3D cell cultures–a comparison of different types of cancer cell cultures. *Archives of medical science*, 14:910.

Li, Q., Sai, Y., Kato, Y., Tamai, I. & Tsuji, A. 2003. Influence of drugs and nutrients on transporter gene expression levels in Caco-2 and LS180 intestinal epithelial cell lines. Pharmaceutical research, 20:1119-1124.

Leist, M., Single, B., Naumann, H., Fava, E., Simon, B., Kühnle, S. & Nicotera, P. 1999. Inhibition of mitochondrial ATP generation by nitric oxide switches apoptosis to necrosis. *Experimental cell research*, 249:396-403.

Leist, M. & Jäättelä, M. 2001. Four deaths and a funeral: from caspases to alternative mechanisms. *Nature reviews molecular cell biology*, 2:589-599.

Squirrell, D. & Murphy, J. 1997. Rapid detection of very low numbers of micro-organisms using adenylate kinase as a cell marker. *A practical guide to industrial uses of ATP luminescence in rapid microbiology*, 107-113.

Swanepoel, R.A. 2018. *In vitro* evaluation of the efficacy of selected medicinal plant extracts against multidrug resistant cancer cells. Potchefstroom:NWU. (Dissertation- MSc).

APPENDIX A

This appendix presents the certificates of analysis of *Sutherlandia frutescens* (SFFW790) and *Xysmalobium undulatum* (XU174), purchased from AfriNatural Holdings.

AfriNatural

African Botanicals, Cold Pressed Oils & Butters

CERTIFICATE OF ANALYSIS

Sutherlandia frutescens - Milled

Herbapulv sic (400 micron)

Batch number: SFFW790
Manufacturing date: Mar 2017
Re-test date: Mar 2020

Characteristic	Specification	Result
Appearance	Green	Yes
Odour& Taste	Typical	Yes
Moisture	< 12%	Yes
Sieve test	95% < 400 micron	Yes
Foreign matter	< 2%	Yes
TLC	Compare to reference	
Heavy Metals		
Lead	< 3 mg / Kg	Not tested
Cadmium	< 1 mg / Kg	Not tested
Mercury	< 0.1 mg / Kg	Not tested
Arsenic	< 3 mg / Kg	Not tested
Microbiological		
TMA	< 1 000 000 CFU's / g	Not tested
Yeast &Moulds	< 10 000 CFU's / g	Not tested
E. coli	Absent	
Staph. Aureus	Absent	
Salmonella	Absent	

Normally not irradiated.

WA Joubert

Executives: Adolf Joubert (CEO) & Annemarie Rautenbach
Afrinatural Phytomedicine cc t/a Afrinatural · Cc 2007 / 108262 / 23

Tel: +27 (0) 28 316 4550 · Email: info@afrinatural.com · Web: www.afrinatural.com
Address : 23 Protea Ave, Onrus River, Hermanus 7201 · PO Box 2121, Hermanus, 7200, South Africa

Figure A.1. The certificates of analysis of *Sutherlandia frutescens* (SFFW790)

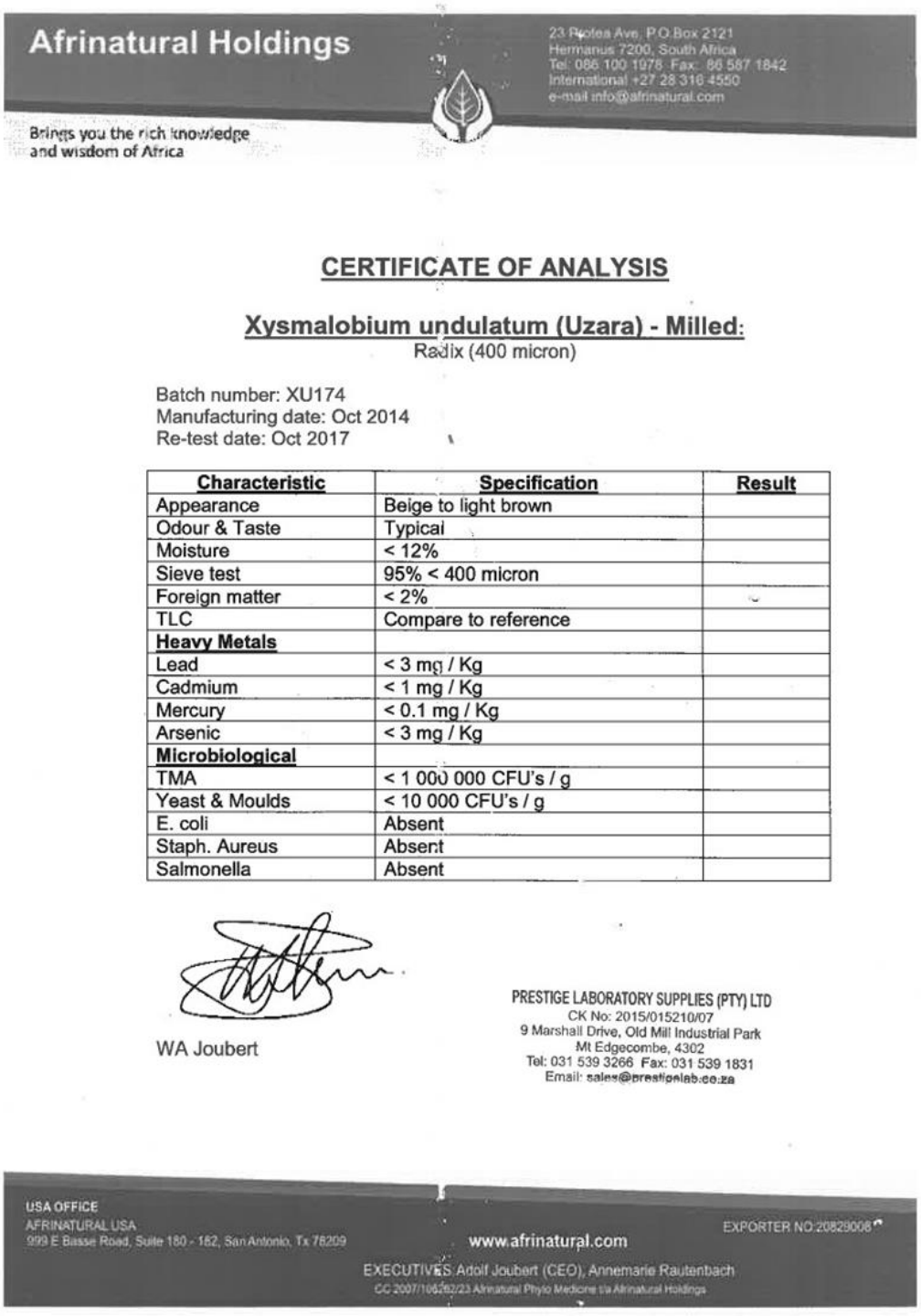

Afrinatural Holdings

Brings you the rich knowledge and wisdom of Africa

23 Protea Ave, P.O.Box 2121
Hermanus 7200, South Africa
Tel: 086 100 1978 Fax: 86 587 1842
International +27 28 316 4550
e-mail info@afrinatural.com

CERTIFICATE OF ANALYSIS

Xysmalobium undulatum (Uzara) - Milled:

Radix (400 micron)

Batch number: XU174
Manufacturing date: Oct 2014
Re-test date: Oct 2017

Characteristic	Specification	Result
Appearance	Beige to light brown	
Odour & Taste	Typical	
Moisture	< 12%	
Sieve test	95% < 400 micron	
Foreign matter	< 2%	
TLC	Compare to reference	
Heavy Metals		
Lead	< 3 mg / Kg	
Cadmium	< 1 mg / Kg	
Mercury	< 0.1 mg / Kg	
Arsenic	< 3 mg / Kg	
Microbiological		
TMA	< 1 000 000 CFU's / g	
Yeast & Moulds	< 10 000 CFU's / g	
E. coli	Absent	
Staph. Aureus	Absent	
Salmonella	Absent	

WA Joubert

PRESTIGE LABORATORY SUPPLIES (PTY) LTD
CK No: 2015/015210/07
9 Marshall Drive, Old Mill Industrial Park
Mt Edgecombe, 4302
Tel: 031 539 3266 Fax: 031 539 1831
Email: sales@prestigelab.co.za

USA OFFICE
AFRINATURAL USA
999 E Basse Road, Suite 180 - 182, San Antonio, Tx 78209

www.afrinatural.com

EXPORTER NO:20829008

EXECUTIVES: Adolf Joubert (CEO), Annemarie Rautenbach
CC 2007/106262/23 Afrinatural Phyto Medicine t/a Afrinatural Holdings

Figure A.2. The certificates of analysis of *Xysmalobium undulatum* (XU174).

APPENDIX B

This appendix presents the chemical fingerprint analyses of the crude aqueous extract of *Sutherlandia frutescens.*

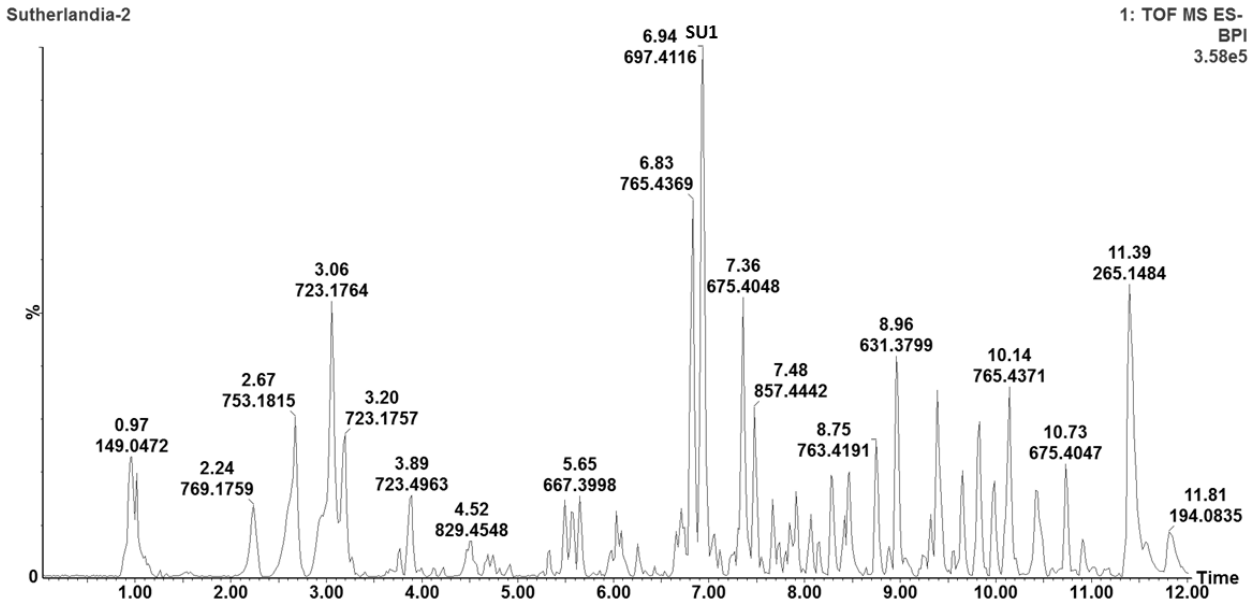

Figure B. The LC-MS chromatogram of the crude aqueous *Sutherlandia frutescens* extract.

APPENDIX C

This appendix presents the chemical fingerprint analyses of the crude aqueous extract of *Xysmalobium undulatum.*

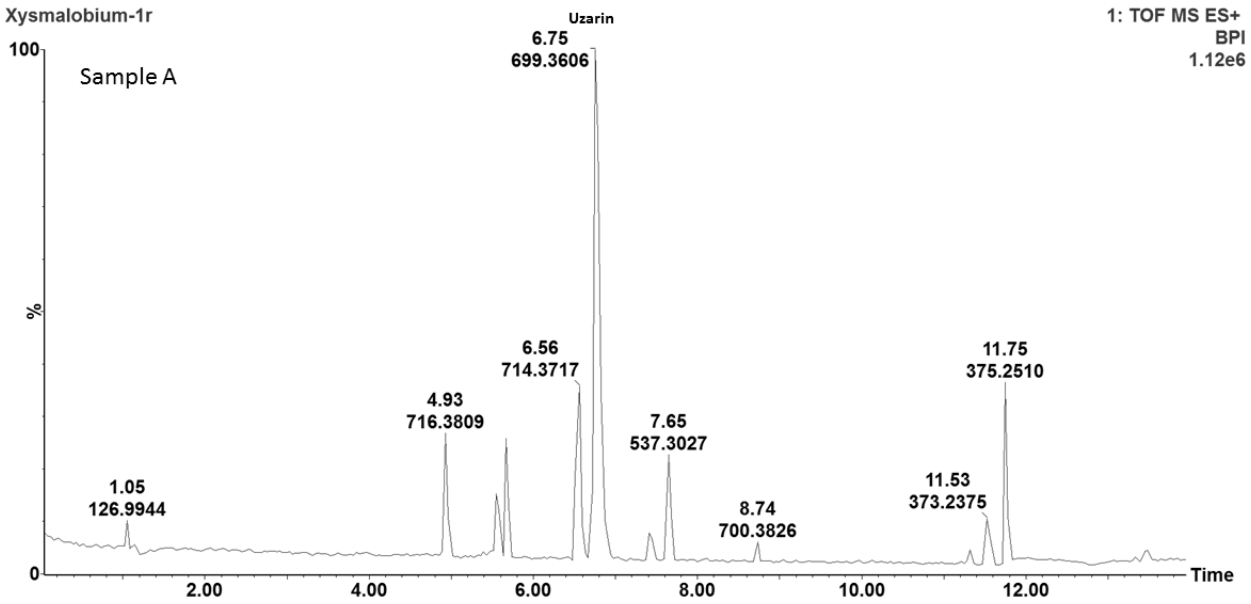

Figure C. The UPLC chromatogram of the the crude aqueous *Xysmalobium undulatum* extract.

APPENDIX D

This appendix presents the raw MTT data obtained following 96 h of exposure to different concentration of paclitaxel on the LS180 cell line.

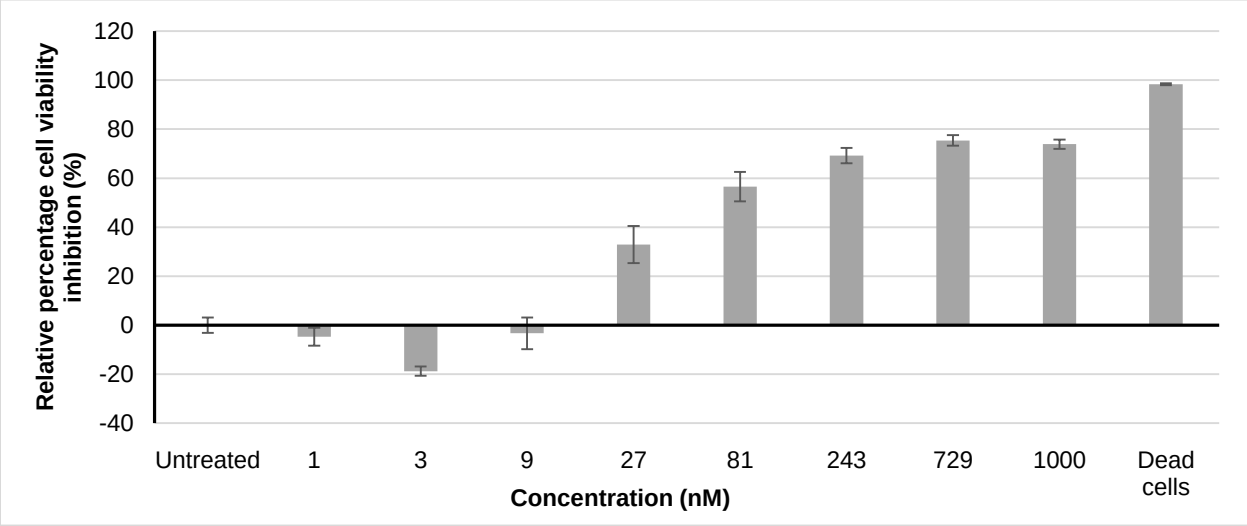

Figure D. Percentage cell viability inhibition (IC) relative to an untreated control following 96 h of exposure to different concentration of paclitaxel on the LS180 cell line. (n = 6, error bars = standard deviation). The positive control consisted of cells treated with Triton X-100 (dead cells).

APPENDIX E

This appendix presents the raw MTT data obtained following 96 h of exposure to different concentration of *Sutherlandia frutescens* on the LS180 cell line.

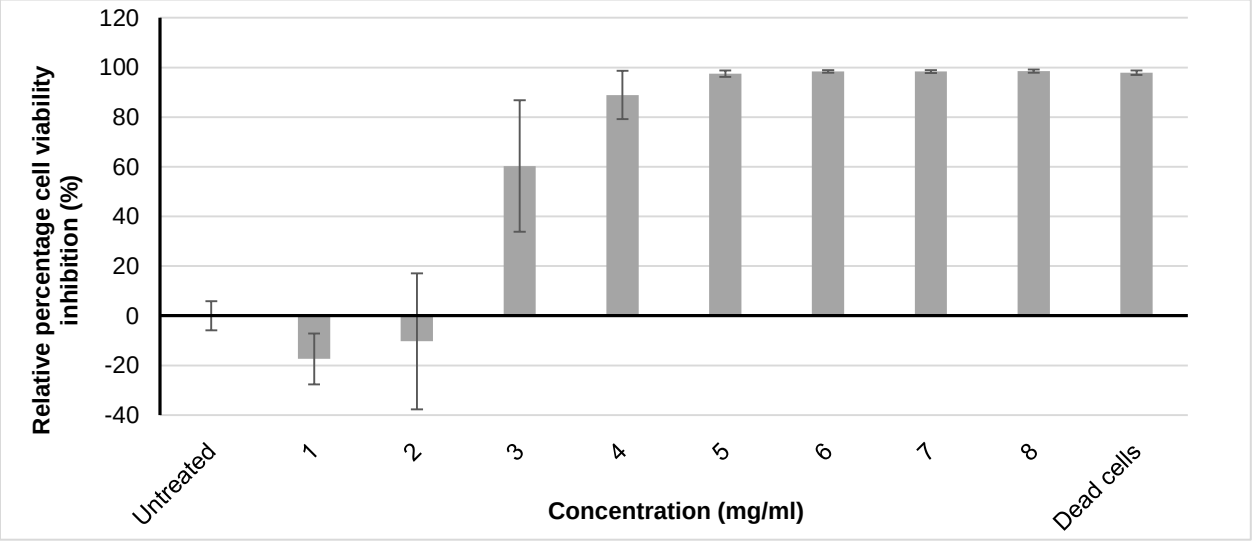

Figure E. Percentage cell viability inhibition (IC) relative to an untreated control following 96 h of exposure to different concentration of *Sutherlandia frutescens* on the LS180 cell line. (*n* = 6, error bars = standard deviation). The positive control consisted of cells treated with Triton X-100 (dead cells).

APPENDIX F

This appendix presents the raw MTT data obtained following 96 h of exposure to different concentration of *Xysmalobium undulatum* on the LS180 cell line.

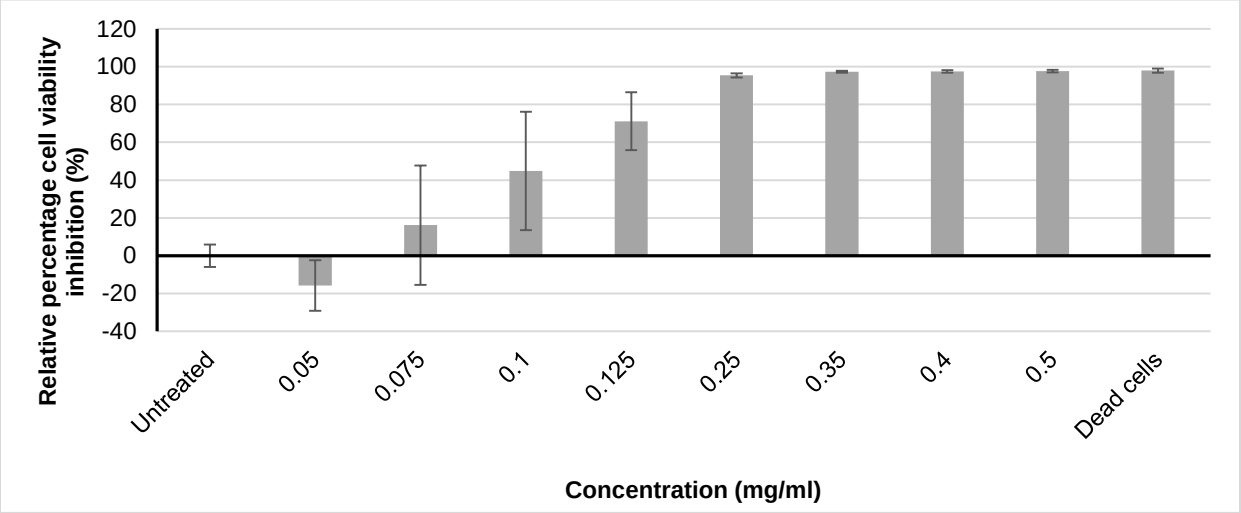

Figure F. Percentage cell viability inhibition (IC) relative to an untreated control following 96 h of exposure to different concentration of *Xysmalobium undulatum* on the LS180 cell line. (*n* = 6, error bars = standard deviation). The positive control consisted of cells treated with Triton X-100 (dead cells).

APPENDIX G

This appendix presents the amplification data following qRT-PCR.

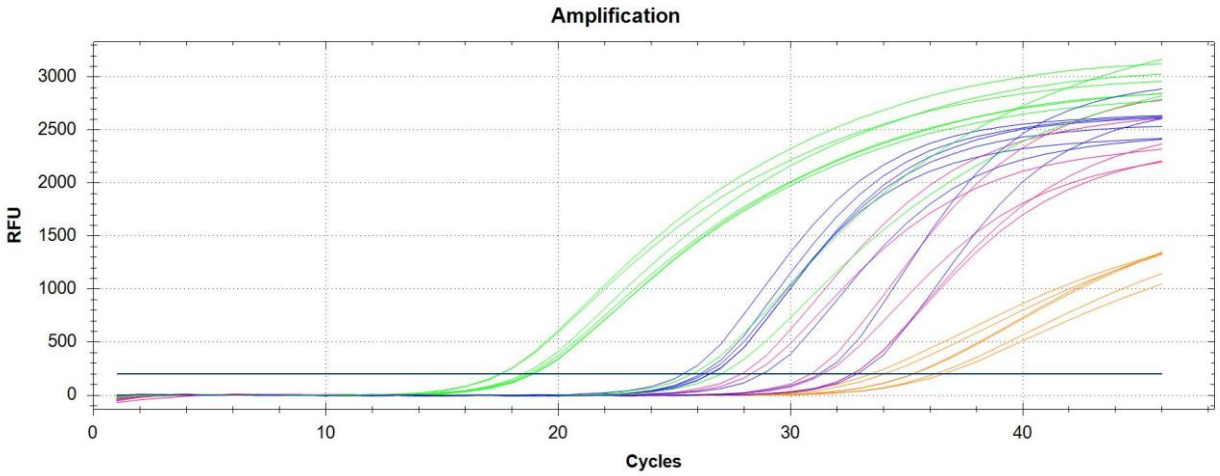

Figure G.1. This figure provides the amplification data following qRT-PCR of the untreated control group. Housekeeping genes namely glyceraldehyde 3-phosphate dehydrogenase (GADPH) and TATA-box binding protein (*TBP*) are indicated and present (indicated in green and blue respectively). The pink and yellow respectively indicates the presence of CYP3A4 and CYP2D6.

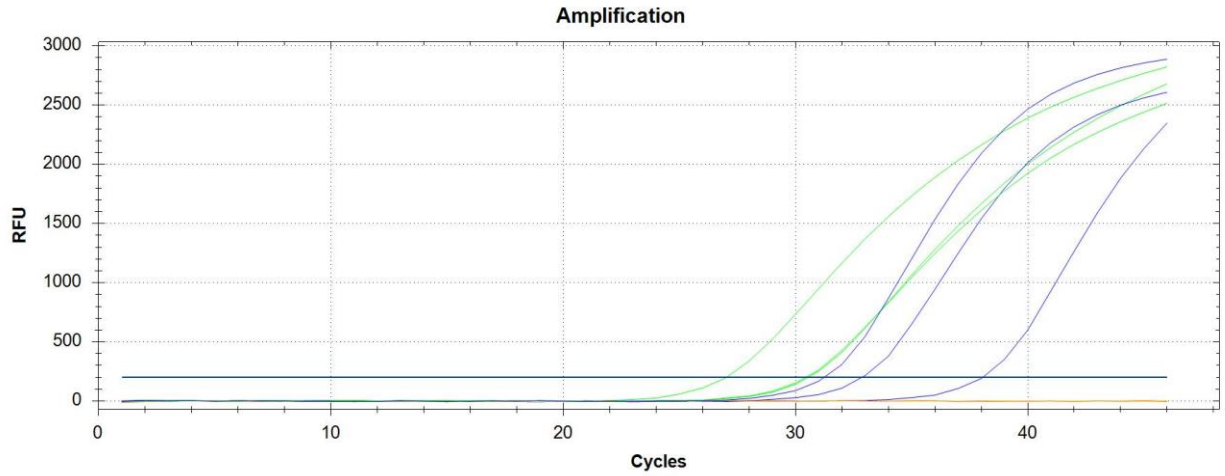

Figure G.2. This figure provides the amplification data following qRT-PCR of the groups treated with *Sutherlandia frutescens*. Housekeeping genes namely glyceraldehyde 3-phosphate dehydrogenase (GADPH) and TATA-box binding protein (*TBP*) are indicated and present (indicated in green and blue respectively). In the figure it is evident that CYP3A4 and CYP2D6 could not be detected in any of the samples (yellow line).

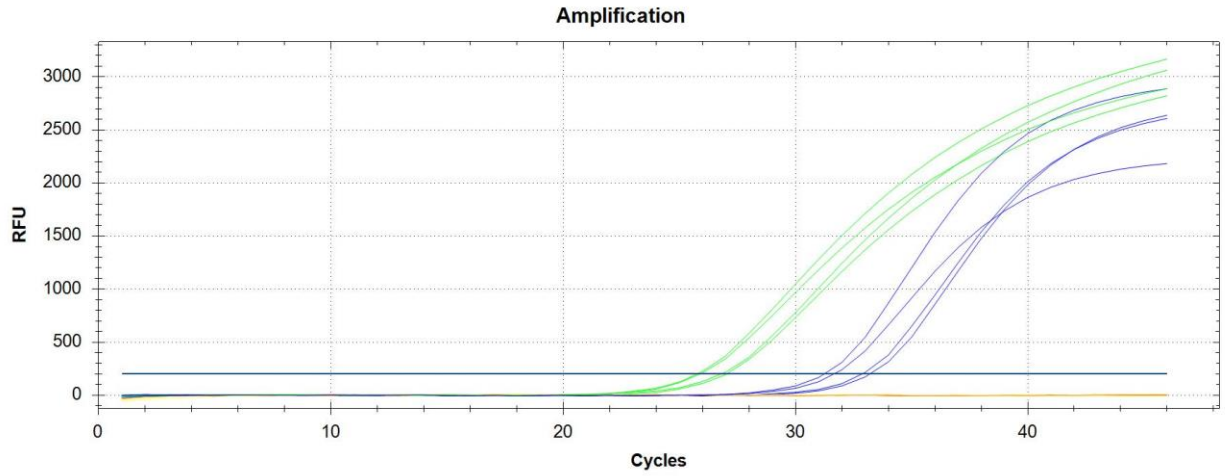

Figure G.3. This figure provides the amplification data following qRT-PCR of the groups treated with *Xysmalobium undulatum*. Housekeeping genes namely glyceraldehyde 3-phosphate dehydrogenase (GADPH) and TATA-box binding protein (*TBP*) are indicated and present (indicated in green and blue respectively). In the figure it is evident that CYP3A4 and CYP2D6 could not be detected in any of the samples (yellow line).